```
  * * * * * * * * * * * * * * STN  Columbus  * * * * * * * * * * * * * * *

FILE 'HOME' ENTERED AT 13:26:00 ON 29 MAY 2001

=> file medline biosis biotechno

COST IN U.S. DOLLARS                                    SINCE FILE      TOTAL
                                                           ENTRY    SESSION
FULL ESTIMATED COST                                         0.15       0.15

FILE 'MEDLINE' ENTERED AT 13:26:13 ON 29 MAY 2001

FILE 'BIOSIS' ENTERED AT 13:26:13 ON 29 MAY 2001
COPYRIGHT (C) 2001 BIOSIS(R)

FILE 'BIOTECHNO' ENTERED AT 13:26:13 ON 29 MAY 2001
COPYRIGHT (C) 2001 Elsevier Science B.V., Amsterdam. All rights reserved.

=> s ste5

L1          201 STE5

=> s l1 and (t52m or s18r)

L2            0 L1 AND (T52M OR S18R)

=> s ste4

L3          263 STE4

=> s l3 and (G124D or W136G or W136G or w136r or s151c del-L138)

L4            3 L3 AND (G124D OR W136G OR W136G OR W136R OR S151C DEL-L138)

=> dup rem l3
<------User Break------>
u
=> dup rem l4

PROCESSING COMPLETED FOR L4
L5            1 DUP REM L4 (2 DUPLICATES REMOVED)

=> d ibib abs l5


L5   ANSWER 1 OF 1  MEDLINE                                  DUPLICATE 1
ACCESSION NUMBER:   94217719     MEDLINE
DOCUMENT NUMBER:    94217719   PubMed ID: 8164677
TITLE:              Genetic identification of residues involved in association
                    of alpha and beta G-protein subunits.
AUTHOR:             Whiteway M; Clark K L; Leberer E; Dignard D; Thomas D Y
CORPORATE SOURCE:   National Research Council, Biotechnology Research
                    Institute, Montreal, Quebec, Canada.
SOURCE:             MOLECULAR AND CELLULAR BIOLOGY, (1994 May) 14 (5) 3223-9.

                    Journal code: NGY; 8109087. ISSN: 0270-7306.
PUB. COUNTRY:       United States
                    Journal; Article; (JOURNAL ARTICLE)
LANGUAGE:           English
FILE SEGMENT:       Priority Journals
ENTRY MONTH:        199405
ENTRY DATE:         Entered STN: 19940606
```

Updated on STN: 20000303
ered Medline: 19940525

AB The GPA1, **STE4**, and STE18 genes of Saccharomyces cerevisiae encode the alpha, beta, and gamma subunits, respectively, of a G protein involved in the mating response pathway. We have found that mutations **G124D**, **W136G**, **W136R**, and delta L138 and double mutations **W136R** L138F and **W136G** S151C of the **Ste4** protein cause constitutive activation of the signaling pathway. The **W136R** L138F and **W136G** S151C mutant **Ste4** proteins were tested in the two-hybrid protein association assay and found to be defective in association with the Gpa1 protein. A mutation at position E307 of the Gpa1 protein both suppresses the constitutive signaling phenotype of some mutant **Ste4** proteins and allows the mutant alpha subunit to physically associate with a specific mutant G beta subunit. The mutation in the Gpa1 protein is adjacent to the hinge, or switch, region that is required for the conformational change which triggers subunit dissociation, but the mutation does not affect the interaction of the alpha subunit with the wild-type beta subunit. Yeast cells constructed to contain only the mutant alpha and beta subunits mate and respond to pheromones, although they exhibit partial induction of the pheromone response pathway. Because the ability of the modified G alpha subunit to suppress the **Ste4** mutations is allele specific, it is likely that the residues defined by this analysis play a direct role in G-protein subunit association.

=> d his

(FILE 'HOME' ENTERED AT 13:26:00 ON 29 MAY 2001)

FILE 'MEDLINE, BIOSIS, BIOTECHNO' ENTERED AT 13:26:13 ON 29 MAY 2001

```
L1          201 S STE5
L2            0 S L1 AND (T52M OR S18R)
L3          263 S STE4
L***          1 S L3 AND (G124D OR W136G OR W136G OR W136R OR S151C
DEL-L***)
L***          1 S L3 AND (G124D OR W136G OR W136G OR W136R OR S151C
DEL-L***)
L***          1 S L3 AND (G124D OR W136G OR W136G OR W136R OR S151C
DEL-L***)
L4            3 S L3 AND (G124D OR W136G OR W136G OR W136R OR S151C DEL-L***)
```

```
  * * * * * * * * * * * * * * STN  Columbus  * * * * * * * * * * * * * * *

FILE 'HOME' ENTERED AT 13:26:00 ON 29 MAY 2001

=> file medline biosis biotechno

COST IN U.S. DOLLARS                                    SINCE FILE      TOTAL
                                                           ENTRY    SESSION
FULL ESTIMATED COST                                         0.15       0.15

FILE 'MEDLINE' ENTERED AT 13:26:13 ON 29 MAY 2001

FILE 'BIOSIS' ENTERED AT 13:26:13 ON 29 MAY 2001
COPYRIGHT (C) 2001 BIOSIS(R)

FILE 'BIOTECHNO' ENTERED AT 13:26:13 ON 29 MAY 2001
COPYRIGHT (C) 2001 Elsevier Science B.V., Amsterdam. All rights reserved.

=> s ste5

L1          201 STE5

=> s l1 and (t52m or s18r)

L2            0 L1 AND (T52M OR S18R)

=> s ste4

L3          263 STE4

=> s l3 and (G124D or W136G or W136G or w136r or s151c del-L138)

L4            3 L3 AND (G124D OR W136G OR W136G OR W136R OR S151C DEL-L138)

=> dup rem l3
<------User Break------>
u
=> dup rem l4

PROCESSING COMPLETED FOR L4
L5            1 DUP REM L4 (2 DUPLICATES REMOVED)

=> d ibib abs l5


L5   ANSWER 1 OF 1  MEDLINE                                  DUPLICATE 1
ACCESSION NUMBER:   94217719     MEDLINE
DOCUMENT NUMBER:    94217719   PubMed ID: 8164677
TITLE:              Genetic identification of residues involved in association
                    of alpha and beta G-protein subunits.
AUTHOR:             Whiteway M; Clark K L; Leberer E; Dignard D; Thomas D Y
CORPORATE SOURCE:   National Research Council, Biotechnology Research
                    Institute, Montreal, Quebec, Canada.
SOURCE:             MOLECULAR AND CELLULAR BIOLOGY, (1994 May) 14 (5) 3223-9.

                    Journal code: NGY; 8109087. ISSN: 0270-7306.
PUB. COUNTRY:       United States
                    Journal; Article; (JOURNAL ARTICLE)
LANGUAGE:           English
FILE SEGMENT:       Priority Journals
ENTRY MONTH:        199405
ENTRY DATE:         Entered STN: 19940606
```

Updated on STN: 20000303
Entered Medline: 19940525

AB The GPA1, **STE4**, and STE18 genes of Saccharomyces cerevisiae encode the alpha, beta, and gamma subunits, respectively, of a G protein involved in the mating response pathway. We have found that mutations **G124D**, **W136G**, **W136R**, and delta L138 and double mutations **W136R** L138F and **W136G** S151C of the **Ste4** protein cause constitutive activation of the signaling pathway. The **W136R** L138F and **W136G** S151C mutant **Ste4** proteins were tested in the two-hybrid protein association assay and found to be defective in association with the Gpa1 protein. A mutation at position E307 of the Gpa1 protein both suppresses the constitutive signaling phenotype of some mutant **Ste4** proteins and allows the mutant alpha subunit to physically associate with a specific mutant G beta subunit. The mutation in the Gpa1 protein is adjacent to the hinge, or switch, region that is required for the conformational change which triggers subunit dissociation, but the mutation does not affect the interaction of the alpha subunit with the wild-type beta subunit. Yeast cells constructed to contain only the mutant alpha and beta subunits mate and respond to pheromones, although they exhibit partial induction of the pheromone response pathway. Because the ability of the modified G alpha subunit to suppress the **Ste4** mutations is allele specific, it is likely that the residues defined by this analysis play a direct role in G-protein subunit association.

=> d his

(FILE 'HOME' ENTERED AT 13:26:00 ON 29 MAY 2001)

FILE 'MEDLINE, BIOSIS, BIOTECHNO' ENTERED AT 13:26:13 ON 29 MAY 2001

```
L1           201 S STE5
L2             0 S L1 AND (T52M OR S18R)
L3           263 S STE4
L***           1 S L3 AND (G124D OR W136G OR W136G OR W136R OR S151C
DEL-L***)
L***           1 S L3 AND (G124D OR W136G OR W136G OR W136R OR S151C
DEL-L***)
L***           1 S L3 AND (G124D OR W136G OR W136G OR W136R OR S151C
DEL-L***)
L4             3 S L3 AND (G124D OR W136G OR W136G OR W136R OR S151C DEL-L***)
L5             1 DUP REM L4 (2 DUPLICATES REMOVED)
```

* * * * * * * * * * * * * * * STN Columbus * * * * * * * * * * * * * * *

FILE 'HOME' ENTERED AT 13:16:31 ON 29 MAY 2001

=> file medline biosis biotechno

COST IN U.S. DOLLARS	SINCE FILE ENTRY	TOTAL SESSION
FULL ESTIMATED COST	0.15	0.15

FILE 'MEDLINE' ENTERED AT 13:16:43 ON 29 MAY 2001

FILE 'BIOSIS' ENTERED AT 13:16:43 ON 29 MAY 2001

FILE 'BIOTECHNO' ENTERED AT 13:16:43 ON 29 MAY 2001

=> s NF-kappa-B

L1 18421 NF-KAPPA-B

=> s (positive feedback) or autopositive or (auto-positive) or amplif?

L2 207912 (POSITIVE FEEDBACK) OR AUTOPOSITIVE OR (AUTO-POSITIVE) OR AMPLIF
?

=> s l1 and l2

L3 287 L1 AND L2

=> s l3 and autopositive

L4 0 L3 AND AUTOPOSITIVE

=> s l3 and auto-positive

L5 0 L3 AND AUTO-POSITIVE

=> s l3 and positive

L6 51 L3 AND POSITIVE

=> dup rem l6

PROCESSING COMPLETED FOR L6
L7 29 DUP REM L6 (22 DUPLICATES REMOVED)

=> d ibib abs 1-29

L7 ANSWER 1 OF 29 MEDLINE
ACCESSION NUMBER: 2001226343 MEDLINE
DOCUMENT NUMBER: 21113392 PubMed ID: 11179195
TITLE: xIAP induces cell-cycle arrest and activates nuclear factor-kappaB : new survival pathways disabled by caspase-mediated cleavage during apoptosis of human endothelial cells.
COMMENT: Comment in: Circ Res. 2001 Feb 16;88(3):262-4
AUTHOR: Levkau B; Garton K J; Ferri N; Kloke K; Nofer J R; Baba H A; Raines E W; Breithardt G

CORPORATE SOURCE: Institute of Arteriosclerosis Research, University of Munster, Munster, Germany.
CONTRACT NUMBER: HL18645 (NHLBI)
SOURCE: CIRCULATION RESEARCH, (2001 Feb 16) 88 (3) 282-90.
Journal code: DAJ; 0047103. ISSN: 1524-4571.
PUB. COUNTRY: United States
Journal; Article; (JOURNAL ARTICLE)
LANGUAGE: English
FILE SEGMENT: Priority Journals
ENTRY MONTH: 200104
ENTRY DATE: Entered STN: 20010502
Last Updated on STN: 20010521
Entered PubMed: 20010222
Entered Medline: 20010426

AB Survival of human vascular endothelial cells depends on their ability to activate the transcription factor nuclear factor-kappaB (NF-kappaB), a regulator of antiapoptotic genes, such as the X chromosome-linked inhibitor of apoptosis protein (xIAP). In the present study, we demonstrated expression of xIAP in the endothelial lining of normal human arteries and veins and elevated levels in highly malignant human endothelial tumors. Using retroviral infection of human endothelial cells, we identified two novel survival mechanisms mediated by xIAP in endothelial cells. First, xIAP can activate the transcription factor NF-kappaB, a known survival factor for human endothelial cells. This **positive feedback** loop induced by xIAP is mediated via phosphorylation and sustained degradation of inhibitor (I) kappaBalpha. Second, xIAP can inhibit cell proliferation via downregulation of cyclins A and D1 and induction of the cyclin-dependent kinase inhibitors p21(Cip1/Waf1) and p27(Kip1). Cleavage of xIAP by caspases during endothelial cell apoptosis disables both of these biological functions of xIAP. Thus, caspase-mediated cleavage of xIAP interrupts a **positive** regulatory cytoprotective loop between NF-kappaB and xIAP and increases the vulnerability of the cell to apoptosis by releasing it from an xIAP-mediated quiescent state.

L7 ANSWER 2 OF 29 MEDLINE
ACCESSION NUMBER: 2001172008 MEDLINE
DOCUMENT NUMBER: 21089204 PubMed ID: 11272279
TITLE: Involvement of protein kinases in the potentiation of lipopolysaccharide-induced inflammatory mediator formation by thapsigargin in peritoneal macrophages.
AUTHOR: Chen B C; Hsieh S L; Lin W W
CORPORATE SOURCE: Department of Pharmacology, College of Medicine, National Taiwan University, Taipei.
SOURCE: JOURNAL OF LEUKOCYTE BIOLOGY, (2001 Feb) 69 (2) 280-8.
Journal code: IWY; 8405628. ISSN: 0741-5400.
PUB. COUNTRY: United States
Journal; Article; (JOURNAL ARTICLE)
LANGUAGE: English
FILE SEGMENT: Priority Journals
ENTRY MONTH: 200103
ENTRY DATE: Entered STN: 20010404
Last Updated on STN: 20010404
Entered PubMed: 20010222
Entered Medline: 20010329

AB We have explored the regulatory roles played by Ca2+-dependent signaling on lipopolysaccharide (LPS)-induced nitric oxide (NO), prostaglandin E2 (PGE2), tumor necrosis factor alpha (TNF-alpha), and interleukin-6 (IL-6) release in mouse peritoneal macrophages. To elevate intracellular Ca2+, we used thapsigargin (TG) and UTP. Although LPS alone cannot stimulate NO synthesis, co-addition with TG, which sustainably increased [Ca2+]i, resulted in NO release. UTP, via acting on P2Y6 receptors, can stimulate phosphoinositide (PI) turnover and transient [Ca2+]i increase, however, it did not possess the NO priming effect. LPS alone triggered the release of PGE2, TNF-alpha, and IL-6; all of which were potentiated by the presence of TG, but not of UTP. The stimulatory effect of LPS plus TG on NO release

was inhibited by the presence of Ro 31-8220, Go6976, KN-93, PD 098059, or SB 203580, and abolished by BAPTA/AM and nuclear factor kappaB (NF-kappaB)
inhibitor, PDTC. PGE2, TNF-alpha, and IL-6 release by LPS alone were attenuated by Ro 31-8220, Go6976, PD 098059, SB 203580, and PDTC. Using L-NAME, soluble TNF-alpha receptor, IL-6 antibody, NS-398, and indomethacin, we performed experiments to understand the cross-regulation by the four mediators. The results revealed that TNF-alpha up-regulated NO, PGE2, and IL-6 synthesis; PGE2 up-regulated NO, but down-regulated TNF-alpha synthesis; and PGE2 and IL-6 mutually up-regulated reciprocally.
Taken together, murine peritoneal macrophages required a sustained [Ca2+]i
increase, which proceeds after TG, but not UTP, stimulation, to enhance LPS-mediated release of inflammatory mediators, particularly for NO induction. Activation of PKC-, ERK-, and p38 MAPK-dependent signaling also
are essential for LPS action. The **positive** regulatory interactions among these mediators might **amplify** the inflammatory response caused by endotoxin.

L7 ANSWER 3 OF 29 BIOSIS COPYRIGHT 2001 BIOSIS DUPLICATE 1
ACCESSION NUMBER: 2001:84307 BIOSIS
DOCUMENT NUMBER: PREV200100084307
TITLE: Toll-like receptor 4: The missing link of the cerebral innate immune response triggered by circulating gram-negative bacterial cell wall components.
AUTHOR(S): Laflamme, Nathalie; Rivest, Serge (1)
CORPORATE SOURCE: (1) Laboratory of Molecular Endocrinology, CHUL Research Center and Department of Anatomy and Physiology, Laval University, 2705, Boul. Laurier, Quebec, PQ, G1V 4G2: Serge.Rivest@crchul.ulaval.ca Canada
SOURCE: FASEB Journal, (January, 2001) Vol. 15, No. 1, pp. 155-163.
print.
ISSN: 0892-6638.
DOCUMENT TYPE: Article
LANGUAGE: English
SUMMARY LANGUAGE: English
AB The recent characterization of human homologues of Toll may be the missing
link for the transduction events leading to NF-kappaB activity and proinflammatory gene transcription during innate immune response. Indeed, CD14 is not thought to participate directly in the cell signaling, but rather one or more of the mammalian Toll-like receptors (TLRs) acts in concert with the lipopolysaccharide (LPS) receptor to discriminate between
microbial pathogens or their products and initiate transmembrane signaling. Mammalian cells may express as many as 10 distinct TLRs, although the importance of TLR4 in response to gram-negative bacteria and LPS is now supported by the fact that TLR4-mutated mice are LPS resistant.
We investigated the expression of TLR4 across the rat brain under basal conditions and in response to systemic LPS and IL-1beta injection. We first cloned the rat TLR4 cDNA via RNA isolation and polymerase chain reaction (PCR) **amplification** with a proofreading polymerase. Total RNA was isolated from the rat liver tissue using Tri-Reagent and reverse transcribed into cDNA using Superscript II reverse transcriptase and an oligonucleotide primer with a degenerate 3' end of sequence 5'-T12(GAC)N-3'. **Positive** hybridization signal was found in the leptomeninges, choroid plexus (chp), subfornical organ, organum vasculosum
of the lamina terminalis, median eminence, and area postrema. Scattered small cells also displayed a convincing hybridization signal within the brain parenchyma. Few well-defined nuclei exhibited **positive** TLR4 transcript: the supramamillary nucleus, cochlear nucleus, and the lateral reticular nucleus. The circumventricular organs, the leptomeninges, and chp also exhibited constitutive expression of the LPS receptor mCD14. In contrast to the strong up-regulation of the gene

encoding mCD14 during endotoxemia, neither LPS nor IL-1beta caused a convincing increase in the TLR4 mRNA levels across the CNS. A down-regulation of the gene encoding TLR4 was found in the cerebral tissue of immune-challenged animals. The constitutive expression of both mCD14 and TLR4 may explain the innate immune response in the brain, which originates from the structures devoid of blood-brain barrier in presence of circulating LPS.

L7 ANSWER 4 OF 29 BIOTECHNO COPYRIGHT 2001 Elsevier Science B.V.
ACCESSION NUMBER: 2000:30756781 BIOTECHNO
TITLE: **Positive** and negative regulation of apoptotic pathways by cytotoxic agents in hematological malignancies
AUTHOR: Solary E.; Droin N.; Bettaieb A.; Corcos L.; Dimanche-Boitrel M.-T.; Garrido C.
CORPORATE SOURCE: E. Solary, INSERM Unite 517, 7 boulevard Jeanne d'Arc, 21000 Dijon, France.
SOURCE: Leukemia, (2000), 14/10 (1833-1849), 222 reference(s)
CODEN: LEUKED ISSN: 0887-6924
DOCUMENT TYPE: Journal; Article
COUNTRY: United Kingdom
LANGUAGE: English
SUMMARY LANGUAGE: English
AN 2000:30756781 BIOTECHNO
AB Most chemotherapeutic drugs can induce tumor cell death by apoptosis. Analysis of the molecular mechanisms that regulate apoptosis has indicated that anticancer agents simultaneously activate several pathways that either positively or negatively regulate the death process. The main pathway from specific damage induced by the drug to apoptosis involves activation of caspases in the cytosol by pro-apoptotic molecules such as cytochrome c released from the mitochondrial intermembrane space. At least in some cell types, anticancer drugs also upregulate the expression of death receptors and sensitize tumor cells to their cognate ligands. The Fas-mediated pathway could contribute to the early steps of drug-induced apoptosis while sensitization to the cytokine TRAIL could be used to **amplify** the response to cytotoxic drugs. The Bcl-2 family of proteins, that includes anti- and pro-apoptotic molecules, regulates cell sensitivity mainly at the mitochondrial level. Anticancer drugs modulate their expression (eg through p53-dependent gene transcription), their activity (eg by phosphorylating Bcl-2) and their subcellular localization (eg by inducing the translocation of specific BH3-only pro-apoptotic proteins). Very early after interacting with tumor cells, anticancer drugs also activate lipid-dependent signaling pathways that either increase or decrease cell ability to die by apoptosis. In addition, cytotoxic agents can activate protective pathways that involve activation of **NF.kappa.B** transcription factor, accumulation of heat shock proteins such as Hsp27 and activation of proteins involved in cell cycle regulation. This review discusses how modulation of the balance between noxious and protective signals that regulate drug-induced apoptosis could be used to improve the efficacy of current therapeutic regimens in hematological malignancies.

L7 ANSWER 5 OF 29 MEDLINE DUPLICATE 2
ACCESSION NUMBER: 2001052198 MEDLINE
DOCUMENT NUMBER: 20482106 PubMed ID: 11025338
TITLE: Adenosine as a biological signal mediating sleepiness following prolonged wakefulness.
AUTHOR: Basheer R; Porkka-Heiskanen T; Strecker R E; Thakkar M M; McCarley R W
CORPORATE SOURCE: Neuroscience Laboratory, Department of Psychiatry, Harvard Medical School and VA Medical Center, Brockton, MA 02401,

CONTRACT NUMBER: [redacted]SA.
R37 39,683 (NIMH)
MH01798-01 (NIMH)
SOURCE: BIOLOGICAL SIGNALS AND RECEPTORS, (2000 Nov-Dec) 9 (6) 319-27. Ref: 43
Journal code: C4C. ISSN: 1422-4933.
PUB. COUNTRY: Switzerland
Journal; Article; (JOURNAL ARTICLE)
General Review; (REVIEW)
(REVIEW, TUTORIAL)
LANGUAGE: English
FILE SEGMENT: Priority Journals
ENTRY MONTH: 200012
ENTRY DATE: Entered STN: 20010322
Last Updated on STN: 20010322
Entered Medline: 20001211

AB Recent reports from our laboratory have shown that extracellular adenosine levels selectively increase in basal forebrain during prolonged wakefulness in cats and rats. Furthermore, microdialysis perfusion of adenosine into the basal forebrain (BF) increased sleepiness and decreased wakefulness in both the species, whereas perfusion of the A(1)-receptor-selective antagonist, cyclopentyl-1, 3-dimethylxanthine resulted in increased wakefulness, an observation similar to that found with caffeine or theophylline administration. The selective participation of the A(1) subtype of the adenosine receptor in mediating the effects of adenosine in the BF was further examined by the technique of single unit recording performed in conjunction with microdialysis perfusion of selective agonists and antagonists. Perfusion of the A(1) agonist cyclohexyladenosine, inhibited the activity of wake-active neurons in the basal forebrain. The effect of prolonged wakefulness-induced increases in adenosine levels were further investigated by determining the changes in the BF in the levels of A(1) receptor binding and the levels of its mRNA. We observed that A(1) receptor mRNA levels increase after 6 h of sleep deprivation. One of the transcription factors that showed increased DNA-binding activity was nuclear factor kappaB (NF-kappaB) and may regulate the expression of A(1) mRNA. We observed, using a gel shift assay, that the DNA-binding activity of NF-kappaB increased following 3 h of sleep deprivation. This was further supported by the increased appearance of NF-kappaB protein in the nuclear extracts and the consequent disappearance of cytoplasmic protein inhibitor kappaB (I-kappaB). Together our results reviewed in this report suggest that the somnogenic effects of adenosine in the BF area may be mediated by the A(1) subtype of adenosine receptor, and its expression might be regulated by induction in the NF-kappaB protein as its transcription factor. This **positive feedback** might mediate some of long-duration effects of sleep deprivation, including 'sleep debt'.

L7 ANSWER 6 OF 29 MEDLINE DUPLICATE 3
ACCESSION NUMBER: 2000092331 MEDLINE
DOCUMENT NUMBER: 20092331 PubMed ID: 10628750
TITLE: Angiotensin II induces nuclear factor (NF)-kappaB1 isoforms to bind the angiotensinogen gene acute-phase response element: a stimulus-specific pathway for NF-kappaB activation.
AUTHOR: Jamaluddin M; Meng T; Sun J; Boldogh I; Han Y; Brasier A R
CORPORATE SOURCE: Department of Internal Medicine, University of Texas Medical Branch, Galveston 77555-1060, USA.
CONTRACT NUMBER: P30 ES06676 (NIEHS)
R01 55630-03
SOURCE: MOLECULAR ENDOCRINOLOGY, (2000 Jan) 14 (1) 99-113.
Journal code: NGZ; 8801431. ISSN: 0888-8809.
PUB. COUNTRY: United States

Journal; Article; (JOURNAL ARTICLE)
LANGUAGE: English
FILE SEGMENT: Priority Journals
ENTRY MONTH: 200001
ENTRY DATE: Entered STN: 20000204
Last Updated on STN: 20000204
Entered Medline: 20000124

AB The vasopressor angiotensin II (AII) activates transcriptional expression of its precursor, angiotensinogen. This biological "**positive feedback** loop" occurs through an angiotensin receptor-coupled pathway that activates a multihormone-responsive enhancer of the angiotensinogen promoter, termed the acute-phase response element (APRE). Previously, we showed that the APRE is a cytokine [tumor necrosis factor-alpha (TNFalpha)]- inducible enhancer by binding the heterodimeric nuclear factor-kappaB (NF-kappaB) complex Rel A x NF-kappaB1. Here, we compare the mechanism for NF-kappaB activation by the AII agonist, Sar1 AII, with TNFalpha in HepG2 hepatocytes. Although Sar1 AII and TNFalpha both rapidly activate APRE-driven transcription within 3 h of treatment, the pattern of inducible NF-kappaB binding activity in electrophoretic mobility shift assay is distinct. In contrast to the TNFalpha mechanism, which strongly induces Rel A x NF-kappaB1 binding, Sar1 AII selectively activates a heterogenous pattern of NF-kappaB1 binding. Using a two-step microaffinity DNA binding assay, we observe that Sar1 AII recruits 50-, 56-, and 96-kDa NF-kappaB1 isoforms to bind the APRE. Binding of all three NF-kappaB1 isoforms occurs independently of changes in their nuclear abundance or proteolysis of cytoplasmic IkappaB inhibitors. Phorbol ester-sensitive protein kinase C (PKC) isoforms are required because PKC down-regulation completely blocks AII-inducible transcription and inducible NF-kappaB1 binding. We conclude that AII stimulates the NF-kappaB transcription factor pathway by activating latent DNA-binding activity of NF-kappaB subunits through a phorbol ester-sensitive (PKC-dependent) mechanism.

L7 ANSWER 7 OF 29 MEDLINE DUPLICATE 4
ACCESSION NUMBER: 2000234838 MEDLINE
DOCUMENT NUMBER: 20234838 PubMed ID: 10774805
TITLE: Increased promoter diversity reveals a complex phylogeny of human immunodeficiency virus type 1 subtype C in India.
AUTHOR: Choudhury S; Montano M A; Womack C; Blackard J T; Maniar J K; Saple D G; Tripathy S; Sahni S; Shah S; Babu G P; Essex M
CORPORATE SOURCE: Department of Immunology and Infectious Diseases, Harvard School of Public Health, Boston, Massachusetts 02115, USA.
CONTRACT NUMBER: CA-39805 (NCI)
SOURCE: JOURNAL OF HUMAN VIROLOGY, (2000 Jan-Feb) 3 (1) 35-43. Journal code: DA6; 9805755. ISSN: 1090-9508.
PUB. COUNTRY: United States
Journal; Article; (JOURNAL ARTICLE)
LANGUAGE: English
FILE SEGMENT: Priority Journals
OTHER SOURCE: GENBANK-AF169762; GENBANK-AF169763; GENBANK-AF169764; GENBANK-AF169765; GENBANK-AF169766; GENBANK-AF169767; GENBANK-AF169768; GENBANK-AF169769; GENBANK-AF169770; GENBANK-AF169771; GENBANK-AF169772; GENBANK-AF169773; GENBANK-AF169774; GENBANK-AF169775; GENBANK-AF169776; GENBANK-AF169777; GENBANK-AF169778; GENBANK-AF169779; GENBANK-AF169780; GENBANK-AF169781; GENBANK-AF169782; GENBANK-AF169783; GENBANK-AF169784; GENBANK-AF169785; GENBANK-AF169786; GENBANK-AF169787; GENBANK-AF169788; GENBANK-AF169789
ENTRY MONTH: 200006
ENTRY DATE: Entered STN: 20000706
Last Updated on STN: 20000706
Entered Medline: 20000622

AB OBJECTIVE: To evaluate human immunodeficiency virus type 1 (HIV-1) long terminal repeat (LTR) sequence diversity among distinct populations within

India and to determine the prevalent subtype. STUDY DESIGN/METHODS: Analysis of the LTR was conducted from 28 HIV-positive samples: 1992-1993 (Pune, New Delhi) and 1995-1996 (Pune, Mumbai and Vellore). Genomic DNA was extracted from cocultivated peripheral blood mononuclear cells (PBMCs) and used for polymerase chain reaction (PCR) **amplification** and sequencing using dye terminator chemistry. Sequences were edited, aligned, and analyzed phylogenetically utilizing gap-stripped and bootstrapping parameters. Mobility shift assays were used to confirm binding activity. RESULTS: All nucleotide sequences were HWV-1 subtype C based on phylogenetic analysis. The isolates from Pune/Delhi formed subclusters when analyzed separately, irrespective of time or sample source. However, no significant subclustering was observed with isolates from Mumbai or Vellore or with the entire sample set when analyzed collectively. Subtype-specific enhancer analysis revealed an expected third NF-kappaB site but also revealed six isolates with insertions and deletions not previously described, one of which resembles an AP-1 binding site. CONCLUSIONS: The results confirm the prevalence of HIV-1C and suggest increasingly complex phylogeny of HIV-1C within India, such that the previously observed subclustering may no longer adequately reflect the diversity of isolates currently circulating throughout India.

L7 ANSWER 8 OF 29 MEDLINE
ACCESSION NUMBER: 1999248183 MEDLINE
DOCUMENT NUMBER: 99248183 PubMed ID: 10229841
TITLE: Signaling through the lymphotoxin-beta receptor stimulates HIV-1 replication alone and in cooperation with soluble or membrane-bound TNF-alpha.
AUTHOR: Marshall W L; Brinkman B M; Ambrose C M; Pesavento P A; Uglialoro A M; Teng E; Finberg R W; Browning J L; Goldfeld A E
CORPORATE SOURCE: Center for Blood Research and Division of Adult Oncology, Dana-Farber Cancer Institute, Boston, MA 02115, USA.
CONTRACT NUMBER: AI28691-06 (NIAID)
CA58735 (NCI)
P30CA06516-33 (NCI)
+
SOURCE: JOURNAL OF IMMUNOLOGY, (1999 May 15) 162 (10) 6016-23.
Journal code: IFB; 2985117R. ISSN: 0022-1767.
PUB. COUNTRY: United States
Journal; Article; (JOURNAL ARTICLE)
LANGUAGE: English
FILE SEGMENT: Abridged Index Medicus Journals; Priority Journals
ENTRY MONTH: 199906
ENTRY DATE: Entered STN: 19990628
Last Updated on STN: 19990628
Entered Medline: 19990614

AB The level of ongoing HIV-1 replication within an individual is critical to HIV-1 pathogenesis. Among host immune factors, the cytokine TNF-alpha has previously been shown to increase HIV-1 replication in various monocyte and T cell model systems. Here, we demonstrate that signaling through the TNF receptor family member, the lymphotoxin-beta (LT-beta) receptor (LT-betaR), also regulates HIV-1 replication. Furthermore, HIV-1 replication is cooperatively stimulated when the distinct LT-betaR and TNF receptor systems are simultaneously engaged by their specific ligands. Moreover, in a physiological coculture cellular assay system, we show that membrane-bound TNF-alpha and LT-alpha1beta2 act virtually identically to their soluble forms in the regulation of HIV-1 replication. Thus, cosignaling via the LT-beta and TNF-alpha receptors is probably involved in the modulation of HIV-1 replication and the subsequent determination of HIV-1 viral burden in monocytes. Intriguingly, surface expression of LT-alpha1beta2 is up-regulated on a T cell line acutely infected with HIV-1, suggesting a **positive feedback** loop between HIV-1 infection, LT-alpha1beta2 expression, and HIV-1 replication. Given the critical role that LT-alpha1beta2 plays in lymphoid architecture, we

speculate that [redacted]-alphalbeta2 may be involved in [redacted]IV-associated abnormalities of the lymphoid organs.

L7 ANSWER 9 OF 29 MEDLINE
ACCESSION NUMBER: 1999247639 MEDLINE
DOCUMENT NUMBER: 99247639 PubMed ID: 10232679
TITLE: Dual effect of nitric oxide donors on cyclooxygenase-2 expression in human mesangial cells.
AUTHOR: Diaz-Cazorla M; Perez-Sala D; Lamas S
CORPORATE SOURCE: Departamento de Estructura y Funcion de Proteinas, Centro de Investigaciones Biologicas and Instituto Reina Sofia de Investigaciones Nefrologicas, C.S.I.C., Velazquez, Madrid, Spain.
SOURCE: JOURNAL OF THE AMERICAN SOCIETY OF NEPHROLOGY, (1999 May) 10 (5) 943-52.
Journal code: A6H; 9013836. ISSN: 1046-6673.
PUB. COUNTRY: United States
Journal; Article; (JOURNAL ARTICLE)
LANGUAGE: English
FILE SEGMENT: Priority Journals
ENTRY MONTH: 199906
ENTRY DATE: Entered STN: 19990712
Last Updated on STN: 20000303
Entered Medline: 19990622

AB Nitric oxide (NO) is emerging as a key regulator of gene expression, capable of playing either **positive** or negative roles. The results of this study indicate that NO exerts a dual effect on cyclooxygenase-2 (COX-2) expression in human mesangial cells (HMC). Treatment of HMC with NO synthase inhibitors attenuated interleukin-1beta (IL-1beta/tumor necrosis factor-alpha (TNF-alpha)-elicited COX-2 protein and mRNA expression, suggesting a **positive** role of endogenous NO on COX-2 induction. However, NO donors (sodium nitroprusside [SNP] and S-nitroso-N-acetylpenicillamine [SNAP]) **amplified** cytokine-elicited COX-2 expression at early time points of treatment (up to 8 h for mRNA and up to 24 h for protein expression), but were inhibitory at later times. Oligonucleotide decoy experiments confirmed the importance of nuclear factor kappaB (NF-kappaB) activation for COX-2 induction by IL-1beta/TNF-alpha. Treatment with N(G)-nitro-L-arginine methyl ester (L-NAME) did not affect initial activation of NF-kappaB by IL-1beta/TNF-alpha, but unveiled an inhibitory effect of NO generation on NF-kappaB activity after 4 h. In HMC supplemented with SNP, cytokine-induced NF-kappaB activation was potentiated at early times of induction (5 to 15 min), but inhibited at later times (1 to 4 h), suggesting a dual effect of NO donors on NF-kappaB activation. Interestingly, IkappaBalpha protein levels followed a reciprocal pattern of expression: IkappaBalpha levels were lower at early times of induction in NO donor-supplemented cells; however, after 1 h of treatment, IkappaBalpha levels became higher than in cells treated only with cytokines. In the presence of SNP, cytokine-elicited IkappaBalpha mRNA induction was initially delayed, but was **amplified** at later times. These changes in IkappaBalpha expression could contribute to the dual effects of NO donors on NF-kappaB activation and COX-2 expression in HMC.

L7 ANSWER 10 OF 29 MEDLINE
ACCESSION NUMBER: 1999328613 MEDLINE
DOCUMENT NUMBER: 99328613 PubMed ID: 10402163
TITLE: Nuclear factor kappaB (NF-kappaB) pathway as a therapeutic target in rheumatoid arthritis.
AUTHOR: Jue D M; Jeon K I; Jeong J Y
CORPORATE SOURCE: Department of Biochemistry, College of Medicine, The Catholic University of Korea, Seoul.. dmjue@cmc.cuk.ac.kr
SOURCE: JOURNAL OF KOREAN MEDICAL SCIENCE, (1999 Jun) 14 (3) 231-8.
Ref: 79
Journal code: AH4; 8703518. ISSN: 1011-8934.
PUB. COUNTRY: KOREA (SOUTH)
Journal; Article; (JOURNAL ARTICLE)

eral Review; (REVIEW)
VIEW, TUTORIAL)
LANGUAGE: English
FILE SEGMENT: Priority Journals
ENTRY MONTH: 199909
ENTRY DATE: Entered STN: 19990925
Last Updated on STN: 19990925
Entered Medline: 19990916

AB Rheumatoid arthritis (RA) is a chronic inflammatory disease characterized by persistent joint swelling and progressive destruction of cartilage and bone. Current RA treatments are largely empirical in origin and their precise mechanism of action is uncertain. Increasing evidence shows that chronic inflammatory diseases such as RA are caused by prolonged production of proinflammatory cytokines including tumor necrosis factor (TNF) and interleukin 1 (IL-1). The nuclear factor kappaB (NF-kappaB) plays an essential role in transcriptional activation of TNF and IL-1. NF-kappaB is induced by many stimuli including TNF and IL-1, forming a **positive** regulatory cycle that may **amplify** and maintain RA disease process. NF-kappaB and enzymes involved in its activation can be a target for anti-inflammatory treatment. Aspirin and sodium salicylate inhibit activation of NF-KB by blocking IkappaB kinase, a key enzyme in NF-kappaB activation. Glucocorticoids suppress expression of inflammatory genes by binding glucocorticoid receptor with NF-kappaB, and increasing expression of inhibitory protein of NF-kappaB, IkappaBalpha. Sulfasalazine and gold compounds also inhibit NF-kappaB activation. Continuing advances in our understanding of action mechanism of antirheumatic agents will benefit the future development of RA regimens with greater efficacy and less toxicity.

L7 ANSWER 11 OF 29 BIOSIS COPYRIGHT 2001 BIOSIS
ACCESSION NUMBER: 1999:408852 BIOSIS
DOCUMENT NUMBER: PREV199900408852
TITLE: Role of TNF in mediating renal insufficiency following cardiac surgery: Evidence of a postbypass cardiorenal syndrome.
AUTHOR(S): Meldrum, Daniel R. (1); Donnahoo, Kirstan K.
CORPORATE SOURCE: (1) Johns Hopkins Hospital, 600 North Wolfe Street, 618 Blalock Building, Baltimore, MD, 21205 USA
SOURCE: Journal of Surgical Research, (Aug., 1999) Vol. 85, No. 2, pp. 185-199.
ISSN: 0022-4804.
DOCUMENT TYPE: General Review
LANGUAGE: English
SUMMARY LANGUAGE: English

AB Recent evidence has implicated proinflammatory mediators such as TNF-alpha in the pathophysiology of ischemia-reperfusion (I/R) injury. Clinically, serum levels of TNF-alpha are increased after myocardial infarction and after cardiopulmonary bypass. Both cardiopulmonary bypass and renal ischemia-reperfusion injury induce a cascade of events leading to cellular damage and organ dysfunction. Tumor necrosis factor (TNF), a potent proinflammatory cytokine, is released from both the heart and the kidney in response to ischemia and reperfusion. TNF released during cardiopulmonary bypass induces glomerular fibrin deposition, cellular infiltration, and vasoconstriction, leading to a reduction in glomerular filtration rate (GFR). The signaling cascade through which renal ischemia-reperfusion induces TNF production is beginning to be elucidated.
Oxidants released following reperfusion activate p38 mitogen-activated protein kinase (p38 MAP kinase) and the TNF transcription factor, NFkappaB, leading to subsequent TNF synthesis. In a **positive feedback**, proinflammatory fashion, binding of TNF to specific TNF membrane receptors can reactivate NFkappaB. This provides a mechanism by which TNF can upregulate its own expression as well as facilitate the expression of other genes pivotal to the inflammatory response. Following its production and release, TNF results in both renal and myocardial

apoptosis and [redacted] function. An understanding of [redacted] mechanisms may allow the adjuvant u[redacted] of anti-TNF therapeutic strateg[redacted] in the treatment of renal injury. The purposes of this review are: (1) to evaluate the evidence which indicates that TNF is produced by the heart following cardiopulmonary bypass; (2) to examine the effect of TNF on myocardial performance; (3) to outline the mechanisms by which the kidney produces significant TNF in response to ischemia and reperfusion; (5) to investigate the role of TNF in renal ischemia-reperfusion injury, (6) to describe the mechanisms of TNF-induced renal cell apoptosis, and (7) to suggest potential anti-TNF strategies designed to reduce renal insufficiency following cardiac surgery.

L7 ANSWER 12 OF 29 MEDLINE DUPLICATE 5
ACCESSION NUMBER: 1999239779 MEDLINE
DOCUMENT NUMBER: 99239779 PubMed ID: 10225273
TITLE: Functional analysis of different LMP1 proteins isolated from Epstein-Barr virus-**positive** carriers.
AUTHOR: Fischer N; Kopper B; Graf N; Schlehofer J R; Grasser F A; Mueller-Lantzsch N
CORPORATE SOURCE: Institut fur Medizinische Mikrobiologie und Hygiene, Abteilung Virologie, Universitatskliniken, Homburg/Saar, Germany.
SOURCE: VIRUS RESEARCH, (1999 Mar) 60 (1) 41-54.
Journal code: X98; 8410979. ISSN: 0168-1702.
PUB. COUNTRY: Netherlands
Journal; Article; (JOURNAL ARTICLE)
LANGUAGE: English
FILE SEGMENT: Priority Journals
ENTRY MONTH: 199906
ENTRY DATE: Entered STN: 19990714
Last Updated on STN: 19990714
Entered Medline: 19990629

AB The Epstein-Barr virus (EBV) is the causative agent of infectious mononucleosis and is implicated in the development of several human malignancies. Latent membrane protein 1 (LMP1), an EBV protein with known oncogenic properties, may be important in the pathogenesis of EBV-associated tumors, particularly nasopharyngeal carcinoma (NPC) and Hodgkin's disease (HD). Several reports suggested that sequence variations in the LMP1 gene may define a more aggressive, geographically restricted EBV-genotype. Most mutations in the LMP1 gene described are located within the C-terminus of the protein. However, the effect of these mutations on the biological function of the protein remains widely unknown. Therefore, this study aimed in investigating whether mutations detected in LMP1 genes isolated from different EBV-**positive** carriers have an effect on the biological function of the protein. For this purpose the LMP1 genes were **amplified** by nested PCR from DNA out of bone marrow and peripheral blood lymphocytes and sequenced. Three functional assays were performed in order to evaluate the biological activity of the different isolates: activation of the transcription factors NF-kappaB and AP-1 as well as the anchorage independent growth of LMP1 transfected ratl cells in soft agar. The results suggested that whereas differences in the activation of NF-kappaB through the various LMP1 isolates correlated tightly with their different expression levels, the outgrowth of transfected cells in soft agar did not and the transcription factor NF-kappaB therefore appeared not to be the major effector for the transformation of the rodent cell line ratl by LMP1. The various LMP1-isolates also differed in their capacity in activating the transcription factor AP-1. We found no correlation between the transforming ability of the LMPI isolates and activation of AP-1 suggesting that other so far uncharacterized domains also influence the transforming ability of the protein.

L7 ANSWER 13 OF 29 BIOSIS COPYRIGHT 2001 BIOSIS
ACCESSION NUMBER: 1998:491601 BIOSIS
DOCUMENT NUMBER: PREV199800491601

TITLE: Transforming growth factor-beta stimulates the production of osteoprotegerin/osteoclastogenesis inhibitory factor by bone marrow stromal cells.
AUTHOR(S): Takai, Hiroyuki; Kanematsu, Masahiro; Yano, Kazuki; Tsuda, Eisuke; Higashio, Kanji; Ikeda, Kyoji; Watanabe, Ken; Yamada, Yoshiji (1)
CORPORATE SOURCE: (1) Dep. Geriatr. Res., Natl. Inst. Longevity Sci., 36-3 Gengo, Morioka, Obu, Aichi 474-8522 Japan
SOURCE: Journal of Biological Chemistry, (Oct. 16, 1998) Vol. 273, No. 42, pp. 27091-27096.
ISSN: 0021-9258.
DOCUMENT TYPE: Article
LANGUAGE: English

AB Osteoprotegerin (OPG)/osteoclastogenesis inhibitory factor (OCIF) is a recently identified cytokine that belongs to the tumor necrosis factor receptor superfamily and regulates bone mass by inhibiting osteoclastic bone resorption. The present study was undertaken to determine whether OPG/OCIF is produced in bone microenvironment and how the expression is regulated. A transcript for OPG/OCIF at 3.1 kilobases was detected in bone marrow stromal cells (ST2 and MC3T3-G2/PA6) as well as in osteoblastic cells (MC3T3-E1). Transforming growth factor-beta1 (TGF-beta1) markedly increased the steady-state level of OPG/OCIF mRNA in a dose-dependent manner, while TGF-beta1 suppressed the mRNA expression of tumor necrosis factor-related activation-induced cytokine (TRANCE)/receptor activator of NF-kappaB ligand (RANKL), a **positive** regulator of osteoclastogenesis to which OPG/OCIF binds. The effect of TGF-beta1 on the expression of OPG/OCIF mRNA was transient, with a peak level at 3-6 h. The up-regulation of OPG/OCIF mRNA by TGF-beta1 in ST2 cells did not require de novo protein synthesis and involved both a transcriptional and a post-transcriptional mechanism. Western blot analysis and an enzyme-linked immunosorbent assay revealed that TGF-beta1 significantly increased the secretion of OPG/OCIF protein by ST2 cells at 6-24 h. In murine bone marrow cultures, TGF-beta1 markedly inhibited the formation of tartrateresistant acid phosphatase-**positive** multinucleated osteoclast-like cells in the presence of 1,25-dihydroxyvitamin D3, whose effect was significantly reversed by a neutralizing antibody against OPG/OCIF. These results suggest that TGF-beta1 negatively regulates osteoclastogenesis, at least in part, through the induction of OPG/OCIF by bone marrow stromal cells and that the balance between OPG/OCIF and TRANCE/RANKL in local environment may be an important determinant of osteoclastic bone resorption.

L7 ANSWER 14 OF 29 MEDLINE
ACCESSION NUMBER: 1999032221 MEDLINE
DOCUMENT NUMBER: 99032221 PubMed ID: 9817309
TITLE: Potential role of rel/nuclear factor-kappaB in the pathogenesis of interstitial cystitis.
AUTHOR: Abdel-Mageed A B; Ghoniem G M
CORPORATE SOURCE: Department of Urology, Tulane University School of Medicine, New Orleans, Louisiana 70112, USA.
SOURCE: JOURNAL OF UROLOGY, (1998 Dec) 160 (6 Pt 1) 2000-3.
Journal code: KC7; 0376374. ISSN: 0022-5347.
PUB. COUNTRY: United States
Journal; Article; (JOURNAL ARTICLE)
LANGUAGE: English
FILE SEGMENT: Abridged Index Medicus Journals; Priority Journals
ENTRY MONTH: 199812
ENTRY DATE: Entered STN: 19990115
Last Updated on STN: 19990115
Entered Medline: 19981223

AB PURPOSE: Despite assertive investigation in the last 2 decades, interstitial cystitis remains an unresolved problem in clinical urology, and its etiology and the mechanisms involved in its pathogenesis are still

a matter of conjecture. Recently nuclear factor (NF)-KB has been implicated in chronic inflammatory diseases, and is thought to be a key regulator of genes involved in response to infection, inflammation and stress. We document the presence, pattern and distribution of NF-kappaB in bladder biopsies from patients with interstitial cystitis. MATERIALS AND METHODS: Bladder biopsies from 7 women clinically diagnosed with interstitial cystitis according to National Institute for Diabetes and Digestive and Kidney Diseases criteria and 5 women diagnosed with urinary incontinence were used for immunohistochemical localization of p65, an NF-kappaB subunit. RESULTS: Our immunohistochemical localization experiments indicate that NF-kappaB was predominantly activated in bladder urothelial cells and cells of the submucosal layer in biopsies from patients with interstitial cystitis compared to controls. While activation was evident by intense nuclear localization of NF-kappaB in all interstitial cystitis specimens, diffuse and faint immunostaining was observed in control samples. The results also indicate that activation of NF-kappaB correlated with disease occurrence. CONCLUSIONS: The fact that NF-kappaB is capable of transactivating pro-inflammatory mediators, which in turn can **amplify** NF-kappaB activation by a **positive** regulatory loop, suggests that inflammatory and/or immune responses in interstitial cystitis can be exacerbated possibly by persistent activation of this nuclear factor. We believe that our study provides a novel basis for investigating the role of NF-kappaB activation in the pathophysiology of interstitial cystitis and further opens a frontier for the development of an innovative therapeutic approach to interstitial cystitis.

L7 ANSWER 15 OF 29 BIOSIS COPYRIGHT 2001 BIOSIS
ACCESSION NUMBER: 1999:16243 BIOSIS
DOCUMENT NUMBER: PREV199900016243
TITLE: **Positive feedback** loops maintaining elevated peroxynitrite levels.
AUTHOR(S): Pall, Martin L. (1)
CORPORATE SOURCE: (1) Dep. Biochem/Biophys, Program Basic Med. Sciences, Washington State Univ., Pullman, WA 99164-4660 USA
SOURCE: Molecular Biology of the Cell, (Nov., 1998) Vol. 9, No. SUPPL., pp. 372A.
Meeting Info.: 38th Annual Meeting of the American Society for Cell Biology San Francisco, California, USA December 12-16, 1998 American Society for Cell Biology
. ISSN: 1059-1524.
DOCUMENT TYPE: Conference
LANGUAGE: English

L7 ANSWER 16 OF 29 MEDLINE DUPLICATE 6
ACCESSION NUMBER: 1998373896 MEDLINE
DOCUMENT NUMBER: 98373896 PubMed ID: 9710122
TITLE: Hypoxia induces high-mobility-group protein I(Y) and transcription of the cyclooxygenase-2 gene in human vascular endothelium.
AUTHOR: Ji Y S; Xu Q; Schmedtje J F Jr
CORPORATE SOURCE: Sealy Center for Molecular Cardiology, Department of Medicine, The University of Texas Medical Branch, Galveston, USA.
SOURCE: CIRCULATION RESEARCH, (1998 Aug 10) 83 (3) 295-304.
Journal code: DAJ; 0047103. ISSN: 0009-7330.
PUB. COUNTRY: United States
Journal; Article; (JOURNAL ARTICLE)
LANGUAGE: English
FILE SEGMENT: Priority Journals
ENTRY MONTH: 199809
ENTRY DATE: Entered STN: 19980910
Last Updated on STN: 19980910
Entered Medline: 19980901
AB Cyclooxygenases catalyze a rate-limiting step in the synthesis of vascular

endothelial prostaglandins. Expression of the inducible cyclooxygenase-2 (COX-2) gene is increased by hypoxia in human vascular endothelial cells via the nuclear factor (NF)-kappaB p65 transcription factor, which is necessary but not sufficient to fully induce COX-2 transcription in response to hypoxia. After finding that cytoplasmic NF-kappaB p65 and IkappaBalpha (an inhibitory protein that binds NF-kappaB p65 precursors) levels are not changed by hypoxia, we hypothesized that other factors might play a role in regulating the COX-2 promoter, like the high-mobility-group (HMG) I(Y) family of proteins, which features multiple A.T hooks and is associated with NF-kappaB-mediated transactivation. Nuclear protein obtained from human umbilical vein endothelial cells (HUVECs) was supplemented with HMG I(Y) during electrophoretic mobility shift assays using an NF-kappaB-3' element probe. These data suggested that HMG I(Y) proteins interact with NF-kappaB p65 to induce COX-2 promoter activity. We also found that TATA-box DNA demonstrated increased electrophoretic shifting indicative of DNA binding after incubation with either hypoxic HUVEC nuclear protein or normoxic nuclear protein supplemented with HMG I(Y). Transfection of HUVECs with an expression vector containing the COX-2 promoter ligated to HMG I(Y) cDNA demonstrated **positive feedback** on COX-2 promoter activity in hypoxia. We confirmed that COX-2 is transcriptionally regulated by hypoxia using a nuclear runoff assay. Hypoxia increased steady-state cellular levels of HMG I(Y) mRNA as an early event, corresponding with increases in HMG I(Y) protein. Overexpression of HMG I(Y) was associated in a dose-response relationship with increasing prevalence of the COX-2 protein in hypoxic HUVECs. Furthermore, sense (and antisense) HMG I(Y) overexpression caused stimulation (or inhibition) of COX-2 promoter activity as measured by luciferase reporter gene expression. The physiological significance of these findings was demonstrated by cyclooxygenase-dependent release of prostaglandin E2 by HUVECs in hypoxia. We concluded that hypoxia increases expression of HMG I(Y) proteins while facilitating transactivation of the COX-2 promoter. The HMG I(Y) family of proteins may therefore function as part of a hypoxia-induced enhanceosome that helps to promote transcription of COX-2.

L7 ANSWER 17 OF 29 MEDLINE DUPLICATE 7

ACCESSION NUMBER: 1998230439 MEDLINE
DOCUMENT NUMBER: 98230439 PubMed ID: 9570512
TITLE: Human immunodeficiency virus type 1 long terminal repeat quasispecies differ in basal transcription and nuclear factor recruitment in human glial cells and lymphocytes.
AUTHOR: Krebs F C; Mehrens D; Pomeroy S; Goodenow M M; Wigdahl B
CORPORATE SOURCE: Department of Microbiology and Immunology, The Pennsylvania State University College of Medicine, Hershey 17033, USA.
CONTRACT NUMBER: NS 27405 (NINDS)
NS 32092 (NINDS)
R01 HL58005 (NHLBI)
SOURCE: JOURNAL OF BIOMEDICAL SCIENCE, (1998) 5 (1) 31-44.
Journal code: C2K; 9421567. ISSN: 1021-7770.
PUB. COUNTRY: Switzerland
Journal; Article; (JOURNAL ARTICLE)
LANGUAGE: English
FILE SEGMENT: Priority Journals
ENTRY MONTH: 199805
ENTRY DATE: Entered STN: 19980529
Last Updated on STN: 19980529
Entered Medline: 19980521

AB The generation of genomic diversity during the course of infection has the potential to affect all aspects of HIV-1 replication, including expression of the proviral genome. To gain a better understanding of the impact of long terminal repeat (LTR) sequence diversity on LTR-directed gene expression in cells of the central nervous system (CNS) and immune system,

we **amplified** and cloned LTRs from proviral DNA i[redacted]IV-1-infected peripheral blo[redacted]Sequence analysis of nineteen [redacted]s cloned from 2 adult and 3 pediatric patients revealed an average of 33 nucleotide changes (with respect to the sequence of the LAI LTR) within the 455-bp U3 region.

Transient expression analyses in cells of neuroglial and lymphocytic origin demonstrated that some of these LTRs had activities which varied significantly from the LAI LTR in U-373 MG cells (an astrocytoma cell line) as well as in Jurkat cells (a CD4-**positive** lymphocyte cell line). While LTRs which demonstrated the highest activities in U-373 MG cells also yielded high activities in Jurkat cells, the LTRs were generally more active in Jurkat cells when compared to the LAI LTR. Differences in LTR sequence also resulted in differences in transcription factor recruitment to cis-acting sites within the U3 region of the LTR, as

demonstrated by electrophoretic mobility shift assays. In particular, naturally occurring sequence variation impacted transcription factor binding to an activating transcription factor/cAMP response element binding (ATF/CREB) binding site (located between the LEF-1 and distal NF-kappaB transcription factor binding sites) that we identified in previous studies of the HIV-1 LTR. These findings suggest that LTR sequence changes can significantly affect basal LTR function and transcription factor recruitment, which may, in turn, alter the course of viral replication in cells of CNS and immune system origin.

L7 ANSWER 18 OF 29 MEDLINE DUPLICATE 8
ACCESSION NUMBER: 1998024165 MEDLINE
DOCUMENT NUMBER: 98024165 PubMed ID: 9356483
TITLE: Parasite-mediated nuclear factor kappaB regulation in lymphoproliferation caused by Theileria parva infection.
AUTHOR: Palmer G H; Machado J Jr; Fernandez P; Heussler V; Perinat T; Dobbelaere D A
CORPORATE SOURCE: Institute of Animal Pathology, University of Bern, Bern 3012, Switzerland.
SOURCE: PROCEEDINGS OF THE NATIONAL ACADEMY OF SCIENCES OF THE UNITED STATES OF AMERICA, (1997 Nov 11) 94 (23) 12527-32.

Journal code: PV3; 7505876. ISSN: 0027-8424.
PUB. COUNTRY: United States
Journal; Article; (JOURNAL ARTICLE)
LANGUAGE: English
FILE SEGMENT: Priority Journals
ENTRY MONTH: 199712
ENTRY DATE: Entered STN: 19980109
Last Updated on STN: 19980109
Entered Medline: 19971216

AB Infection of cattle with the protozoan Theileria parva results in uncontrolled T lymphocyte proliferation resulting in lesions resembling multicentric lymphoma. Parasitized cells exhibit autocrine growth characterized by persistent translocation of the transcriptional regulatory factor nuclear factor kappaB (NFkappaB) to the nucleus and consequent enhanced expression of interleukin 2 and the interleukin 2 receptor. How T. parva induces persistent NFkappaB activation, required for T cell activation and proliferation, is unknown. We hypothesized that the parasite induces degradation of the IkappaB molecules which normally sequester NFkappaB in the cytoplasm and that continuous degradation requires viable parasites. Using T. parva-infected T cells, we showed that

the parasite mediates continuous phosphorylation and proteolysis of IkappaBalpha. However, IkappaBalpha reaccumulated to high levels in parasitized cells, which indicated that T. parva did not alter the normal NFkappaB-mediated **positive feedback** loop which restores cytoplasmic IkappaBalpha. In contrast, T. parva mediated continuous degradation of IkappaBbeta resulting in persistently low cytoplasmic IkappaBbeta levels. Normal IkappaBbeta levels were only restored following T. parva killing, indicating that viable parasites are required for IkappaBbeta degradation. Treatment of T. parva-infected cells

with pyrrolidine dithiocarbamate, a metal chelator, blocked both IkappaB

degradation and consequent enhanced expression of NFkappaB dependent genes. However, treatment using the antioxidant N-acetylcysteine had no effect on either IkappaB levels or NFkappaB activation, indicating that the parasite subverts the normal IkappaB regulatory pathway downstream of the requirement for reactive oxygen intermediates. Identification of the critical points regulated by T. parva may provide new approaches for disease control as well as increase our understanding of normal T cell function.

L7 ANSWER 19 OF 29 MEDLINE DUPLICATE 9
ACCESSION NUMBER: 97439816 MEDLINE
DOCUMENT NUMBER: 97439816 PubMed ID: 9294162
TITLE: Suppression of tumor necrosis factor-induced cell death by inhibitor of apoptosis c-IAP2 is under NF-kappaB control.
AUTHOR: Chu Z L; McKinsey T A; Liu L; Gentry J J; Malim M H; Ballard D W
CORPORATE SOURCE: Howard Hughes Medical Institute, Department of Microbiology and Immunology, Vanderbilt University School of Medicine, Nashville, TN 37232-0295, USA.
SOURCE: PROCEEDINGS OF THE NATIONAL ACADEMY OF SCIENCES OF THE UNITED STATES OF AMERICA, (1997 Sep 16) 94 (19) 10057-62. Journal code: PV3; 7505876. ISSN: 0027-8424.
PUB. COUNTRY: United States
Journal; Article; (JOURNAL ARTICLE)
LANGUAGE: English
FILE SEGMENT: Priority Journals
ENTRY MONTH: 199710
ENTRY DATE: Entered STN: 19971105
Last Updated on STN: 19971105
Entered Medline: 19971021

AB Members of the NF-kappaB/Rel and inhibitor of apoptosis (IAP) protein families have been implicated in signal transduction programs that prevent cell death elicited by the cytokine tumor necrosis factor alpha (TNF). Although NF-kappaB appears to stimulate the expression of specific protective genes, neither the identities of these genes nor the precise role of IAP proteins in this anti-apoptotic process are known. We demonstrate here that NF-kappaB is required for TNF-mediated induction of the gene encoding human c-IAP2. When overexpressed in mammalian cells, c-IAP2 activates NF-kappaB and suppresses TNF cytotoxicity. Both of these c-IAP2 activities are blocked in vivo by coexpressing a dominant form of IkappaB that is resistant to TNF-induced degradation. In contrast to wild-type c-IAP2, a mutant lacking the C-terminal RING domain inhibits NF-kappaB induction by TNF and enhances TNF killing. These findings suggest that c-IAP2 is critically involved in TNF signaling and exerts **positive feedback** control on NF-kappaB via an IkappaB targeting mechanism. Functional coupling of NF-kappaB and c-IAP2 during the TNF response may provide a signal **amplification** loop that promotes cell survival rather than death.

L7 ANSWER 20 OF 29 MEDLINE DUPLICATE 10
ACCESSION NUMBER: 1998056784 MEDLINE
DOCUMENT NUMBER: 98056784 PubMed ID: 9394802
TITLE: Involvement of nuclear factor-kappa B in platelet-activating factor-mediated tumor necrosis factor-alpha expression.
AUTHOR: Im S Y; Han S J; Ko H M; Choi J H; Chun S B; Lee D G; Ha T Y; Lee H K
CORPORATE SOURCE: Department of Microbiology, College of Natural Sciences, Chonnam National University, Kwangju, Republic of Korea.
SOURCE: EUROPEAN JOURNAL OF IMMUNOLOGY, (1997 Nov) 27 (11) 2800-4. Journal code: EN5; 1273201. ISSN: 0014-2980.
PUB. COUNTRY: GERMANY: Germany, Federal Republic of
Journal; Article; (JOURNAL ARTICLE)
LANGUAGE: English
FILE SEGMENT: Priority Journals
ENTRY MONTH: 199801

ENTRY DATE: Entered STN: 19980122
Last Updated on STN: 19980122
Entered Medline: 19980102

AB Tumor necrosis factor (TNF)-alpha and platelet-activating factor (PAF) are important mediators of inflammatory reactions, and their release is controlled by a **positive feedback** network. However, the regulatory mechanisms underlying the interaction of these two molecules are unknown. Within 10 min of the injection of lipopolysaccharide (LPS) into C57BL/6 mice, effects inducible by PAF such as anaphylactic shock-like symptoms, disseminated intravascular coagulation, and hemorrhage in renal medullae were observed, and all these pathological changes were prevented by the PAF antagonist, BN 50739. The plasma level of PAF after LPS injection reached a peak at 5 min. TNF-alpha gene expression was evident 20 min after LPS injection and was maximal at 40 min, and the level of serum TNF-alpha reached a peak at 1 h. Pretreatment with BN 50739 inhibited LPS-induced TNF-alpha gene expression and protein synthesis in a dose-dependent manner. Injection of PAF or treatment of the macrophage cell line, J774A.1, with PAF activated the transcription factor, nuclear factor (**NF**)-**kappa B**, which is essential for inducible TNF-alpha transcription. The activation of **NF-kappa B** by PAF preceded the LPS-mediated TNF-alpha gene expression. Pretreatment with BN 50739 inhibited LPS-induced mobilization of **NF-kappa B** in a dose-dependent manner in vivo as well as in vitro. These data suggest that PAF, which is released immediately or shortly after LPS injection, induces the expression of TNF-alpha through the activation of **NF-kappa B**.

L7 ANSWER 21 OF 29 MEDLINE DUPLICATE 11
ACCESSION NUMBER: 97311088 MEDLINE
DOCUMENT NUMBER: 97311088 PubMed ID: 9166419
TITLE: Perturbation of the T lymphocyte lineage in transgenic mice expressing a constitutive repressor of nuclear factor (NF)-kappaB.
AUTHOR: Boothby M R; Mora A L; Scherer D C; Brockman J A; Ballard D W
CORPORATE SOURCE: Department of Microbiology and Immunology, Vanderbilt University Medical Center, Nashville, Tennessee 37232, USA.
CONTRACT NUMBER: AI-33839 (NIAID)
AI-36997 (NIAID)
GM-42550 (NIGMS)
SOURCE: JOURNAL OF EXPERIMENTAL MEDICINE, (1997 Jun 2) 185 (11) 1897-907.
Journal code: I2V; 2985109R. ISSN: 0022-1007.
PUB. COUNTRY: United States
Journal; Article; (JOURNAL ARTICLE)
LANGUAGE: English
FILE SEGMENT: Priority Journals
ENTRY MONTH: 199706
ENTRY DATE: Entered STN: 19970716
Last Updated on STN: 20000303
Entered Medline: 19970630

AB Members of the nuclear factor (NF)-kappaB/Rel family transcription factors are induced during thymic selection and in mature T lymphocytes after ligation of the T cell antigen receptor (TCR). Despite these findings, disruption of individual NF-kappaB/Rel genes has revealed no intrinsic defect in the development of mature T cells, perhaps reflecting functional redundancy. To circumvent this possibility, the T cell lineage was targeted to express a trans-dominant form of IkappaBalpha that constitutively represses the activity of multiple NF-kappaB/Rel proteins.

Transgenic cells expressing this inhibitor exhibit a significant proliferative defect, which is not reversed by the addition of exogenous interleukin-2. Moreover, mitogenic stimulation of splenocytes leads to increased apoptosis of transgenic T cells as compared with controls. In addition to deregulated T cell growth and survival, transgene expression impairs the development of normal T cell populations as evidenced by diminished numbers of TCRhi CD8 single-**positive** thymocytes. This defect was significantly **amplified** in the periphery and was accompanied by a decrease in CD4(+) T cells. Taken together, these in vivo findings indicate that the NF-kappaB/Rel signaling pathway contains compensatory components that are essential for the establishment of normal T cell subsets.

L7 ANSWER 22 OF 29 MEDLINE DUPLICATE 12
ACCESSION NUMBER: 97460006 MEDLINE
DOCUMENT NUMBER: 97460006 PubMed ID: 9312180
TITLE: Interleukin 6 is autoregulated by transcriptional mechanisms in cultures of rat osteoblastic cells.
AUTHOR: Franchimont N; Rydziel S; Canalis E
CORPORATE SOURCE: Department of Research, Saint Francis Hospital and Medical Center, Hartford, Connecticut 06105, USA.
CONTRACT NUMBER: AR-21707 (NIAMS)
SOURCE: JOURNAL OF CLINICAL INVESTIGATION, (1997 Oct 1) 100 (7) 1797-803.
Journal code: HS7; 7802877. ISSN: 0021-9738.
PUB. COUNTRY: United States
Journal; Article; (JOURNAL ARTICLE)
LANGUAGE: English
FILE SEGMENT: Abridged Index Medicus Journals; Priority Journals
ENTRY MONTH: 199710
ENTRY DATE: Entered STN: 19971224
Last Updated on STN: 19971224
Entered Medline: 19971029

AB Interleukin 6 (IL-6), a cytokine produced by skeletal cells, stimulates osteoclast recruitment. The IL-6 soluble receptor (sIL-6R) increases IL-6 activity, and IL-6 and sIL-6R levels are increased in conditions of increased bone resorption. We examined the production of IL-6 by primary rat osteoblasts (Ob cells) cultured in the presence of IL-6 and sIL-6R. IL-6 alone did not induce IL-6 transcripts, but IL-6 was stimulatory in the presence of sIL-6R. Furthermore, sIL-6R by itself increased IL-6 transcripts. Cycloheximide superinduced IL-6 transcripts and did not prevent the effect of IL-6 and sIL-6R. IL-6 in the presence of sIL-6R stimulated IL-6 rates of transcription and the activity of IL-6 promoter fragments in transiently transfected Ob cells. 5' deletions of the IL-6 promoter and targeted mutations of the multiple response element (MRE)/cAMP responsive element (CRE), the nuclear factor for IL-6 (NF-IL-6), and the nuclear factor-kappaB (NF-kappaB) binding sites indicated that NF-IL-6 and NF-kappaB, in combination with MRE/CRE, binding sites are required for the induction of the IL-6 promoter by IL-6. In conclusion, IL-6 induces its own synthesis in osteoblasts by transcriptional mechanisms. This **positive feedback** may be important in conditions of increased bone resorption.

L7 ANSWER 23 OF 29 BIOSIS COPYRIGHT 2001 BIOSIS DUPLICATE 13
ACCESSION NUMBER: 1997:19407 BIOSIS
DOCUMENT NUMBER: PREV199799318610
TITLE: Elf-1 and Stat5 bind to a critical element in a new enhancer of the human interleukin-2 receptor alpha gene.
AUTHOR(S): Lecine, Patrick; Algarte, Michele; Rameil, Pascal; Beadling, Carol; Bucher, Philipp; Nabholz, Markus; Imbert, Jean (1)
CORPORATE SOURCE: (1) INSERM U119, 27 Boulevard Lei Roure, 13009 Marseille France
SOURCE: Molecular and Cellular Biology, (1996) Vol. 16, No. 12, pp.
6829-6840.

ISSN: 0270-7306.
DOCUMENT TYPE: Article
LANGUAGE: English
AB The interleukin 2 receptor alpha-chain (IL-2R-alpha) gene is a key regulator of lymphocyte proliferation. IL-2R-alpha is rapidly and potently induced in T cells in response to mitogenic stimuli. Interleukin 2 (IL-2) stimulates IL-2R-alpha transcription, thereby **amplifying** expression of its own high-affinity receptor. IL-2Ra. transcription is at least in part controlled by two **positive** regulatory regions, PRRI and PRRII. PRRI is an inducible proximal enhancer, located between nucleotides -276 and -244, which contains **NF-kappa-B** and SRE/CArG motifs. PRRII is a T-cell-specific enhancer, located between nucleotides -137 and -64, which binds the T-cell-specific Ets protein Elf-1 and HMG-I(Y) proteins. However, none of these proximal regions account for the induction of IL-2R-alpha transcription by IL-2. To find new regulatory regions of the IL-2R-alpha gene, 8.5 kb of the 5' end noncoding sequence of the IL-2R-alpha gene have been sequenced. We identified an 86-nucleotide fragment that is 90% identical to the recently characterized murine IL-2-responsive element (mIL-2rE). This putative human IL-2rE, designated PRRIII, confers IL-2 responsiveness on a heterologous promoter. PRRIII contains a Stat protein binding site that overlaps with an EBS motif (GASd/EBSd). These are essential for IL-2 inducibility of PRRIII/CAT reporter constructs. IL-2 induced the binding of Stat5a and b proteins to the human GASd element. To confirm the physiological relevance of these findings, we carried out in vivo footprinting experiments which showed that stimulation of IL-2R-alpha expression correlated with occupancy of the GASd element. Our data demonstrate a major role of the GASd/EBSd element in IL-2R-alpha regulation and suggest that the T-cell-specific Elf-1 factor can serve as a transcriptional repressor.

L7 ANSWER 24 OF 29 MEDLINE DUPLICATE 14
ACCESSION NUMBER: 97024614 MEDLINE
DOCUMENT NUMBER: 97024614 PubMed ID: 8870842
TITLE: HIV type 1 glycoprotein 120 **amplifies** tumor necrosis factor-induced **NF-kappa B** activation in Jurkat cells.
AUTHOR: Shatrov V A; Ratter F; Gruber A; Droge W; Lehmann V
CORPORATE SOURCE: Division of Immunochemistry, Deutsches Krebsforschungszentrum, Heidelberg, Germany.
SOURCE: AIDS RESEARCH AND HUMAN RETROVIRUSES, (1996 Sep 1) 12 (13) 1209-16.
Journal code: ART; 8709376. ISSN: 0889-2229.
PUB. COUNTRY: United States
Journal; Article; (JOURNAL ARTICLE)
LANGUAGE: English
FILE SEGMENT: Priority Journals
ENTRY MONTH: 199701
ENTRY DATE: Entered STN: 19970128
Last Updated on STN: 20000303
Entered Medline: 19970113
AB This article demonstrates that human immunodeficiency virus type 1 (HIV-1) gp120 **amplifies** the activity of tumor necrosis factor alpha (TNF-alpha), a cytokine that stimulates HIV-1 replication through activation of **NF-kappa B**. In CD4-**positive** Jurkat cells, gp120 potentiates TNF-induced **NF-kappa B** activation. TNF-mediated activation of **NF-kappa B** is known to involve the intracellular formation of reactive oxygen intermediates (ROIs). Accordingly, we examined the influence of gp120 on the cellular redox state. We found that gp 120-modulated TNF-induced NK-kappa B activation was inhibited by the antioxidant butylated hydroxyanisole, indicating the involvement of redox-dependent mechanisms. In addition, we showed that gp120 induces intracellular formation of hydrogen peroxide, which is accompanied by a decrease in the ratio of glutathione to glutathione

disulfide. In contrast, in the p56lck-deficient CaM1.6 T cell line, a derivative of Jurkat cell line, gp120 was unable to stimulate hydrogen peroxide, to decrease the ratio of GSH to GSSG, and has no effect on TNF-induced **NF-kappa B** activation. This demonstrated that p56lck protein tyrosine kinase plays an active role in transmitting a signal that increases the oxidative state of the cell and as a consequence **amplifies** TNF-mediated **NF-kappa B** DNA binding. We have demonstrated that Tat protein decreased both the Mn-dependent superoxide dismutase (MnSOD) and the cellular glutathione content (GSH). Here we show that, in contrast to Tat, gp120 is unable to inhibit activity and expression of MnSOD and to decrease GSH content. Taken together, our data suggest that gp120 potentiates TNF-induced **NF-kappa B** activation by stimulating a signal pathway that involves p56lck and the increased formation of reactive oxygen intermediates such as H2O2. These findings may be relevant for the regulation of HIV-1 replication in T cells.

L7 ANSWER 25 OF 29 MEDLINE DUPLICATE 15
ACCESSION NUMBER: 96430529 MEDLINE
DOCUMENT NUMBER: 96430529 PubMed ID: 8833654
TITLE: Angiotensinogen gene activation by angiotensin II is mediated by the rel A (nuclear factor-kappaB p65) transcription factor: one mechanism for the renin angiotensin system **positive feedback** loop in hepatocytes.
AUTHOR: Li J; Brasier A R
CORPORATE SOURCE: Departments Internal Medicine and Sealy Center for Molecular Science, University of Texas Medical Branch, Galveston, USA.
CONTRACT NUMBER: 1R29-HL-45500 (NHLBI)
SOURCE: MOLECULAR ENDOCRINOLOGY, (1996 Mar) 10 (3) 252-64. Journal code: NGZ; 8801431. ISSN: 0888-8809.
PUB. COUNTRY: United States
Journal; Article; (JOURNAL ARTICLE)
LANGUAGE: English
FILE SEGMENT: Priority Journals
ENTRY MONTH: 199705
ENTRY DATE: Entered STN: 19970507
Last Updated on STN: 20000303
Entered Medline: 19970501

AB The renin-angiotensin system controls blood pressure through the enzymatic production of the vasopressor angiotensin II (AII) from the angiotensinogen (AGT) precursor. Intravascular AII production stimulates de novo synthesis of its precursor in a **positive feedback** loop through increased gene expression. In this study, we investigate the effects of AII on AGT gene expression. At nanomolar concentrations, All activates transcription of the native AGT gene; this region is mapped to the AGT gene multihormone-inducible enhancer (-615 to -470). Within the multihormone-inducible enhancer, site-directed mutations of the acute-phase response element (APRE) that interfere with nuclear factor-kappa B (**NF-kappa B**) transcription factor binding also abolish All responsiveness. The APRE functions as a rapidly inducible All-inducible enhancer with peak reporter activity detected after a 4-h stimulation; this effect occurs only when the type 1 AII receptor is expressed. All induces sequence-specific NF-KB binding to the APRE in HepG2 nuclear extracts. Moreover, AII infusions of primary rat hepatocyte cultures produces a rapid 4-fold increase in sequence-specific **NF-kappa B** binding to the APRE. Antibodies against the transcriptional activator subunit, Rel A, quantitatively supershift the nucleoprotein complex, whereas antibodies to other **NF-kappa B** members do not, demonstrating that Rel A APRE-binding activity is AII-inducible. Transient overexpression of Rel A(1-551) activates the AGT multihormone-inducible enhancer. AII-inducible domains of Rel A were mapped by cotransfecting a chimeric

GAL4-Rel A fusion protein with a reporter gene containing GAL4-binding sites. GAL4-Rel A(1-551) was an AII-inducible transactivator. Deletion of the NH(2)-terminal 254 amino acids of Rel A produces a constitutive transactivator, indicating that Rel A is activated by AII in a manner dependent on its NH(2) terminus. These studies define one mechanism for the renin-angiotensin system **positive feedback** loop in hepatocyctes.

L7 ANSWER 26 OF 29 MEDLINE
ACCESSION NUMBER: 95246748 MEDLINE
DOCUMENT NUMBER: 95246748 PubMed ID: 7729429
TITLE: Absolute dependence on kappa B responsive elements for initiation and Tat-mediated **amplification** of HIV transcription in blood CD4 T lymphocytes.
AUTHOR: Alcami J; Lain de Lera T; Folgueira L; Pedraza M A; Jacque J M; Bachelerie F; Noriega A R; Hay R T; Harrich D; Gaynor R B; +
CORPORATE SOURCE: Servicio de Microbiologia, Hospital 12 de Octubre, Madrid, Spain.
SOURCE: EMBO JOURNAL, (1995 Apr 3) 14 (7) 1552-60.
Journal code: EMB; 8208664. ISSN: 0261-4189.
PUB. COUNTRY: ENGLAND: United Kingdom
Journal; Article; (JOURNAL ARTICLE)
LANGUAGE: English
FILE SEGMENT: Priority Journals
ENTRY MONTH: 199505
ENTRY DATE: Entered STN: 19950608
Last Updated on STN: 19970203
Entered Medline: 19950530

AB The role of **NF-kappa B**-dependent signals in activating the transcriptional activity of the HIV regulatory region (LTR) was analyzed by systematic comparison of HIV LTR activity in human CD4 T cells purified from peripheral blood and a transformed lymphoblastoid T cell line. In normal CD4 T cells we also analyzed the role played by the viral kappa B responsive elements in HIV replication. Analysis of nuclear extracts of resting, normal T lymphocytes revealed the presence of the p50, but not the p65, **NF-kappa B** subunit and the induction by phorbol esters of bona fide (p50-p65) **NF-kappa B** complexes. In parallel, we observed clear enhancer-dependent HIV LTR transactivation comparable in intensity with that observed in lymphoblastoid cells. We show that unstimulated CD4 T lymphocytes offer a cellular environment of very low permissivity to HIV LTR functioning. This was in sharp contrast to the high spontaneous LTR activity observed in lymphoblastoid T cells, where LTR activity was essentially independent of kappa B-responsive elements. Due to the low basal LTR activity in resting T lymphocytes, **NF-kappa B**-dependent transactivation was a sine qua non event for induction of the HIV LTR. Surprisingly, even the function of HIV Tat in resting CD4 T lymphocytes was found to be absolutely dependent on LTR kappa B responsive elements. The relevance of these observations obtained in transient transfections was confirmed by the incapacity of blood CD4 T lymphocytes infected with an HIV infectious provirus carrying critical point mutations in the kappa B responsive elements to show any detectable transcriptional activity upon cell activation and prolonged culture in vitro.(ABSTRACT TRUNCATED AT 250 WORDS)

L7 ANSWER 27 OF 29 MEDLINE DUPLICATE 16
ACCESSION NUMBER: 96091343 MEDLINE
DOCUMENT NUMBER: 96091343 PubMed ID: 8529098
TITLE: Genomic organization and sequence of the human NRAMP gene: identification and mapping of a promoter region polymorphism.
AUTHOR: Blackwell J M; Barton C H; White J K; Searle S; Baker A M; Williams H; Shaw M A
CORPORATE SOURCE: University of Cambridge Clinical School, Department of Medicine, Addenbrooke's Hospital, United Kingdom.
SOURCE: MOLECULAR MEDICINE, (1995 Jan) 1 (2) 194-205.
Journal code: CG3; 9501023. ISSN: 1076-1551.

PUB. COUNTRY: United States
Journal; Article; (JOURNAL ARTICLE)
LANGUAGE: English
FILE SEGMENT: Priority Journals
OTHER SOURCE: GENBANK-X82015; GENBANK-X82016
ENTRY MONTH: 199601
ENTRY DATE: Entered STN: 19960220
Last Updated on STN: 19960220
Entered Medline: 19960129

AB BACKGROUND: Murine Nramp is a candidate for the macrophage resistance gene
Ity/Lsh/Bcg. Sequence analysis of human NRAMP was undertaken to determine its role in man. MATERIALS AND METHODS: A yeast artificial chromosome carrying NRAMP was subcloned and **positive** clones sequenced. The transcriptional start site was mapped using 5' RACE PCR. Polymorphic variants were **amplified** by PCR. Linkage analysis was used to map NRAMP. RESULTS: NRAMP spans 12kb and has 15 exons encoding a 550 amino acid protein showing 85% identity (92% similarity) with Nramp. Two conserved PKC sites occur in exon 2 encoding the Pro/Ser rich SH3 binding domain, and in exon 3. Striking sequence similarities (57 and 53%) were observed with yeast mitochondrial proteins, SMF1 and SMF2, especially within putative functional domains: exon 6 encoding the second transmembrane spanning domain, site of the murine susceptibility mutation;
and exon 11 encoding a conserved transport motif. No mutations comparable to the murine susceptibility mutation were found. The transcriptional initiation site mapped 148 bp 5' of the translational initiation codon. 440bp of 5' flanking sequence contained putative promoter region elements:
6 interferon-gamma response elements, 3 W-elements, 3 **NF kappa B** binding sites and 1 AP-1 site. Nine purine-rich GGAA core motifs for the myeloid-specific PU.1 transcription factor were identified, two combining with imperfect AP1-like sites to create PEA3 motifs. TATA, GC and CCAAT boxes were absent. A possible enhancer element containing the Z-DNA forming dinucleotide repeat t(gt),ac(gt),ac(gt),g was
polymorphic (4 alleles; n = 4,9,10,11), and was used to map NRAMP to 2q35.
CONCLUSIONS: This analysis provides important resources to study the role of NRAMP in human disease.

L7 ANSWER 28 OF 29 MEDLINE DUPLICATE 17
ACCESSION NUMBER: 93352583 MEDLINE
DOCUMENT NUMBER: 93352583 PubMed ID: 8349660
TITLE: Tumor necrosis factor-alpha (TNF-alpha) signal transduction
through ceramide. Dissociation of growth inhibitory effects
of TNF-alpha from activation of nuclear factor-kappa B.
AUTHOR: Dbaibo G S; Obeid L M; Hannun Y A
CORPORATE SOURCE: Department of Medicine, Duke University Medical Center, Durham, North Carolina 27710.
CONTRACT NUMBER: GM-43825 (NIGMS)
SOURCE: JOURNAL OF BIOLOGICAL CHEMISTRY, (1993 Aug 25) 268 (24) 17762-6.
Journal code: HIV; 2985121R. ISSN: 0021-9258.
PUB. COUNTRY: United States
Journal; Article; (JOURNAL ARTICLE)
LANGUAGE: English
FILE SEGMENT: Priority Journals
ENTRY MONTH: 199309
ENTRY DATE: Entered STN: 19931001
Last Updated on STN: 19970203
Entered Medline: 19930916

AB Tumor necrosis factor-alpha (TNF-alpha) exerts pleiotropic biologic effects. Although TNF-alpha appears to activate a number of signal transduction pathways, the role of second messengers in mediating the different effects of TNF-alpha are not well defined. In this study, we investigated the role of ceramide as an intracellular mediator of

TNF-alpha acti[redacted] In Jurkat T cells, TNF-alpha c[redacted]ed early activation of the sphingomye[redacted] cycle with peak hydrolysis of [redacted]ingomyelin observed at 30 min following addition of TNF-alpha. In this cell line, TNF-alpha caused potent activation of nuclear factor-kappa B (**NF-kappa B**) and exerted potent cytostatic/cytocidal activity. C2-ceramide mimicked the effects of TNF-alpha on cell growth in a dose-dependent manner, but C2-ceramide was unable to induce activation of **NF-kappa B** under multiple conditions investigated. C2-ceramide, however, enhanced activation of **NF-kappa B** in response to TNF-alpha with peak effects observed at a concentration of C2-ceramide of 5 microM. Thus, ceramide functions as a selective mediator of the cytostatic/cytotoxic effects of TNF-alpha and plays a **positive feedback** role in activation of **NF-kappa B**. TNF-alpha signaling, therefore, involves multiple second-messenger pathways that function independently or coordinately to transduce distinct functions of TNF-alpha.

L7 ANSWER 29 OF 29 MEDLINE
ACCESSION NUMBER: 90272009 MEDLINE
DOCUMENT NUMBER: 90272009 PubMed ID: 1971917
TITLE: Sequence analysis and acute pathogenicity of molecularly cloned SIVSMM-PBj14.
COMMENT: Comment in: Nature. 1990 Jun 14;345(6276):572-3
AUTHOR: Dewhurst S; Embretson J E; Anderson D C; Mullins J I; Fultz P N
CORPORATE SOURCE: Harvard University, School of Public Health, Boston, Massachusetts 02115.
SOURCE: NATURE, (1990 Jun 14) 345 (6276) 636-40.
Journal code: NSC; 0410462. ISSN: 0028-0836.
PUB. COUNTRY: ENGLAND: United Kingdom
Journal; Article; (JOURNAL ARTICLE)
LANGUAGE: English
FILE SEGMENT: Priority Journals
OTHER SOURCE: GENBANK-M31325
ENTRY MONTH: 199007
ENTRY DATE: Entered STN: 19900810
Last Updated on STN: 19970203
Entered Medline: 19900712

AB The PBj14 isolate of simian immunodeficiency virus from sooty mangabey monkeys (SIVSMM-PBj14) is the most acutely pathogenic primate lentivirus so far described, always causing fatal disease in pig-tailed macaques (Macaca nemestrina) within 8 days of inoculation. As a first step in identifying viral genes and gene products that influence pathogenicity, the SIVSMM-PBj14 genome was **amplified** by the polymerase chain reaction as 5' and 3' genomic halves of 5.1 and 5.8 kilobases, respectively, and molecularly cloned. DNA sequence analysis revealed a high degree of conservation with other SIVs, except for a 22-base-pair duplication in the enhancer region of the viral long terminal repeat which included a second binding site for the transcription factor **NF-kappa B**. Of six genomic halves examined, four contributed to the formation of infectious virus that induced acute disease and death in pig-tailed macaques as early as 6 days post-inoculation, with pathology, disease syndromes and kinetics indistinguishable from those induced by the uncloned isolate. To our knowledge this is the first example of acute immunodeficiency disease induced by a molecularly defined lentivirus. Furthermore, the molecularly cloned SIVSMM-PBj14 viruses share with the uncloned virus cytopathicity for mangabey CD4+ cells, a property that may correlate with their observed pathogenicity in vivo.

=> s autopositive or (auto-positive)

L8 54 AUTOPOSITIVE OR (AUTO-POSITIVE)

=> dup rem l8

PROCESSING COMPLETED FOR L8
L9 40 DUP REM L8 (14 DUPLICATES REMOVED)

=> s l9 and py <1999

2 FILES SEARCHED...
L10 33 L9 AND PY <1999

=> d ibib abs 1-33

L10 ANSWER 1 OF 33 MEDLINE
ACCESSION NUMBER: 1999170748 MEDLINE
DOCUMENT NUMBER: 99170748 PubMed ID: 10070176
TITLE: Ventilatory care in status asthmaticus.
AUTHOR: Smyth R J
CORPORATE SOURCE: Department of Anaesthesia, York County Hospital, Newmarket,
Canada.
SOURCE: CANADIAN RESPIRATORY JOURNAL, **(1998 Nov-Dec)** 5 (6) 485-90. Ref: 43
Journal code: C1W; 9433332. ISSN: 1198-2241.
PUB. COUNTRY: Canada
Journal; Article; (JOURNAL ARTICLE)
General Review; (REVIEW)
(REVIEW, TUTORIAL)
LANGUAGE: English
FILE SEGMENT: Priority Journals
ENTRY MONTH: 199904
ENTRY DATE: Entered STN: 19990413
Last Updated on STN: 19990413
Entered Medline: 19990401

AB Asthma continues to pose a significant medical problem in terms of both morbidity and mortality. A number of patients with a severe exacerbation of asthma fail medical therapy and require urgent intubation and mechanical ventilation. New modalities of ventilatory support, including noninvasive ventilation, have been shown to provide effective ventilation even in the presence of severe bronchoconstriction. An intrinsically high level of **auto positive** end-expiratory pressure in these patients requires a precise balance between respiratory frequency, tidal volume and inspiratory flow rates. Pressure support ventilation reduces the risk of barotrauma and lowers the work of breathing in these patients. Adjuvant therapy with inhaled anesthetics and bronchoalveolar lavage may also be indicated in patients requiring high pressures to achieve adequate ventilation.

L10 ANSWER 2 OF 33 MEDLINE
ACCESSION NUMBER: 1999021198 MEDLINE
DOCUMENT NUMBER: 99021198 PubMed ID: 9806361
TITLE: Inducible cAMP early repressor ICER down-regulation of CREB
gene expression in Sertoli cells.
AUTHOR: Walker W H; Daniel P B; Habener J F
CORPORATE SOURCE: Laboratory of Molecular Endocrinology, Massachusetts General Hospital, Howard Hughes Medical Institute, Harvard Medical School, Boston 02114, USA.
CONTRACT NUMBER: DK25532 (NIDDK)
SOURCE: MOLECULAR AND CELLULAR ENDOCRINOLOGY, **(1998 Aug 25)** 143 (1-2) 167-78.
Journal code: E69; 7500844. ISSN: 0303-7207.
PUB. COUNTRY: Ireland
Journal; Article; (JOURNAL ARTICLE)
LANGUAGE: English
FILE SEGMENT: Priority Journals
ENTRY MONTH: 199901
ENTRY DATE: Entered STN: 19990115
Last Updated on STN: 19990115

ered Medline: 19990105

AB The cAMP respon[redacted]element binding protein (CREB) [redacted]d the cAMP-responsive element modulator (CREM) are cyclically expressed in the seminiferous tubules during spermatogenesis. In the somatic Sertoli cells, which are the major supporters of germ cell development in the seminiferous tubules, the expression of CREB is cyclical and appears to be regulated by the levels of cAMP produced in response to the pituitary derived follicle-stimulating hormone FSH. Cyclic AMP response elements (CREs) located in the promoter of the CREB gene were shown earlier to be implicated in an **autopositive** feedback loop that up-regulates the expression of CREB. Here we show that in Sertoli cells FSH-mediated induction of the CREM repressor isoform, ICER (inducible cAMP early repressor) is correlated with the inhibition and delay of CREB gene expression in the seminiferous tubules. ICER binds to the two CREs located in the promoter of the CREB gene and in transient transfection assays of Sertoli cells, ICER expression vectors down-regulate transcription of a reporter gene driven by the CREB gene promoter. In addition, analyses of ICER and CREB gene expression in isolated segments of rat seminiferous tubules reveals stage-specific and cycle-dependent expression of ICER. The periods of enhanced expression of ICER correspond to the stages of spermatogenesis with the lowest levels of CREB expression. We suggest that the expression of ICER in Sertoli cells may contribute to the periodic repression of CREB gene expression during the repeated 12-day cycles of spermatogenesis, and may be required to reset the levels of activator CREB prior to the initiation of each new cycle of spermatogenesis.

L10 ANSWER 3 OF 33 MEDLINE
ACCESSION NUMBER: 97028990 MEDLINE
DOCUMENT NUMBER: 97028990 PubMed ID: 8875002
TITLE: **Auto-positive** end-expiratory pressure and dynamic hyperinflation.
AUTHOR: Ranieri V M; Grasso S; Fiore T; Giuliani R
CORPORATE SOURCE: Istituto di Anestesiologia e Rianimazione, Ospedale Policlinico, Universita di Bari, Italy.
SOURCE: CLINICS IN CHEST MEDICINE, **(1996 Sep)** 17 (3) 379-94. Ref: 50
Journal code: DLR; 7907612. ISSN: 0272-5231.
PUB. COUNTRY: United States
Journal; Article; (JOURNAL ARTICLE)
General Review; (REVIEW)
(REVIEW, TUTORIAL)
LANGUAGE: English
FILE SEGMENT: Priority Journals
ENTRY MONTH: 199701
ENTRY DATE: Entered STN: 19970128
Last Updated on STN: 19970128
Entered Medline: 19970115

AB PEEP is indicated in patients with COPD only to unload the respiratory muscles from the auto-PEEP resulting from expiratory flow limitation. If auto-PEEP is not caused by flow limitation, application of PEEP will cause further hyperinflation, worsening respiratory mechanics, muscle activity, and hemodynamics. To assess the presence of expiratory flow limitation correctly, to measure auto-PEEP correctly, and to identify the maximal PEEP level to be used, measurements of flow and opening pressure must be obtained during a brief period of suspended respiratory muscle activity (obtained by sedation) with the patient's own breathing pattern reproduced accurately.

L10 ANSWER 4 OF 33 MEDLINE
ACCESSION NUMBER: 96322888 MEDLINE
DOCUMENT NUMBER: 96322888 PubMed ID: 8706501
TITLE: Unilateral lung hyperinflation and **auto-**

po[redacted]tive end-expiratory pressure du[redacted]o a ruptured right hemidiaphragm.

AUTHOR: Burchell S A; Takiguchi S A; Myers S A; Yu M
CORPORATE SOURCE: Department of Surgery, University of Hawaii, Honolulu 96813-7825, USA.
SOURCE: CRITICAL CARE MEDICINE, **(1996 Aug)** 24 (8) 1418-21.
Journal code: DTF; 0355501. ISSN: 0090-3493.
PUB. COUNTRY: United States
Journal; Article; (JOURNAL ARTICLE)
LANGUAGE: English
FILE SEGMENT: Abridged Index Medicus Journals; Priority Journals
ENTRY MONTH: 199609
ENTRY DATE: Entered STN: 19960919
Last Updated on STN: 19960919
Entered Medline: 19960910

L10 ANSWER 5 OF 33 MEDLINE
ACCESSION NUMBER: 96196060 MEDLINE
DOCUMENT NUMBER: 96196060 PubMed ID: 8610857
TITLE: **Auto-positive** end-expiratory pressure during one-lung ventilation using a double-lumen endobronchial tube.
COMMENT: Comment in: Anesth Analg. 1996 Nov;83(5):1131
AUTHOR: Yokota K; Toriumi T; Sari A; Endou S; Mihira M
CORPORATE SOURCE: Department of Anesthesiology and Intensive Care Medicine, Kawasaki Medical School, Okayama, Japan.
SOURCE: ANESTHESIA AND ANALGESIA, **(1996 May)** 82 (5) 1007-10.
Journal code: 4R8; 1310650. ISSN: 0003-2999.
PUB. COUNTRY: United States
Journal; Article; (JOURNAL ARTICLE)
LANGUAGE: English
FILE SEGMENT: Abridged Index Medicus Journals; Priority Journals
ENTRY MONTH: 199605
ENTRY DATE: Entered STN: 19960605
Last Updated on STN: 19980206
Entered Medline: 19960524

AB The present study was undertaken to investigate the possible relationships between the magnitude of **autopositive** end-expiratory pressure (auto-PEEP) and measured PaO2 during one-lung ventilation (OLV). Forty-one adults received OLV anesthesia using a tidal volume of 8 mL/kg and a respiratory rate of 12 breaths/min. Auto-PEEP was quantified using an end-expiratory port occlusion method. During two-lung ventilation (2LV), auto-PEEP was observed in 18 of 41 patients and ranged from 0.5 to 2.5 cm H2O. During OLV, auto-PEEP was observed in 34 of 41 patients and ranged from 0.5 to 10 cm H2O. The mean (+/- SD) value of auto-PEEP was significantly higher during OLV than during 2LV (3.2 +/- 3.3 cm H2O versus 0.5 +/- 0.7 cm H2O, P < 0.0001). Auto-PEEP during OLV correlated inversely with preoperative forced expiratory volume in 1 s/forced vital capacity (y = 12.5 - 0.13x, r = -.05, P < 0.005). During OLV, there was no significant correlation between auto-PEEP and measured PaO2. These findings confirm that many patients do not exhale completely to functional residual capacity during OLV.

L10 ANSWER 6 OF 33 MEDLINE
ACCESSION NUMBER: 96194350 MEDLINE
DOCUMENT NUMBER: 96194350 PubMed ID: 8625647
TITLE: Low measured **auto-positive** end-expiratory pressure during mechanical ventilation of patients with severe asthma: hidden **auto-positive** end-expiratory pressure.
COMMENT: Comment in: Crit Care Med. 1996 Mar;24(3):379-80

AUTHOR: [redacted]therman J W; Ravenscraft S A
CORPORATE SOURCE: [redacted]artment of Medicine, Hennepin [redacted]nty Medical Center, Minneapolis, MN 55415, USA.
SOURCE: CRITICAL CARE MEDICINE, **(1996 Mar)** 24 (3) 541-6.
Journal code: DTF; 0355501. ISSN: 0090-3493.
PUB. COUNTRY: United States
Journal; Article; (JOURNAL ARTICLE)
LANGUAGE: English
FILE SEGMENT: Abridged Index Medicus Journals; Priority Journals
ENTRY MONTH: 199606
ENTRY DATE: Entered STN: 19960708
Last Updated on STN: 19960708
Entered Medline: 19960627

AB OBJECTIVE: To describe the occurrence of low measured auto-end-expiratory pressure (auto-PEEP) during mechanical ventilation of patients severe asthma. DESIGN: Observational clinical study. SETTING: Medical intensive care unit of a university-affiliated county hospital. PATIENTS: Four mechanically ventilated patients with severe asthma who had low measured auto-PEEP despite marked increase in both peak and plateau airway pressures. INTERVENTIONS: None. MEASUREMENTS AND MAIN RESULTS: Peak pressure, plateau pressure, and auto-PEEP were measured at an early time point, when airflow obstruction was most severe, and again at a later time after clinical improvement. Auto-PEEP was measured by the method of end-expiratory airway occlusion. From the early to the late point, there was a marked decrease in peak pressure (76 +/- 7 to 53 +/- 6 cm H2O; p<.001) and in plateau pressure (28 +/- 2 to 18 +/- 3 cm H2O; p<.001), but only minimal change in auto-PEEP (5 +/- 3 to 4 +/- 3 cm H2O). The difference between plateau pressure and auto-PEEP decreased between the early and late time points (23 +/- 1 to 14 +/- 1 cm H2O; p<.01), even though tidal volume was larger at the late time point. In three patients, low auto-PEEP and a large difference between plateau pressure and auto-PEEP was only seen after expiratory time was prolonged. In these three patients, prolongation of expiratory time resulted in a large decrease in measured auto-PEEP (14 +/- 4 to 5 +/- 4 cm H2O), but a much smaller change in plateau pressure (31 +/- 3 to 29 +/- 3 cm H2O). CONCLUSIONS: We conclude that measured auto-PEEP may underestimate end-expiratory alveolar pressure in severe asthma, and that marked pulmonary hyperinflation may be present despite low measured auto-PEEP, especially at low respiratory rates. This phenomenon may be due to widespread airway closure that prevents accurate assessment of alveolar pressure at end-expiration.

L10 ANSWER 7 OF 33 MEDLINE
ACCESSION NUMBER: 96194338 MEDLINE
DOCUMENT NUMBER: 96194338 PubMed ID: 8625635
TITLE: Tracheal gas insufflation combined with high-frequency oscillatory ventilation.
AUTHOR: Dolan S; Derdak S; Solomon D; Farmer C; Johanningman J; Gelineau J; Smith R B
CORPORATE SOURCE: Department of Pulmonary Medicine, Wilford Hall Medical Center, Lackland Air Force Base, San Antonio, TX, USA.
SOURCE: CRITICAL CARE MEDICINE, **(1996 Mar)** 24 (3) 458-65.
Journal code: DTF; 0355501. ISSN: 0090-3493.
PUB. COUNTRY: United States
Journal; Article; (JOURNAL ARTICLE)
LANGUAGE: English
FILE SEGMENT: Abridged Index Medicus Journals; Priority Journals
ENTRY MONTH: 199606
ENTRY DATE: Entered STN: 19960708
Last Updated on STN: 19960708
Entered Medline: 19960627

AB OBJECTIVES: To determine the efficacy of tracheal insufflation delivered by two different catheter designs on CO2 elimination when used in conjunction with high-frequency oscillatory ventilation. DESIGN: A nonrandomized before and after trial. Each animal served as his own control. SUBJECTS: Ten mongrel dogs weighing 20.9 +/- 1.9 kg. Four animals

were assigned to normal lung group and six animals underwent lung injury
by large volume saline lavage. INTERVENTION: Permissive hypercapnia was allowed to occur by selecting oscillator settings that would lead to alveolar hypoventilation. Proximal mean airway pressure was kept constant.
Tracheal gas was insufflated at 1 cm above the carina for 30 min periods at gas flows of 5 to 15 L/min. MEASUREMENTS AND MAIN RESULTS: Carinal pressure, hemodynamic parameters (cardiac output, mean arterial pressure, pulmonary artery occlusion pressure), and gas exchange parameters (PaCO2, PaO2, PaO2/FIO2, shunt fraction, D O2) were measured. For the normal dogs,
at catheter flow of 15 L/min; the forward thrust catheter increased carinal pressure and Pao2/FIO2 BY 30% (p<.003) and 105% (p<.005), respectively. The forward thrust catheter reduced Paco2 by 40% (p<.04). The reverse thrust catheter increased PaO2/FIO2 by 102% (p<.001) and decreased pressure and PaCO2 by 44% (p<.001) and 34% (p<.003), respectively. For the injured dogs, at catheter flow rate of 15 L/min, the
forward thrust catheter increased carinal pressure, PaO2, and PaO2/FIO2 by
6% (p<.001), 23% (p<.001), and 24% (p<.02), respectively. The forward thrust catheter reduced PaCO2 by 29% (p<.002). The reverse thrust catheter
increased PaO2 and PaO2/FIO2 both by 11% (p<.02) and reduced carinal pressure and PaCO2 by 23% (p<.001) and 18% (p<.002), respectively.
CONCLUSIONS: Tracheal gas insufflation is capable of improving oxygenation
and ventilation in acute lung injury when combined with high-frequency oscillatory ventilation. The addition of this second gas flow at the level
of the carina raises or lowers distal airway pressure, the magnitude of which is dependent on the direction and rate of gas flow. The beneficial effects of tracheal gas insufflation may be tempered by the long-term effects of altering distal airway pressure; lowering distal airway pressure may lead to atelectasis, whereas raising distal airway pressure may lead to an **auto-positive** end-expiratory pressure (auto-PEEP) effect.

L10 ANSWER 8 OF 33 MEDLINE
ACCESSION NUMBER: 95044344 MEDLINE
DOCUMENT NUMBER: 95044344 PubMed ID: 7956282
TITLE: Hemodynamic responses to external counterbalancing of **auto-positive** end-expiratory pressure in mechanically ventilated patients with chronic obstructive pulmonary disease.
COMMENT: Comment in: Crit Care Med. 1994 Nov;22(11):1714-7
AUTHOR: Baigorri F; de Monte A; Blanch L; Fernandez R; Valles J; Mestre J; Saura P; Artigas A
CORPORATE SOURCE: Intensive Care Service, Hospital de Sabadell, Barcelona, Spain.
SOURCE: CRITICAL CARE MEDICINE, **(1994 Nov)** 22 (11) 1782-91.
Journal code: DTF; 0355501. ISSN: 0090-3493.
PUB. COUNTRY: United States
Journal; Article; (JOURNAL ARTICLE)
LANGUAGE: English
FILE SEGMENT: Abridged Index Medicus Journals; Priority Journals
ENTRY MONTH: 199411
ENTRY DATE: Entered STN: 19950110
Last Updated on STN: 19950110
Entered Medline: 19941130
AB OBJECTIVE: To study the effect of positive end-expiratory pressure (PEEP) on right ventricular hemodynamics and ejection fraction in patients with chronic obstructive pulmonary disease and positive alveolar pressure throughout expiration by dynamic hyperinflation (auto-PEEP). DESIGN: Open,
prospective, controlled trial. SETTING: General intensive care unit of a community hospital. PATIENTS: Ten patients sedated and paralyzed with an

acute exacerbati[redacted] of chronic obstructive pulmona[redacted] disease undergoing mechanical venti[redacted]ion. INTERVENTIONS: Insertion [redacted]a pulmonary artery catheter modified with a rapid response thermistor and a radial arterial catheter. PEEP was then increased from 0 (PEEP 0) to auto-PEEP level (PEEP = auto-PEEP) and 5 cm H2O above that (PEEP = auto-PEEP +5). MEASUREMENTS: At each level of PEEP, airway pressures, flow and volume, hemodynamic variables (including right ventricular ejection fraction by thermodilution technique), and blood gas analyses were recorded. MAIN RESULTS: The mean auto-PEEP was 6.6 +/- 2.8 cm H2O and the total PEEP reached was 12.2 +/- 2.4 cm H2O. The degree of lung inflation induced by PEEP averaged 145 +/- 87 mL with PEEP = auto-PEEP and 495 +/- 133 mL with PEEP = auto-PEEP + 5. The PEEP = auto-PEEP caused a right ventricular end-diastolic pressure increase, but there was no other significant hemodynamic change. With PEEP = auto-PEEP + 5, there was a significant increase in intravascular pressures; this amount of PEEP reduced cardiac output (from 4.40 +/- 1.38 L/min at PEEP 0 to 4.13 +/- 1.48 L/min; $p < .05$). The cardiac output reduction induced by PEEP = auto-PEEP + 5 was > 10% in only five cases and this group of patients had significantly lower right ventricular volumes than the group with less cardiac output variation (right ventricular end-diastolic volume: 64 +/- 9 vs. 96 +/- 26 mL/m2; right ventricular end-systolic volume: 38 +/- 6 vs. 65 +/- 21 mL/m2; $p < .05$) without significant difference in the other variables that were measured. Neither right ventricular ejection fraction nor right ventricle volumes changed as PEEP increased, but there were marked interpatient differences and also pronounced changes in volume between stages in individual patients. CONCLUSIONS: In the study conditions, PEEP application up to values approaching auto-PEEP did not result in the impairment of right ventricular hemodynamics, while higher levels reduced cardiac output in selected patients.

L10 ANSWER 9 OF 33 MEDLINE
ACCESSION NUMBER: 95006754 MEDLINE
DOCUMENT NUMBER: 95006754 PubMed ID: 7922433
TITLE: A historical perspective on ventilator management.
AUTHOR: Shapiro B A
CORPORATE SOURCE: Department of Anesthesia, Northwestern University Medical School, Chicago IL.
SOURCE: NEW HORIZONS, **(1994 Feb)** 2 (1) 8-18. Ref: 118
Journal code: B45; 9416195. ISSN: 1063-7389.
PUB. COUNTRY: United States
Historical
Journal; Article; (JOURNAL ARTICLE)
General Review; (REVIEW)
(REVIEW LITERATURE)
LANGUAGE: English
FILE SEGMENT: Priority Journals
ENTRY MONTH: 199411
ENTRY DATE: Entered STN: 19941222
Last Updated on STN: 19941222
Entered Medline: 19941108

AB Paralysis via neuromuscular blockade in ICU patients requires mechanical ventilation. This review historically addresses the technological advances and scientific information upon which ventilatory management concepts are based, with special emphasis on the influence such concepts have had on the use of neuromuscular blocking agents. Specific reference is made to the scientific information and technological advances leading to the newer concepts of ventilatory management. Information from > 100 major studies in the peer-reviewed medical literature, along with the author's 25 yrs of clinical experience and academic involvement in acute respiratory care is presented. Nomenclature related to ventilatory management is specifically defined and consistently utilized to present and interpret the data.

Pre-1970 ventilatory management is traced from the clinically unacceptable pressure-limited devices to the reliable performance of volume-limited ventilators. The scientific data and rationale that led to the concept of relatively large tidal volume delivery are reviewed in the light of today's concerns regarding alveolar overdistention, control-mode dyssynchrony, and **auto-positive** end-expiratory pressure. Also presented are the post-1970 scientific rationales for continuous positive airway pressure/positive end-expiratory pressure therapy, avoidance of alveolar hyperxia, and partial ventilatory support techniques (intermittent mandatory ventilation/synchronized intermittent mandatory ventilation). The development of pressure-support devices is discussed and the capability of pressure-control techniques is presented. The rationale for more recent concepts of total ventilatory support to avoid ventilator-induced lung injury is presented. The traditional techniques utilizing volume-preset ventilators with relatively large tidal volumes remain valid and desirable for the vast majority of patients requiring mechanical ventilation. Neuromuscular blockade is best avoided in these patients. However, adequate analgesia, amnesia, and sedation are required. For patients with severe lung disease, alveolar overdistention and hyperoxia should be avoided and may be best accomplished by total ventilatory support techniques, such as pressure control. Total ventilatory support requires neuromuscular blockade and may not provide eucapnic ventilation.

L10 ANSWER 10 OF 33 MEDLINE
ACCESSION NUMBER: 94284401 MEDLINE
DOCUMENT NUMBER: 94284401 PubMed ID: 8014286
TITLE: Comparison of one versus two bronchodilators in ventilated COPD patients.
AUTHOR: Fernandez A; Munoz J; de la Calle B; Alia I; Ezpeleta A; de la Cal M A; Reyes A
CORPORATE SOURCE: Servicio de Cuidados Intensivos, Hospital Universitario de Getafe, Madrid, Spain.
SOURCE: INTENSIVE CARE MEDICINE, **(1994)** 20 (3) 199-202.
Journal code: H2J; 7704851. ISSN: 0342-4642.
PUB. COUNTRY: United States
(CLINICAL TRIAL)
Journal; Article; (JOURNAL ARTICLE)
(RANDOMIZED CONTROLLED TRIAL)
LANGUAGE: English
FILE SEGMENT: Priority Journals
ENTRY MONTH: 199407
ENTRY DATE: Entered STN: 19940810
Last Updated on STN: 19970203
Entered Medline: 19940726

AB OBJECTIVE: To compare the bronchodilating effect of a single drug, ipratropium bromide (IBr), with that of its combination with fenoterol (IBr+F). DESIGN: The study was triple blind and randomized. SETTING: Medical-surgical intensive care unit. PATIENTS: 12 patients with acute exacerbation of chronic obstructive pulmonary disease (COPD) requiring mechanical ventilation for severe respiratory failure. INTERVENTIONS: Before administering each drug, peak airway pressure (Ppeak), end inspiratory pressure (Pei), resistive pressure (Pres), and **auto positive**--end expiratory pressure (auto-PEEP) were measured. Inspiratory system resistance (Rins) and dynamic respiratory system compliance (C) were calculated. Arterial pH and blood gas determinations were made. These measurements were repeated 60 min after administration of each therapeutic regimen. For ipratropium bromide alone the dose was 0.04 mg. When the combination of drugs was used, the doses were 0.04 mg for ipratropium bromide and 0.1 mg for fenoterol. MEASUREMENTS AND RESULTS: With the combination of both drugs, all the pressures in the airway, as well as the auto-PEEP and the Rins were significantly reduced ($p < 0.05$) with respect to baseline values. With ipratropium bromide alone, no significant changes were observed either in the pressures or in the inspiratory resistance. No significant changes were observed either in the

pH or blood gas[redacted] with any of the treatments. The[redacted]ombination of both drugs produced [redacted]nificantly reduction in Pei an[redacted]uto-PEEP when compared with ipratropium bromide alone. CONCLUSIONS: The combination of both drugs is more effective than ipratropium bromide alone at the doses used in this study.

L10 ANSWER 11 OF 33 MEDLINE
ACCESSION NUMBER: 94153668 MEDLINE
DOCUMENT NUMBER: 94153668 PubMed ID: 8110544
TITLE: On-line expiratory flow-volume curves during thoracic surgery: occurrence of auto-PEEP.
AUTHOR: Bardoczky G; d'Hollander A; Yernault J C; Van Meuylem A; Moures J M; Rocmans P
CORPORATE SOURCE: Department of Anesthesiology, Erasme University Hospital, Free University of Brussels, Belgium.
SOURCE: BRITISH JOURNAL OF ANAESTHESIA, **(1994 Jan)** 72 (1) 25-8.
Journal code: AUO; 0372541. ISSN: 0007-0912.
PUB. COUNTRY: ENGLAND: United Kingdom
Journal; Article; (JOURNAL ARTICLE)
LANGUAGE: English
FILE SEGMENT: Priority Journals
ENTRY MONTH: 199403
ENTRY DATE: Entered STN: 19940406
Last Updated on STN: 19940406
Entered Medline: 19940331

AB Flow-volume loops were monitored continuously in 39 patients undergoing thoracic surgery requiring one-lung ventilation. In 26 of the 39 patients (67%), **auto-positive** end-expiratory pressure (auto-PEEP) was seen on the flow-volume curves during both two-lung and one-lung ventilation. Eighty-seven percent of the patients whose trachea was intubated with a smaller size (35- and 37-French gauge) double-lumen tracheal tube exhibited auto-PEEP, compared with patients in whom the tube used was larger (39- or 41-French gauge: 54% and 50%, respectively). Before operation, mean airway resistance was significantly greater in patients who exhibited auto-PEEP during anaesthesia (2.4 cm H2O litre-1 s) than in patients without auto-PEEP (1.7 cm H2O litre-1 s).

L10 ANSWER 12 OF 33 MEDLINE
ACCESSION NUMBER: 94101911 MEDLINE
DOCUMENT NUMBER: 94101911 PubMed ID: 8275734
TITLE: Relationship between expired capnogram and respiratory system resistance in critically ill patients during total ventilatory support.
AUTHOR: Blanch L; Fernandez R; Saura P; Baigorri F; Artigas A
CORPORATE SOURCE: Intensive Care Service, Hospital de Sabadell, Barcelona, Spain.
SOURCE: CHEST, **(1994 Jan)** 105 (1) 219-23.
Journal code: D1C; 0231335. ISSN: 0012-3692.
PUB. COUNTRY: United States
Journal; Article; (JOURNAL ARTICLE)
LANGUAGE: English
FILE SEGMENT: Abridged Index Medicus Journals; Priority Journals
ENTRY MONTH: 199402
ENTRY DATE: Entered STN: 19940218
Last Updated on STN: 19940218
Entered Medline: 19940210

AB To examine the relationship of expired capnograms and respiratory system resistance (Rrs) in intubated critically ill patients, we consecutively studied 41 mechanically ventilated patients to (1) analyze the association between expired CO2 slope and **auto-positive** end-expiratory pressure (auto-PEEP), between Rrs and auto-PEEP, between Rrs and expired CO2 slope, and between Rrs and arterial minus end-tidal PCO2 gradient (PaCO2-PETCO2 gradient) and (2) to investigate the capacity

of the expired CO2 slope and PaCO2-PETCO2 gradient to predict Rrs during mechanical ventilation. Regression analysis found close correlation between Rrs and expired CO2 slope ($r = 0.86$; $p < 0.001$), between Rrs and auto-PEEP ($r = 0.75$; $p < 0.001$), and between auto-PEEP and expired CO2 slope ($r = 0.74$; $p < 0.001$). Weak correlation was found between Rrs and PaCO2-PETCO2 gradient ($r = 0.48$; $p < 0.01$). Prediction interval limits at 95 percent confidence level for Rrs are approximately +/- 7.39 cm H2O/L/s from the predicted value obtained by the regression equation, where Rrs = 11.42 + 2.28 expired CO2 slope. These observations suggest that CO2 elimination in critically ill patients is strongly modulated by lung, airway, endotracheal tube, and ventilator equipment resistances. Although continuous capnogram waveform monitoring at the bedside might be useful to assess Rrs, very accurate predictions could be done only in determinate patients.

L10 ANSWER 13 OF 33 MEDLINE
ACCESSION NUMBER: 91337581 MEDLINE
DOCUMENT NUMBER: 91337581 PubMed ID: 1873115
TITLE: Auto-PEEP: an impediment to weaning in the chronically ventilated patient.
AUTHOR: Geisman L K; Ahrens T
SOURCE: AACN CLINICAL ISSUES IN CRITICAL CARE NURSING, **(1991 Aug)** 2 (3) 391-7.
Journal code: ATW; 9009969. ISSN: 1046-7467.
PUB. COUNTRY: United States
Journal; Article; (JOURNAL ARTICLE)
LANGUAGE: English
FILE SEGMENT: Nursing Journals
ENTRY MONTH: 199109
ENTRY DATE: Entered STN: 19911013
Last Updated on STN: 19911013
Entered Medline: 19910926

AB **Auto-positive** end expiratory pressure (auto-PEEP) is a physiologic event that is a recently recognized phenomenon common to mechanically ventilated patients. Auto-PEEP occurs when forces exist that limit expiration and the subsequent elimination of positive pressure from the lungs. If positive pressure is retained, a potential reduction in cardiac output and increase in complications from barotrauma arise. Because of possible physiologic problems associated with it, auto-PEEP can potentially interfere with weaning from mechanical ventilation. Nursing measures that can reduce the effect of auto-PEEP during weaning are centered on improving the inspiratory/expiratory flow patterns. These efforts include manipulating mechanical ventilator settings and reducing causes of increased respiratory rates (e.g., pain and anxiety). Since auto-PEEP was only recently identified as a potential impediment to weaning from mechanical ventilation, the nurse must be aware of the need to assess for the presence of auto-PEEP in these patients.

L10 ANSWER 14 OF 33 MEDLINE
ACCESSION NUMBER: 90120289 MEDLINE
DOCUMENT NUMBER: 90120289 PubMed ID: 2136979
TITLE: Bronchodilators in patients with chronic obstructive pulmonary disease on mechanical ventilation. Utilization of metered-dose inhalers.
AUTHOR: Fernandez A; Lazaro A; Garcia A; Aragon C; Cerda E
CORPORATE SOURCE: Servicio de Cuidados Intensivos, Hospital Central de la Cruz Roja, Madrid, Spain.
SOURCE: AMERICAN REVIEW OF RESPIRATORY DISEASE, **(1990 Jan)** 141 (1) 164-8.
Journal code: 426; 0370523. ISSN: 0003-0805.
PUB. COUNTRY: United States
Journal; Article; (JOURNAL ARTICLE)
LANGUAGE: English
FILE SEGMENT: Abridged Index Medicus Journals; Priority Journals
ENTRY MONTH: 199002
ENTRY DATE: Entered STN: 19900328

Last Updated on STN: 19900328
Entered Medline: 19900222

AB Bronchodilators are used widely in the acute exacerbations of chronic obstructive pulmonary disease (COPD), although their effectiveness is not clearly established. We used three bronchodilators in 20 patients with COPD who were being mechanically ventilated. Two of the bronchodilators, ipratropium bromide and salbutamol, were administered from metered-dose inhalers (MDI) through an adapter to the endotracheal tube, and the third, aminophylline, was administered in the form of intravenous infusion. Before administering each drug, peak airway pressure, end-inspiratory pressure, resistive pressure, and **auto positive** end-expiratory pressure (auto-PEEP) were measured, and inspiratory resistance (Rins) and compliance were calculated. Heart rate (HR) and blood pressure were also recorded, and arterial pH and blood gas determinations were made. These measurements were repeated 60 min after the administration of aminophylline, 15 and 60 min after administering salbutamol, and 30 and 60 min after administering ipratropium bromide. With these three drugs, airway pressures were reduced, as well as auto-PEEP and Rins, with respect to basal values (p less than 0.05). The changes in compliance were only significant with salbutamol (p less than 0.05). HR was only significantly modified with aminophylline (p less than 0.05). No blood gas change was observed with any of the three drugs. It can be concluded that: (1) the three drugs used in this study were equally effective in producing significant bronchodilation in patients on mechanical ventilation for severe acute exacerbation of COPD; (2) the administration of bronchodilators by MDI in intubated patients through a special adapter was as effective as the intravenous administration of aminophylline.

L10 ANSWER 15 OF 33 MEDLINE

ACCESSION NUMBER: 90008565 MEDLINE
DOCUMENT NUMBER: 90008565 PubMed ID: 2676950
TITLE: Determinants and limits of pressure-preset ventilation: a mathematical model of pressure control.
AUTHOR: Marini J J; Crooke P S 3rd; Truwit J D
CORPORATE SOURCE: Division of Pulmonary and Critical Care Medicine, University of Minnesota, Minneapolis 55101.
CONTRACT NUMBER: HL-07123 (NHLBI)
HL-19153 (NHLBI)
SOURCE: JOURNAL OF APPLIED PHYSIOLOGY, **(1989 Sep)** 67 (3) 1081-92.
Journal code: HEG; 8502536. ISSN: 8750-7587.
PUB. COUNTRY: United States
Journal; Article; (JOURNAL ARTICLE)
LANGUAGE: English
FILE SEGMENT: Priority Journals
ENTRY MONTH: 198911
ENTRY DATE: Entered STN: 19900328
Last Updated on STN: 19970203
Entered Medline: 19891121

AB In recent years, four square-wave modes of pressure-preset mechanical ventilation (PPV)--pressure control, pressure support, inverse ratio, and airway pressure release ventilation--have been introduced to clinical practice. Conceptually, they share important features. Yet, because there remains widespread uncertainty regarding their ventilatory characteristics, efficacy, and appropriate use, the potential range of application is only now being investigated. To construct a unifying mathematical model of PPV, we developed a system of equations for prediction of the major "outcome" variables of PPV--tidal volume, minute ventilation, **auto-positive** end-expiratory pressure, mean alveolar pressure, and mechanical work--from the primary clinical "inputs" from patient (resistance, compliance) and clinician (applied pressure, frequency, inspiratory time fraction). Our analysis revealed distinct bounding limits for the outcome variables of ventilation and pressure and important implications for their clinical determinants. Although simplifying assumptions were required to enable construction of this mathematical analogue of respiratory system behavior, this model

provides a firm conceptual framework for understanding the physiological interactions between PPV and the patients they are intended to help.

L10 ANSWER 16 OF 33 BIOSIS COPYRIGHT 2001 BIOSIS
ACCESSION NUMBER: 1999:129027 BIOSIS
DOCUMENT NUMBER: PREV199900129027
TITLE: Auto-peep calculation based on lungs mechanics simulation during pressure controlled ventilation.
AUTHOR(S): Michnikowski, M. (1); Darowski, M. (1); Slugocki, P.; Grabowski, J.; Rondio, Z.
CORPORATE SOURCE: (1) Inst. Biocybernetics Biomed. Eng., Polish Acad. Sci., Warsaw Poland
SOURCE: European Respiratory Journal, (**Sept., 1998**) Vol. 12, No. SUPPL. 28, pp. 146S.
Meeting Info.: European Respiratory Society Annual Congress
Geneva, Switzerland September 19-23, 1998 The European Respiratory Society
. ISSN: 0903-1936.
DOCUMENT TYPE: Conference
LANGUAGE: English

L10 ANSWER 17 OF 33 BIOSIS COPYRIGHT 2001 BIOSIS
ACCESSION NUMBER: 1995:541771 BIOSIS
DOCUMENT NUMBER: PREV199598556071
TITLE: The effects of applied vs auto-PEEP on local lung unit pressure and volume in a four-unit lung model.
AUTHOR(S): Kacmarek, Robert M. (1); Kirmse, Max; Nishimura, Masaji; Mang, Harald; Kimball, William R.
CORPORATE SOURCE: (1) Respiratory Care, Ellison 401, 32 Fruit Street, Massachusetts Gen. Hosp., Boston, MA 02114 USA
SOURCE: Chest, (1995) Vol. 108, No. 4, pp. 1073-1079.
ISSN: 0012-3692.
DOCUMENT TYPE: Article
LANGUAGE: English
AB Background: The application of positive end-expiratory pressure (PEEP) and maintenance of increased mean airway pressure (MAP) has been associated with improved oxygenation in adult respiratory distress syndrome. Recently, attention has been directed toward elevating MAP by establishing auto-PEEP when ventilating with an inverse inspiratory to expiratory ratio in opposition to applied PEEP. We theorized that FRC distribution and local lung unit end-expiratory pressure (EEP) would be different when equal levels of PEEP were established by applying PEEP or by producing auto-PEEP. Methods: Using a four-chamber lung model with each chamber having a different time constant (TC), we applied equal levels of applied PEEP (I:E ratio 1:3) and auto-PEEP (I:E ratio 3: 1) and evaluated local lung unit EEP and end expiratory lung volume (EELV). Results: During all trials with applied PEEP, local lung unit EEP was equal to applied PEEP, whereas during auto-PEEP local EEP differed (p lt 0.01). At a tracheal auto-PEEP level of 12.7 cm H-2O, the lung unit with the longest TC (slow lung unit) had an EEP of 15.8 cm H-2O, while the shortest TC unit (fast lung unit) had an EEP of 10.1 cm H-2O (P lt 0.01). Similarly, local EELVs were more maldistributed with auto-PEEP than with applied PEEP. At a tracheal PEEP level of 12.7 cm H-2O, the EELV increase in the slow lung unit with auto-PEEP was 1,054 mL vs 918 with applied PEEP (p lt 0.01), whereas the fast lung unit's EELV increase with auto-PEEP was 142 mL compared with 212 mL with applied PEEP (p lt 0.01). Conclusion: Comparing equal levels of auto-PEEP with applied PEEP, a greater maldistribution of local lung unit EEP and EELV was established with the anto-PEEP. During auto-PEEP, the greatest EEP and EELV occurred in the slow lung unit, and the lowest EEP and EELV developed in the fast lung unit.

L10 ANSWER 18 OF 33 BIOSIS COPYRIGHT 2001 BIOSIS
ACCESSION NUMBER: 1995:150385 BIOSIS
DOCUMENT NUMBER: PREV199598164685
TITLE: The effects of external PEEP on hyperinflation and

to-PEEP in anesthetized patients with COPD.
AUTHOR(S): hitvejpaisal, P.; Joshi, G. P. hite, P. F.
CORPORATE SOURCE: Dep. Anesthesiol. Pain Management, Univ. Texas Southwestern
Med. Cent., Dallas, TX USA
SOURCE: Anesthesia & Analgesia, (1995) Vol. 80, No. 2 SUPPL., pp. S528.
Meeting Info.: 69th Clinical and Scientific Congress of the
International Anesthesia Research Society Honolulu, Hawaii March 10-14, 1995
ISSN: 0003-2999.
DOCUMENT TYPE: Conference
LANGUAGE: English

L10 ANSWER 19 OF 33 BIOSIS COPYRIGHT 2001 BIOSIS
ACCESSION NUMBER: 1994:386599 BIOSIS
DOCUMENT NUMBER: PREV199497399599
TITLE: Life-threatening hypotension associated with emergency intubation and the initiation of mechanical ventilation.
AUTHOR(S): Franklin, Cory (1); Samuel, Jacob; Hu, Tzyy-Chyn
CORPORATE SOURCE: (1) Critical Care Med., Ward 15/MICU, Cook County Hosp., 1835 W. Harrison St., Chicago, IL 60612 USA
SOURCE: American Journal of Emergency Medicine, (1994) Vol. 12, No.
4, pp. 425-428.
ISSN: 0735-6757.
DOCUMENT TYPE: Article
LANGUAGE: English
AB To determine the incidence of life-threatening hypotension (LTH) suffered by patients in the initial hours after emergency intubation and mechanical ventilation, prospective, consecutive case series of patients undergoing endotracheal intubation and mechanical ventilation were evaluated in the adult emergency department of a large urban hospital. Eighty-four medical patients who received intubation and mechanical ventilation for ventilatory failure, respiratory failure, or airway protection (trauma patients excluded) were included. LTH, defined as a decrease in mean arterial pressure of 60 mm Hg or an absolute decrease to a systolic blood pressure lt 80 mm Hg in the first 2 hours after intubation, was observed in 24 of the 84 patients who met study criteria (incidence 28.6%). Eleven patients (incidence 13.1%) required treatment for LTH with vasopressors. There was one cardiac arrest, and there were no deaths. There was a statistically significant association between LTH and hypercarbic (PCO-2 gt 50 mm) chronic obstructive pulmonary disease (COPD) (P = .004). There was also a weaker statistical association between LTH and hypoxemic respiratory failure (P = .019). No association could be established between LTH and the other diagnoses, arterial blood gas (ABG) derangements, or the administration of sedatives or paralytic medications.
LTH represents a serious complication of emergency intubation in the initial phase of mechanical ventilation. Because it occurs in more one quarter of all cases, it should be anticipated during intubation and the initial phase of ventilator management, especially in high-risk patients such as those with hypercarbic COPD. The cause of LTH is probably multifactorial, and potential mechanisms include preexisting volume depletion, right ventricular compromise, **auto-positive** end-expiratory pressure (PEEP) and catecholamine reduction during CO. washout. The frequency of LTH after intubation has implications for intubation procedures, ABG monitoring, ventilator adjustment, and fluid and vasopressor resuscitation.

L10 ANSWER 20 OF 33 BIOSIS COPYRIGHT 2001 BIOSIS
ACCESSION NUMBER: 1993:398518 BIOSIS
DOCUMENT NUMBER: PREV199345057343
TITLE: Pressure-controlled inverse ratio ventilation in severe respiratory failure.
AUTHOR(S): Bein, T.; Metz, C.; Eberl-Lehmann, P.; Taeger, K.
CORPORATE SOURCE: Klink Anaesthesiologie, Klinikum Univ. Regensburg,

SOURCE: [redacted]nz-Josef-Strauss-Allee 11, W-84[redacted] Regensburg
[redacted]ensivmedizin und Notfallmedizi[redacted] (1993) Vol. 30, No. 3, pp. 73-78.
ISSN: 0175-3851.
DOCUMENT TYPE: Article
LANGUAGE: German
SUMMARY LANGUAGE: German; English

L10 ANSWER 21 OF 33 BIOSIS COPYRIGHT 2001 BIOSIS
ACCESSION NUMBER: 1993:216867 BIOSIS
DOCUMENT NUMBER: PREV199344101367
TITLE: Inverse ratio ventilation in ARDS: Improved oxygenation without autoPEEP.
AUTHOR(S): Manthous, Constantine A.; Schmidt, Gregory A. (1)
CORPORATE SOURCE: (1) 5841 South Maryland, Chicago 60637
SOURCE: Chest, (1993) Vol. 103, No. 3, pp. 953-954.
ISSN: 0012-3692.
DOCUMENT TYPE: Article
LANGUAGE: English

L10 ANSWER 22 OF 33 BIOSIS COPYRIGHT 2001 BIOSIS
ACCESSION NUMBER: 1992:152309 BIOSIS
DOCUMENT NUMBER: BR42:68509
TITLE: TIME-COURSE OF RESPIRATORY MECHANICS AND GAS EXCHANGE DURING MECHANICAL VENTILATION IN A CASE OF NEAR-FATAL ASTHMA.
AUTHOR(S): BLANCH L; FERNANDEZ R; FERRER A; BAIGORRI F; ARTIGAS A
CORPORATE SOURCE: SERVEI DE MEDICINA INTENSIVA, HOSPITAL SABADELL, APARTAT CORREUS 196, E-08208 SABADELL, SPAIN.
SOURCE: Intensive Care Med., (1991) 17 (8), 506-507.
CODEN: ICMED9. ISSN: 0342-4642.
FILE SEGMENT: BR; OLD
LANGUAGE: English

L10 ANSWER 23 OF 33 BIOSIS COPYRIGHT 2001 BIOSIS
ACCESSION NUMBER: 1992:125301 BIOSIS
DOCUMENT NUMBER: BA93:71101
TITLE: THE EFFECT OF **AUTO-POSITIVE** END-EXPIRATORY PRESSURE ON THE ARTERIAL-END-TIDAL CARBON DIOXIDE PRESSURE GRADIENT AND EXPIRED CARBON DIOXIDE SLOPE IN CRITICALLY ILL PATIENTS DURING TOTAL VENTILATORY SUPPORT.
AUTHOR(S): BLANCH L; FERNANDEZ R; ARTIGAS A
CORPORATE SOURCE: SERVEI DE MEDICINA INTENSIVA, HOSP. DE SABADELL, APARTADO DE CORREOS 196, 08208 SABADELL, SPAIN.
SOURCE: J CRIT CARE, (1991) 6 (4), 202-210.
CODEN: JCCAER. ISSN: 0883-9441.
FILE SEGMENT: BA; OLD
LANGUAGE: English
AB To examine the effect of **auto-positive** end-expiratory pressure (autoPEEP) on the estimation of arterial carbon dioxide pressure (PaCO2) from end-tidal carbon dioxide pressure (PetCO2) during changes in minute ventilation (MV), we studied 24 consecutive sedated and paralyzed patients under controlled mechanical ventilation for acute respiratory failure. The patients were grouped according to whether they had autoPEEP:
group I (n = 11) comprised non-autoPEEP patients and group II (n = 13) comprised autoPEEP patients. Patients were randomly ventilated at three different levels of MV: normal MV (basal tidal volume), high MV (tidal volume 2.5 mL/kg above basal), and low MV (tidal volume 2.5 mL/kg below basal). Respiratory rate and inspiration to expiration ratio were kept constant during the study. In each condition, we measured arterial blood gases, expiratory capnograms, airway pressure, and autoPEEP. We determined
PaCO2-PetCO2 gradient, predicted PaCO2 (Pa'CO2) [Pa'CO2 = PetCO2 for each condition + (PaCO2-PetCO2 gradient at normal MV)], and expired CO2 slope. The PaCO2-PetCO2 gradient only remained stable in group I (mean values for
low, normal, and high MV were 3.3, 3.3, and 3.5 mm Hg, respectively),

while group II showed a significant difference during low MV (12.2 mm Hg) when compared with normal MV (8.4 mm Hg; P < .01) and high MV (8.9 mm Hg; P < .05). PaCO2 and PetCO2 showed significant correlations in both groups (r = .92 in group I and .79 in group II). However, Pa'CO2 could only be safely estimated in patients without autoPEEP when the difference between PaCO2 and Pa'CO2 ranged between 1.6 and -1.9 mm Hg. Slopes of expired CO2 greater than 3 mm Hg/s identified patients with autoPEEP of 89% sensitivity, 93% specificity, 94% positive predictive power, and 95% accuracy. A significant correlation was found between autoPEEP and expired CO2 slope (r = .70; P < .001), between autoPEEP and PaCO2-PetCO2 gradient (r = .46; P < .001), and between CO2 expired slope and PaCO2-PetCO2 gradient (r = .74; P < .001). These results indicate that in patients with acute respiratory failure under controlled mechanical ventilation, the presence of autoPEEP is associated with inaccuracy in the calculation of predicted PaCO2 from PetCO2 after changes in MV at fixed respiratory rates.

L10 ANSWER 24 OF 33 BIOSIS COPYRIGHT 2001 BIOSIS
ACCESSION NUMBER: 1991:333475 BIOSIS
DOCUMENT NUMBER: BR41:30025
TITLE: THE IMPACT OF AUTOPEEP ON THE CAPNOGRAM IN PATIENTS WITH ACUTE RESPIRATORY FAILURE DURING TOTAL VENTILATORY SUPPORT.
AUTHOR(S): BLANCH L; FERNANDEZ F; ARTIGAS A
CORPORATE SOURCE: SERVEI DE MEDICINA INTENSIVA, HOSP. DE SABADELL, UNIVERSITAT AUTONOMA DE BARCELONA, APARTADO CORREOS 196. 08208 SABADELL, SPAIN.
SOURCE: INTERNATIONAL CONFERENCE OF THE AMERICAN LUNG ASSOCIATION AND THE AMERICAN THORACIC SOCIETY, ANAHEIM, CALIFORNIA, USA, MAY 12-15, 1991. AM REV RESPIR DIS, (1991) 143 (4 PART 2), A485.
CODEN: ARDSBL. ISSN: 0003-0805.
DOCUMENT TYPE: Conference
FILE SEGMENT: BR; OLD
LANGUAGE: English

L10 ANSWER 25 OF 33 BIOSIS COPYRIGHT 2001 BIOSIS
ACCESSION NUMBER: 1990:455571 BIOSIS
DOCUMENT NUMBER: BA90:106211
TITLE: EFFECT OF NASAL-CPAP ON PATIENTS WITH CHRONIC OBSTRUCTIVE PULMONARY DISEASE.
AUTHOR(S): LIM T K
CORPORATE SOURCE: DEP. MED., NATL. UNIV. HOSP., LOWER KENT RIDGE RD., SINGAPORE 0511.
SOURCE: SINGAPORE MED J, (1990) 31 (3), 233-237.
CODEN: SIMJA3. ISSN: 0037-5675.
FILE SEGMENT: BA; OLD
LANGUAGE: English
AB Patients with chronic obstructive pulmonary disease [COPD] breath at large lung volumes because of dynamic hyperinflation. Their end-tidal lung volumes will then be much above the equilibrium position of the respiratory system and the elastic recoil pressure would be above zero at end-tidal exhalation. This auto or intrinsic positive end-expiratory pressure [auto-PEEP] contributes to the elastic work of inspiration and the sensation of dyspnoea. The purpose of this study was to offset the auto-PEEP in patients with exacerbated chronic airflow obstruction by applying continuous positive airway pressure via the nose [nasal-CPAP]. Nine out of 14 patients experienced alleviation of dyspnoea while on nasal-CPAP [4 to 8 cmH2O]. These 9 patients had significantly more severe hyperinflation than the 5 patients who did not respond positively to nasal-CPAP. While there is a complex relationship between intrinsic and extrinsically applied PEEP in patients with COPD, the result of this study is consistent with the notion that CPAP may alleviate dyspnoea by reducing auto-PEEP, improving lung mechanics and unloading the inspiratory

muscles. Nasal [redacted]AP may have a potential therape[redacted]ic role in exacerbations of COPD.

L10 ANSWER 26 OF 33 BIOSIS COPYRIGHT 2001 BIOSIS
ACCESSION NUMBER: 1989:500596 BIOSIS
DOCUMENT NUMBER: BR37:110255
TITLE: PRESSURE SUPPORT VENTILATION PSV REVERSES HYPERINFLATION INDUCED ISORHYTHMIC A-V DISSOCIATION.
AUTHOR(S): CONTI G; BUFI M; ANTONELLI M; ROCCO M; GASPARETTO A
CORPORATE SOURCE: UNIV. "LA SAPIENZA" ROMA, IST. ANESTESIOLOGIA RIANIMAZIONE, VIALE DEL POLICLINICO 155, I-00161 ROMA, ITALY.
SOURCE: Intensive Care Med., (1989) 15 (5), 319-321. CODEN: ICMED9. ISSN: 0342-4642.
FILE SEGMENT: BR; OLD
LANGUAGE: English

L10 ANSWER 27 OF 33 BIOSIS COPYRIGHT 2001 BIOSIS
ACCESSION NUMBER: 1987:53915 BIOSIS
DOCUMENT NUMBER: BR32:24136
TITLE: RELATIONSHIP OF ENDOTRACHEAL TUBE SIZE TO **AUTO-POSITIVE** END-EXPIRATORY PRESSURE AT HIGH MINUTE VENTILATION.
AUTHOR(S): SCOTT L R; BENSON M S; BISHOP M J
CORPORATE SOURCE: DEPARTMENT OF RESPIRATORY CARE, ZA-68, HARBORVIEW MEDICAL CENTER, 325 NINTH AVE., SEATTLE, WASHINGTON 98104.
SOURCE: Respir. Care, (1986) 31 (11), 1080-1082. CODEN: RECACP.
FILE SEGMENT: BR; OLD
LANGUAGE: English

L10 ANSWER 28 OF 33 BIOSIS COPYRIGHT 2001 BIOSIS
ACCESSION NUMBER: 1987:53914 BIOSIS
DOCUMENT NUMBER: BR32:24135
TITLE: EFFECT OF INSPIRATORY FLOWRATE AND CIRCUIT COMPRESSIBLE VOLUME ON **AUTO-POSITIVE** END-EXPIRATORY PRESSURE DURING MECHANICAL VENTILATION.
AUTHOR(S): SCOTT L R; BENSON M S; PIERSON D J
CORPORATE SOURCE: 325 NINTH AVE., ZA-62, SEATTLE, WASHINGTON 98104.
SOURCE: Respir. Care, (1986) 31 (11), 1075-1079. CODEN: RECACP.
FILE SEGMENT: BR; OLD
LANGUAGE: English

L10 ANSWER 29 OF 33 BIOSIS COPYRIGHT 2001 BIOSIS
ACCESSION NUMBER: 1987:53913 BIOSIS
DOCUMENT NUMBER: BR32:24134
TITLE: **AUTO-POSITIVE** END-EXPIRATORY PRESSURE IS COMMON IN MECHANICALLY VENTILATED PATIENTS A STUDY OF INCIDENCE SEVERITY AND DETECTION.
AUTHOR(S): BROWN D G; PIERSON D J
CORPORATE SOURCE: HARBORVIEW MEDICAL CENTER, ZA-62, 325 NINTH AVE., SEATTLE, WASHINGTON 98104.
SOURCE: Respir. Care, (1986) 31 (11), 1069-1074. CODEN: RECACP.
FILE SEGMENT: BR; OLD
LANGUAGE: English

L10 ANSWER 30 OF 33 BIOSIS COPYRIGHT 2001 BIOSIS
ACCESSION NUMBER: 1987:14927 BIOSIS
DOCUMENT NUMBER: BR32:5060
TITLE: THE EFFECT OF POSITIVE END-EXPIRATORY PRESSURE ON **AUTO-POSITIVE** END-EXPIRATORY PRESSURE.
AUTHOR(S): SMITH T C; MARINI J J; LAMB V J
CORPORATE SOURCE: VANDERBILT UNIV., NASHVILLE, TN.
SOURCE: 52ND ANNUAL SCIENTIFIC ASSEMBLY OF THE AMERICAN COLLEGE OF CHEST PHYSICIANS, SAN FRANCISCO, CALIF., USA, SEPT. 22-26, 1986. CHEST, (1986) 89 (6 SUPPL), 443S.

CODEN: CHETBF. ISSN: 0012-3692.
DOCUMENT TYPE: Conference
FILE SEGMENT: BR; OLD
LANGUAGE: English

L10 ANSWER 31 OF 33 BIOSIS COPYRIGHT 2001 BIOSIS
ACCESSION NUMBER: 1984:145101 BIOSIS
DOCUMENT NUMBER: BR27:61593
TITLE: EFFECT OF CONTINUOUS POSITIVE AIRWAY PRESSURE CONTROLLED MECHANICAL VENTILATION AND **AUTO POSITIVE** END EXPIRATORY PRESSURE ON EXPIRATORY TIME AND FLOW COMPONENTS.
AUTHOR(S): SACKNER M A; LANG E; GRENVIK S
CORPORATE SOURCE: DIV. PULM. DIS., MT. SINAI MED. CTR., MIAMI BEACH, FL 33140.
SOURCE: 80TH ANNUAL MEETING OF THE AMERICAN LUNG ASSOCIATION, 79TH ANNUAL MEETING OF THE AMERICAN THORACIC SOCIETY, AND 72ND ANNUAL MEETING OF THE CONGRESS OF LUNG ASSOCIATION STAFF, MIAMI BEACH, FLA., USA, MAY. 20-23, 1984. AM REV RESPIR DIS, (1984) 129 (4 SUPPL), A252.
CODEN: ARDSBL. ISSN: 0003-0805.
DOCUMENT TYPE: Conference
FILE SEGMENT: BR; OLD
LANGUAGE: English

L10 ANSWER 32 OF 33 BIOSIS COPYRIGHT 2001 BIOSIS
ACCESSION NUMBER: 1984:138536 BIOSIS
DOCUMENT NUMBER: BR27:55028
TITLE: INDUCTION OF **AUTO POSITIVE** END EXPIRATORY PRESSURE IN NORMAL SUBJECTS.
AUTHOR(S): LANG E; GRENVIK S; SACKNER M A
CORPORATE SOURCE: DIV. PULMONARY DISEASE, MOUNT SINAI MED. CENT., MIAMI BEACH, FLA.
SOURCE: 80TH ANNUAL MEETING OF THE AMERICAN LUNG ASSOCIATION, 79TH ANNUAL MEETING OF THE AMERICAN THORACIC SOCIETY, AND 72ND ANNUAL MEETING OF THE CONGRESS OF LUNG ASSOCIATION STAFF, MIAMI BEACH, FLA., USA, MAY. 20-23, 1984. AM REV RESPIR DIS, (1984) 129 (4 SUPPL), A100.
CODEN: ARDSBL. ISSN: 0003-0805.
DOCUMENT TYPE: Conference
FILE SEGMENT: BR; OLD
LANGUAGE: English

L10 ANSWER 33 OF 33 BIOSIS COPYRIGHT 2001 BIOSIS
ACCESSION NUMBER: 1983:172347 BIOSIS
DOCUMENT NUMBER: BA75:22347
TITLE: OCCULT POSITIVE END EXPIRATORY PRESSURE IN MECHANICALLY VENTILATED PATIENTS WITH AIR FLOW OBSTRUCTION THE **AUTO POSITIVE** END EXPIRATORY PRESSURE EFFECT.
AUTHOR(S): PEPE P E; MARINI J J
CORPORATE SOURCE: RESPIR. DIS. DIV., SEATTLE PUBLIC HEALTH HOSP., 1131 14TH AVE. SOUTH, 1031, SEATTLE, WASH. 98114.
SOURCE: AM REV RESPIR DIS, (1982) 126 (1), 166-170.
CODEN: ARDSBL. ISSN: 0003-0805.
FILE SEGMENT: BA; OLD
LANGUAGE: English
AB Alveolar pressure can remain positive throughout the ventilatory cycle of mechanically-ventilated patients with airflow obstruction, even when positive end-expiratory pressure (PEEP) is not applied intentionally. The increase of intrathoracic pressure associated with this auto-PEEP phenomenon can severely depress cardiac output and elevate the end-expiratory pulmonary artery wedge pressure. Such effects may be exaggerated in patients with chronic obstructive pulmonary disease because abnormally compliant lungs transmit a high fraction of alveolar pressure to intrathoracic vessels. Failure to recognize the hemodynamic consequences of auto-PEEP may lead to inappropriate fluid restriction or unnecessary vasopressor therapy. Although not apparent during normal

ventilator operation, the auto-PEEP effect can be detected and quantified by a simple bedside maneuver: expiratory port occlusion at the end of the set exhalation period.

=> d his

(FILE 'HOME' ENTERED AT 13:16:31 ON 29 MAY 2001)

FILE 'MEDLINE, BIOSIS, BIOTECHNO' ENTERED AT 13:16:43 ON 29 MAY 2001

```
L1         18421 S NF-KAPPA-B
L2        207912 S (POSITIVE FEEDBACK) OR AUTOPOSITIVE OR (AUTO-POSITIVE) OR
AMP
L3           287 S L1 AND L2
L4             0 S L3 AND AUTOPOSITIVE
L5             0 S L3 AND AUTO-POSITIVE
L6            51 S L3 AND POSITIVE
L7            29 DUP REM L6 (22 DUPLICATES REMOVED)
L8            54 S AUTOPOSITIVE OR (AUTO-POSITIVE)
L9            40 DUP REM L8 (14 DUPLICATES REMOVED)
L10           33 S L9 AND PY <1999
```

=> log y

STIC-ILL

From: Brannock, Michael
Sent: Tuesday, May 29, 2001 3:18 PM
To: STIC-ILL
Subject: 09378046

Please provide the following refs:

Whiteway M et al., Molecular and Cellular Biology 14(5)3223-9, 1994

Ji YS et al., Circulation Research 83(3)295-304, 1998

Franchimont N, J. Clinical Investivation 100(7)1797-1803, 1997.

Li, J., et al., Molecular Endocrinology 10(3)252-64, 1996

Thank you,

Michael T. Brannock, Ph.D.
Patent Examiner, AU 1646
Crystal Mall One, 10E18
(703) 306-5876

Hypoxia Induces High-Mobility-Group Protein I(Y) and Transcription of the Cyclooxygenase-2 Gene in Human Vascular Endothelium

Yan-Shan Ji, Qing Xu, John F. Schmedtje, Jr

Abstract—Cyclooxygenases catalyze a rate-limiting step in the synthesis of vascular endothelial prostaglandins. Expression of the inducible cyclooxygenase-2 (COX-2) gene is increased by hypoxia in human vascular endothelial cells via the nuclear factor (NF)-κB p65 transcription factor, which is necessary but not sufficient to fully induce COX-2 transcription in response to hypoxia. After finding that cytoplasmic NF-κB p65 and IκBα (an inhibitory protein that binds NF-κB p65 precursors) levels are not changed by hypoxia, we hypothesized that other factors might play a role in regulating the COX-2 promoter, like the high-mobility-group (HMG) I(Y) family of proteins, which features multiple A·T hooks and is associated with NF-κB–mediated transactivation. Nuclear protein obtained from human umbilical vein endothelial cells (HUVECs) was supplemented with HMG I(Y) during electrophoretic mobility shift assays using an NF-κB-3′ element probe. These data suggested that HMG I(Y) proteins interact with NF-κB p65 to induce COX-2 promoter activity. We also found that TATA-box DNA demonstrated increased electrophoretic shifting indicative of DNA binding after incubation with either hypoxic HUVEC nuclear protein or normoxic nuclear protein supplemented with HMG I(Y). Transfection of HUVECs with an expression vector containing the COX-2 promoter ligated to HMG I(Y) cDNA demonstrated positive feedback on COX-2 promoter activity in hypoxia. We confirmed that COX-2 is transcriptionally regulated by hypoxia using a nuclear runoff assay. Hypoxia increased steady-state cellular levels of HMG I(Y) mRNA as an early event, corresponding with increases in HMG I(Y) protein. Overexpression of HMG I(Y) was associated in a dose-response relationship with increasing prevalence of the COX-2 protein in hypoxic HUVECs. Furthermore, sense (and antisense) HMG I(Y) overexpression caused stimulation (or inhibition) of COX-2 promoter activity as measured by luciferase reporter gene expression. The physiological significance of these findings was demonstrated by cyclooxygenase-dependent release of prostaglandin E_2 by HUVECs in hypoxia. We concluded that hypoxia increases expression of HMG I(Y) proteins while facilitating transactivation of the COX-2 promoter. The HMG I(Y) family of proteins may therefore function as part of a hypoxia-induced enhanceosome that helps to promote transcription of COX-2. (***Circ Res.* 1998;83:295-304.**)

Key Words: endothelium ■ hypoxia ■ HMG I(Y) ■ cyclooxygenase-2 ■ prostaglandin E_2

The high-mobility-group protein family (HMG) I(Y) is a group of nonhistone chromosomal proteins.[1,2] HMG I(Y) binds to A·T-rich regions of DNA with A·T hooks,[3] inducing DNA conformational changes. HMG I(Y) can also regulate the affinity of some transcriptional factors to their DNA-binding elements while interacting with other transcriptional regulators.[4–7] As a architectural protein regulator, HMG I(Y) can either facilitate the binding of some factors to their DNA-binding elements and increase promoter activity or interfere with the binding of some other factors and inhibit promoter activity.[8–15] The affinity of HMG I(Y) binding to DNA depends on the structure of the DNA binding site.[4,16,17] Nuclear factor (NF)-κB is among those factors considered to interact with HMG I(Y).[8]

The inducible cyclooxygenase, cyclooxygenase-2 (COX-2), is considered a rate-limiting enzyme in the synthesis of the prostaglandins from arachidonic acid.[18] COX-2 can be induced rapidly by many physical and chemical stimuli in human endothelial cells, including shear stress, cobalt, mitogenic agents, and cytokines.[19–21] The COX-2 gene has been cloned, and there are several potential response elements upstream from the transcription start site of the COX-2 gene, including Sp1, activator protein-2, NF-κB, NF-IL6, cAMP response element, E box, and TATA.[22,23] In addition, IL-1β regulates the translation of COX-2 gene by binding the 3′ untranslated region and stabilizing mRNA.[24] The NF-IL6 site is responsible for induction of COX-2 by lipopolysaccharides and phorbol ester in vascular endothelial cells.[22] A cAMP response element mediates the effect of v-*src* on COX-2 expression in fibroblasts.[25] In a previous study, we showed that hypoxia induced the expression of COX-2 gene via NF-κB p65 factor in human endothelial cells, demonstrating

Received December 30, 1997; accepted May 6, 1998.

From the Sealy Center for Molecular Cardiology, Department of Medicine, The University of Texas Medical Branch, Galveston, Tex.

Reprint requests to John F. Schmedtje, Jr, MD, Section on Cardiology, Wake Forest University School of Medicine, Medical Center Blvd, Winston-Salem, NC 27157.

that hypoxia increases the binding of NF-κB p65 to the relatively 3′ consensus element in the upstream promoter of the COX-2 gene.[16] We found that the binding of the NF-κB is a necessary, if not sufficient, step for the response of COX-2 to hypoxia. This finding left us with questions as to what other factors could be conveying hypoxia-specific signals to the nucleus, making the p65 interaction with the COX-2 promoter a sufficient stimulus for transactivation.

We hypothesized that the increase in COX-2 gene expression by NF-κB in hypoxia was sensitive to interaction between NF-κB or TATA elements and the HMG I(Y) family of proteins given this background information. We examined the expression of HMG I(Y) gene under hypoxic conditions and found evidence indicating that HMG I(Y) plays a role in the induction of COX-2 expression in hypoxia.

Materials and Methods

Cell Culture and Hypoxia Treatment

Human umbilical vein endothelial cells (HUVECs) (Clonetics) were cultured in medium 199 with 2.2 g $NaHCO_3$/L (Life Technology, Inc), 5% FBS (Hyclone Laboratories), 50 μg/mL endothelial cell growth supplement (Collaborative Biomedical Products), 50 μg/mL heparin, and 1.0 μg/mL hydrocortisone. HUVECs were studied within ≤5 passages from primary culture. HUVECs were exposed to ambient oxygen concentration of 1% (hypoxia) and 21% (normoxia) when the cells were grown to ≈60% to 80% confluence. The medium was preequilibrated to the environmental gas conditions overnight before cellular exposure. The possibility of generating reoxygenation artifacts after removal of the cells from the incubator was carefully prevented by immediately placing cells on ice and replacing hypoxic medium with lysis buffer.

Construction of Plasmids

The full-length human HMG I cDNA (pBS-HMG-I) was a gift from Dr Raymond Reeves. A set of deletion constructions of the COX-2 promoter, extending from −1800, −304, −245, and −45 bp upstream from the transcription start site to +65, were produced with polymerase chain reaction. These deletions were inserted into vector pGL2-basic (Promega) containing a luciferase reporter gene and are referred to as pD4, pD3, pD2, and pD1, respectively. An HMG I(Y) expression plasmid pD3-HMG was driven by the COX-2 promoter through replacement of luciferase reporter gene (*Hin*dIII-*Eco*RV fragment) of pD3 with the HMG I cDNA insert of pBS-HMG-I. The pSV40-HMG(+) and pSV40-HMG(−) plasmids were generated by removing the luciferase reporter gene in pGL-2 promoter (Promega) through restriction endonuclease digestion with *Eco*RV and *Hin*dIII and subsequently ligating HMG I cDNA in sense (+) or antisense (−) orientation with the SV40-driven remnant of pGL-2. The correctness of the recombinant plasmids was confirmed by restriction digest analyses.

Western Blotting

Cell culture dishes were briefly washed with prechilled PBS before adding cell lysis buffer (50 mmol/L HEPES [pH 7.4], 10 mmol/L KCl, 1 mmol/L EDTA, 1 mmol/L EGTA, 1 mmol/L DDT, 0.5 mmol/L phenylmethylsulfonyl fluoride, 1 μg/mL pepstatin A, 1 μg/mL leupeptin, 10 μg/mL trypsin inhibitor, 10 μg/mL aprotinin, and 0.5% Triton). Protein concentration was measured using Bio-Rad protein assay reagent. After electrophoresis in 12% SDS-PAGE gel, the 30 μg cell lysate was blotted to a nitrocellulose membrane. Nonspecific binding was blocked by soaking the membrane in a TBST buffer (20 mmol/L Tris base [pH 7.5], 137 mmol/L NaCl, and 0.1% Tween 20) containing 5% nonfat milk for 30 minutes at 37°C. The membrane was then incubated with polyclonal IgG to NF-κB p65 (1:1500 dilution), the inhibitory protein that binds NF-κB p65 precursors (IκB, 1:1000 dilution), or HMG I(Y) (1:1000 dilution) (Santa Cruz Biotechnology) for 30 minutes at 37°C and washed in TBST for 5 minutes (5 times each). After a similar incubation with horseradish peroxidase–conjugated anti-IgG, the membrane was washed and incubated in luminol ECL detection reagents (Amersham) and exposed to the film. Incubation with IgG monoclonal antibody to chicken α-tubulin (Sigma) at 1:2500 dilution was also performed for comparative purposes.

Electrophoretic Mobility Shift Assay

Nuclear protein extraction and gel shift assays were performed as previously described for NF-κB-3′.[16] The duration of HUVEC exposure to hypoxia was 2 hours. The binding reaction was performed with end-labeled oligonucleotide from the COX-2 promoter and 2 to 6 μg of nuclear extract. The sense strand of the double-stranded TATA box oligo used for electrophoretic mobility shift assay (EMSA) was also taken from the COX-2 promoter region: 5′-TTGGTTTTCAGTCTTATAAAAAGG-3′.

Transfection for Reporter Gene Assay

We performed transfection analysis using luciferase reporter gene constructions in HUVECs, which were grown in 35-mm 6-well plates to 70% to 80% confluence. For each well, 12 μL of lipofectin reagent (GIBCO BRL) was added into 88 μL of Opti-MEM-1 medium (Life Technologies, Inc) and incubated at room temperature for 45 minutes. Then 2.0 μg of pD1-pD4 and 0.5 μg of pSV2PAP, containing the alkaline phosphatase reporter gene downstream from an SV40 promoter, were added into 100 μL Opti-MEM-1 medium. The lipofectin and DNA solution were mixed and incubated at room temperature for 15 minutes, and then another 800 μL of Opti-MEM-1 medium was added to the mixture. After the HUVECs were rinsed once with the Opti-MEM-1 medium, the lipofectin and DNA mixture was overlaid on the cells and incubated at 37°C for 8 hours. We then replaced the mixture with the original medium and let the cells recover overnight. HUVEC cells were exposed to hypoxia or further normoxia for 24 hours before reporter gene assay. An additional 0.5 to 4.0 μg of HMG I expression plasmid (as indicated in Figure 5) was added into the DNA mixture. A control plasmid containing only the COX-2 promoter but no reporter gene was used to make the DNA quantity constant. Luciferase activity was determined in cell lysates through single photon counting on a microplate scintillation counter. Alkaline phosphatase activity was determined as previously described to control transfection efficiency.[16] The values for luciferase (counts per second) and alkaline phosphatase (optical density) were reported as a ratio, thereby correcting for discrepancies in transfection efficiency.

Northern Blotting

Total RNA was extracted from HUVECs treated with normoxia and hypoxia with the use of RNAzol B (TEL-TEST, Inc). Total RNA (20 μg/well) was loaded in a 1.2% formaldehyde agarose gel. After electrophoresis, the nucleic acids were transferred to a nylon membrane by blotting. A *Sac*I fragment of HMG I cDNA (1186 bp) was randomly labeled with ^{32}P as a probe. Randomly labeled 18S RNA was also used for comparative purposes.

Nuclear Runoff Assay for COX-2 Transcripts

Nuclei were harvested from HUVECs as follows: cells were rinsed twice with ice-cold PBS, and then 5 to 8×10^7cells were scraped into a 50-mL tube with 4 mL of ice-cold PBS, centrifuged for 5 minutes at 500*g* and 4°C, loosened by vortexing gently, and then lysed with 4 mL of NP-40 lysis buffer (10 mmol/L Tris-HCl [pH 7.5], 1.5 mmol/L $MgCl_2$, 140 mmol/L NaCl, and 1% NP-40). We incubated lysed cells for ≈3 to 5 minutes on ice, checked the cell lysate with a phase-contrast microscope, and then centrifuged the nuclei at 500*g* at 4°C for 5 minutes. The nuclei were washed twice in 1 mL of 20 mmol/L Tris-HCl (pH 8.0), 20% glycerol, 140 mmol/L KCl, 10 mmol/L $MgCl_2$, 1 mmol/L $MnCl_2$, and 14 mmol/L β-mercaptoethanol. After centrifugation at 650*g* for 4 minutes, we resuspended the nuclei in 200 μL of this buffer and stored them in liquid nitrogen. Frozen nuclei were thawed to 25°C, and nascent

transcripts were labeled with 20 μL of 10 mCi/mL [α-^{32}P]UTP(800 Ci/mmol) and 2.5 μL of 100 mmol/L ATP, CTP, and GTP for 30 minutes at 30°C. RNA was extracted from the nuclei by adding 0.9 mL RNazol B and 0.12 mL chloroform. The aqueous content was separated, and RNA was precipitated with isopropanol and washed with 70% ethanol. The RNA was resuspended in 100 μL Tris-EDTA solution and 1 μL of RNase inhibitor. Limited alkaline hydrolysis was achieved with the addition of 20 μL of 1 mol/L NaOH and incubation on ice for 10 minutes, followed by neutralization with 40 μL of 1 mol/L HEPES at pH 7.9. RNA was precipitated with sodium acetate and ethanol. RNA was hybridized to nitrocellulose to which DNA for COX-1 and COX-2, along with a negative control, had been slot-blotted. The radiolabeled RNA transcripts that hybridized to the membrane were identified by exposure to film for 4 days.

GST-HMG Fusion Protein

The full-length HMG I(Y) cDNA coding region was inserted into the glutathione-*S*-transferase (GST) fusion protein expression vector pGEX-4T-1 by ligation to *Eco*RI and *Sma*I restriction sites. *Escherichia coli* BL21, transformed with the recombinant plasmid, was grown in LB medium supplemented with 100 μg/mL ampicillin at 37°C overnight. The cells were then diluted 1:10 in fresh LB and grown for another hour. Expression of the GST-HMG fusion protein was induced by incubation with 1.0 mmol/L isopropyl-β-D-thiogalactoside for 4 hours. The cells were then resuspended in PBS and lysed by sonication. The proteins were brought into solution with 1% Triton X-100. A crude extract was separated by centrifugation and added to a 50% slurry of glutathione Sepharose 4B equilibrated with PBS. After gentle agitation at room temperature for 30 minutes, the matrix was sedimented and washed with PBS. Then GST-HMG was eluted by 10 mmol/L reduced glutathione, and the fusion protein was analyzed by SDS-PAGE.

Radioimmunoassay of PGE_2

HUVEC cells were grown to 70% to 80% confluence and exposed to 2 hours, 6 to 10 hours, 24 hours, and 48 hours of normoxic or hypoxic conditions. Immediately after stimulation, the culture medium was collected into prechilled polypropylene tubes coated with a solution of 4.5 mmol/L EDTA combined with 10 μg/mL indomethacin to inhibit further prostaglandin synthesis. Prostaglandin E_2 (PGE_2) levels were determined using a commercially available ^{125}I radioimmunoassay kit (Dupont). PGE_2 levels were assayed directly from medium as follows: 100 μL sample, 100 μL rabbit anti-serum, and 100 μL tracer (iodinated analogue of PGE_2) were incubated together overnight at 4°C. Then 1 mL cold precipitating reagent (16% PEG 6000 and 0.05% sodium azide in 50 mmol/L phosphate buffer, pH 6.8) was added to precipitate the antibody-bound tracer. After centrifugation, the pellet containing the antibody-antigen complex was counted in a gamma counter. Results from a serial dilution of standard concentrate were used to construct standard (dose-response) curves from which the unknowns were read by interpolation. The value in the medium at time zero was subtracted from each value to yield an index of cellular prostanoid production above that baseline over time. Protein concentration in each cell culture dish was measured after 2 washings with PBS. NaOH (0.62 mol/L) was added to solubilize the protein. The protein concentrations from each dish were then measured with a modified Bradford method (Bio-Rad) using BSA as a standard.[76] The results of PGE_2 measurements were reported as picograms per milligram of protein.

Results

Search for Hypoxia-Related Regulatory Elements in COX-2 Promoter

Hypoxia is known to regulate transcription via multiple factors. For instance, hypoxia-inducible factor 1 (HIF-1), which mediates erythropoietin induction in hypoxia, also regulates the transcription of genes encoding glycolytic enzymes. The presence of a HIF-1 binding site is necessary but not sufficient to direct the hypoxia-induced transcription of these genes.[27] There are several potential *cis*-acting elements within the 350 bases upstream from the COX-2 transcription start site (Figure 1A). The known hypoxia-inducible element 1 (HIE-1), which binds HIF-1, has not been found upstream or downstream from the COX-2 coding region. We performed several transfections with a set of deletions of the COX-2 promoter to search for a hypoxia regulatory element (Figure 1B). The D4 region is the intact COX-2 promoter. It displayed full COX-2 promoter activity and a full reporter gene response to hypoxia induction when transfected in a vector. Transfection using pD3, which features 1496 bp less of the COX-2 upstream promoter than does D4, showed no significant decrease of the promoter activity. The smallest construct, pD1, containing the basal promoter of COX-2 and a TATA box, displayed a minimal response to hypoxia. Although insignificant in itself, this minimal response suggested to us that hypoxia may induce the COX-2 gene through not only the NF-κB binding site but also the TATA box and other DNA-protein binding sites.

Mechanism of NF-κB Activation by Hypoxia

Previous work from our laboratory indicated that hypoxia activates the binding of NF-κB p65 to a consensus NF-κB oligonucleotide. We noticed that the NF-κB 5′-binding site in the COX-2 promoter, which is −440 bp upstream from the transcription start site, did not have any contribution to the COX-2 promoter activity but did constitutively bind with normoxic and hypoxic HUVEC nuclear protein extracts. By comparison, hypoxia enhances protein binding to the NF-κB-3′ binding site in the COX-2 promoter. We examined IκB-α and NF-κB p65 by Western blot in HUVEC cell lysates (Figure 2). α-Tubulin was used as an equivalent loading control. The protein level of both factors did not change between normoxia and hypoxia (from 30 minutes to 24 hours). This suggests that the activation of NF-κB by hypoxia is regulated by posttranslational modification and/or binding factors such as IκB-α in HUVECs. We reasoned that other factors like HMG I(Y) may play a role in the hypoxia-specific binding of NF-κB transactivation factors to certain NF-κB elements. This hypoxia-specific interaction might occur through cooperative binding of HMG I(Y) to the A·T region, facilitating binding of NF-κB p65 to the NF-κB-3′ element.

Hypoxia, HMG I(Y), and Nuclear Protein Binding to NF-κB-3′ and TATA

Hypoxic nuclear protein caused our radiolabeled NF-κB-3′ oligonucleotide probe to shift electrophoretically. The combination of nuclear protein from hypoxic cells and the GST-HMG fusion protein produced a synergistically enhanced shift, as seen in Figure 3. The range of GST-HMG protein used in a series of EMSA experiments revealed a maximal shift at 1 to 3 ng with a definite decrease in NF-κB-3′ shift above this amount. We also recorded that a GST protein without HMG had no effect on electrophoretic mobility. When hypoxic nuclear protein was used in this experiment, the shift intensified and was observed at lower

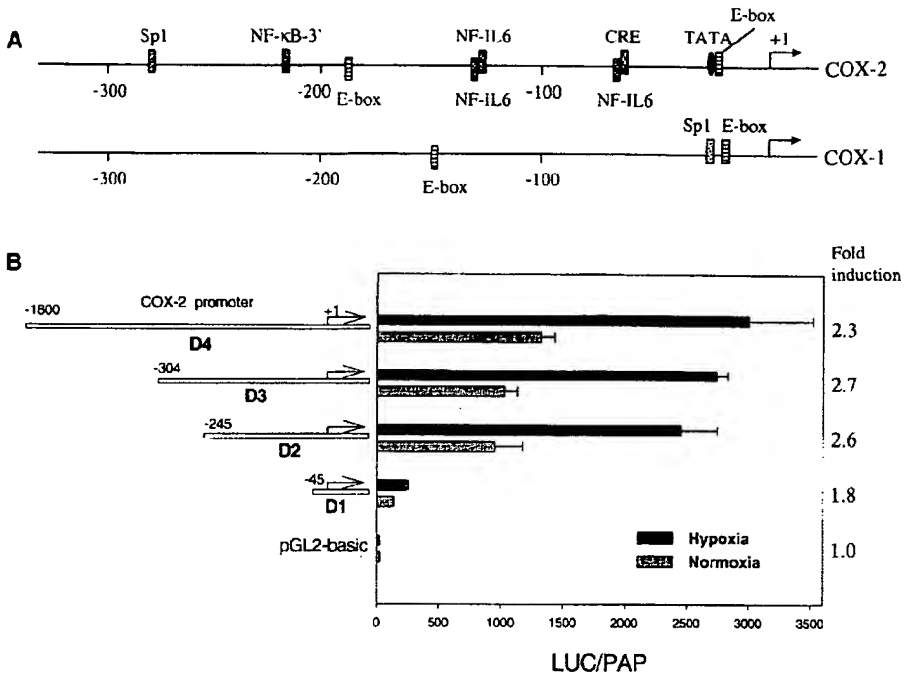

Figure 1. The search for hypoxia-related regulatory elements within the COX-2 promoter region. A, Schematic representation of the promoter regions of COX-2[23] and COX-1[39] relative to transcriptional start sites. Potential factor binding sites are shown on both the direct (up) and complementary (down) strands within −350 bp. CRE indicates cAMP response element. B, Transfection of HUVECs with plasmids driven by COX-2 promoter deletion constructs ligated to the luciferase reporter gene. Regions from −1800 bp, −304 bp, −245 bp, and −45 bp to +65 bp of the COX-2 promoter were cloned into pGL2-basic as pD4, pD3, pD2, and pD1, respectively. After transfection by 2 μg of each construct and 0.5 μg of pSV2PAP and subsequent stimulation by hypoxia for 24 hours, luciferase activity (LUC) and alkaline phosphatase activity (PAP) were assayed. The results are presented as ratios of LUC to PAP. Descriptive statistics (mean±SEM) were based on 3 to 5 independent experiments.

doses of GST-HMG. When a TATA oligo was used for EMSA (Figure 4), multiple bands were shifted, corresponding to the shift of HMG I(Y) and TATA-binding protein (TBP) recorded in a previous study of TATA DNA-protein interactions.[12] Hypoxia induced increased shifting, as did HMG I(Y), suggesting a functional correlation between hypoxic induction of transcription and DNA binding with HMG I(Y) proteins at the TATA box as well as at the NF-κB-3′ element of the COX-2 promoter. However, we cannot conclude that this DNA-protein interaction is of

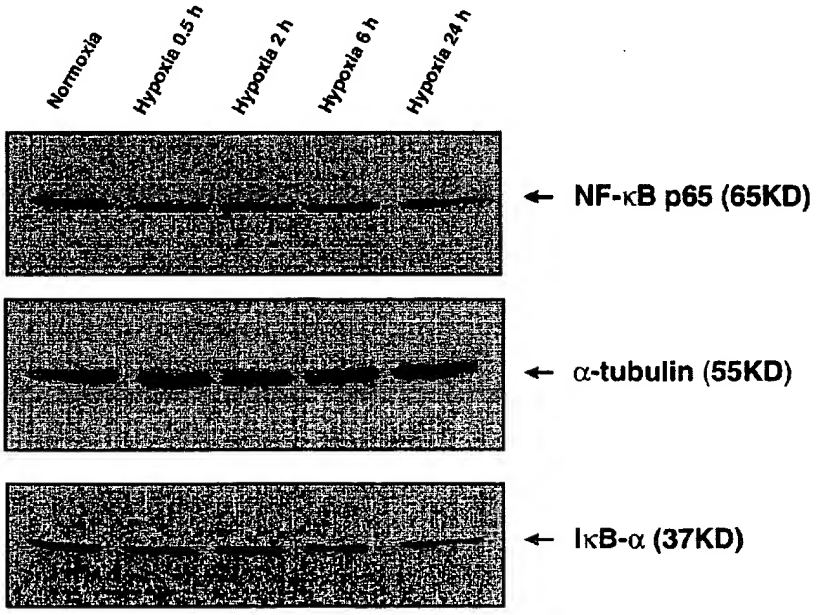

Figure 2. Western blot analysis of NF-κB p65 and IκB-α protein in HUVECs. Each lane contains 30 μg cell lysate from HUVECs treated with a time course of hypoxia and normoxia as indicated. The same blot was hybridized to anti–NF-κB p65 and then to anti–IκB-α antibody. The hybridization to anti–α-tubulin was used as a loading control. NF-κB and IκB-α did not show any change during hypoxia. The results represent 3 independent experiments.

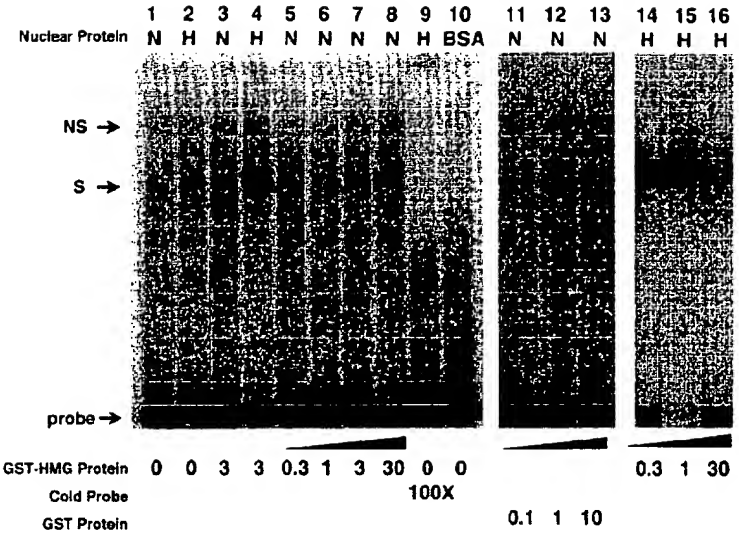

Figure 3. Hypoxic nuclear protein (H) and HMG I(Y) both bind to NF-κB by EMSA, with the use of 2×10^4 cpm NF-κB-3′ oligonucleotide as a probe. Nuclear protein of HUVECs treated with continued normoxia or 2 hours of hypoxia was assayed: 2.7 μg was used in lanes 1 to 9, 4.0 μg was used in lanes 11 to 13, and 2.5 μg was used in lanes 14 to 16. Lanes 1 to 4 demonstrate the synergy between hypoxic nuclear protein and GST-HMG fusion protein in shifting the NF-κB-3′ probe. NF-κB-3′ was maximally shifted in normoxic nuclear protein (N) experiments by 3.0 ng GST-HMG fusion protein (range, 0.3 to 30.0 ng in lanes 5 to 8). When hypoxic nuclear protein was added to NF-κB-3′ probe and GST-HMG (0.3 to 30 ng in lanes 14 to 16), more shifting occurred with less GST-HMG. A 100-fold excess of cold NF-κB-3′ oligo was added to block specific binding in lane 9. BSA (5 μg) was added to lane 10 instead of nuclear protein. Lanes 11 to 13 demonstrate that GST protein (without the HMG fusion) has no effect on DNA-protein binding. S indicates specific shift bands; NS, nonspecific shift band.

functional significance given the limitations of EMSA; therefore, further experiments were performed to examine the effect of HMG I(Y) proteins on COX-2 promoter function and gene expression.

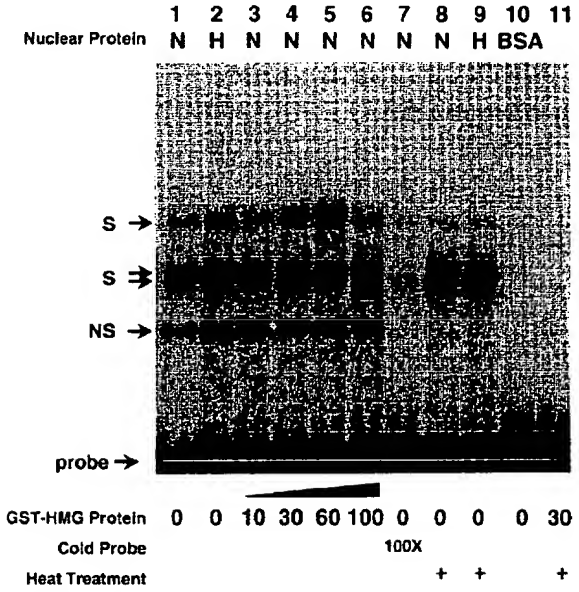

Figure 4. Hypoxia and HMG I(Y) both increase nuclear protein binding to the COX-2 promoter TATA box by EMSA, with the use of 2×10^4 cpm double-stranded TATA oligonucleotide as a probe. The top band appears to be attributable to HMG I(Y) binding to TATA DNA. Nuclear protein of HUVECs (6.0 μg) treated with continued normoxia or 2 hours of hypoxia was used. Lanes 1 to 2 demonstrate increased DNA-protein interaction in hypoxia. Lanes 3 to 6 show that HMG I(Y) protein can mimic the effect of hypoxia in a dose-dependent manner. Cold probe (100×) in lane 7 blocks shifting. Heat treatment of the DNA-protein binding product at 60°C for 5 minutes (lanes 8 to 9) reduced the amount of HMG I(Y)–attributable gel shifting. Lanes 10 and 11 are controls, in which BSA and HMG I(Y) protein were used alone. S indicates specific shift bands; NS, nonspecific shift band; N, normoxic nuclear protein; and H, hypoxic nuclear protein. Note that the nonspecific band (lanes 8 and 9) is heat labile when compared with the specific bands.

Upregulation of COX-2 Promoter Activity by HMG I(Y)

To understand how HMG I(Y) regulates the expression of the COX-2 gene under hypoxia, we constructed an HMG I expression plasmid by replacing the luciferase gene with HMG I cDNA in the COX-2 promoter construct pD3, making pD3-HMG, in which the expression of the HMG I gene was driven by the COX-2 promoter. COX-2 promoter constructs ligated to luciferase reporters or HMG I were used to cotransfect the HUVECs. Expression of HMG I(Y) remarkably increased the COX-2 promoter activity in a dose-dependent manner under hypoxia (Figure 5A). Since HMG I(Y) itself is upregulated by hypoxia, as described later, the synergistic effect of HMG I(Y) and hypoxia greatly increased the expression of reporter gene compared with baseline. This stimulation is conspicuous and as strong as that of phorbol ester and lipopolysaccharide[22] or 20% FCS.[20] pD1 contains the basal promoter of the COX-2 gene. We found that increased HMG I(Y) could also upregulate the basal promoter activity of COX-2 in cotransfected HUVECs under hypoxia (Figure 5B). This effect was not dependent on the linkage between hypoxia-sensitive elements in the COX-2 promoter and HMG I(Y) expression, as modeled with the pD3-HMG vector. Repeating these experiments with a constitutively active expression vector, pSV40-HMG(+), demonstrated that a sufficient amount of HMG I(Y) could stimulate reporter gene expression by the COX-2 promoter as much as hypoxia could (Figure 5C).

Transcription of COX-2 in Hypoxia

Hypoxia had been previously shown to regulate the transcription of COX-2 via the NF-κB p65 transactivation protein. We confirmed this finding using a nuclear runoff assay by hybridization of radiolabeled nascent transcripts to immobilized pBS-hgCOX-2-3′, containing the 3′ end (bases 4490 to 10488) of the human genomic COX-2 sequence.[28] The positive control was demonstrated by hybridization to pBS-hCOX-1, containing a 1750-bp insert

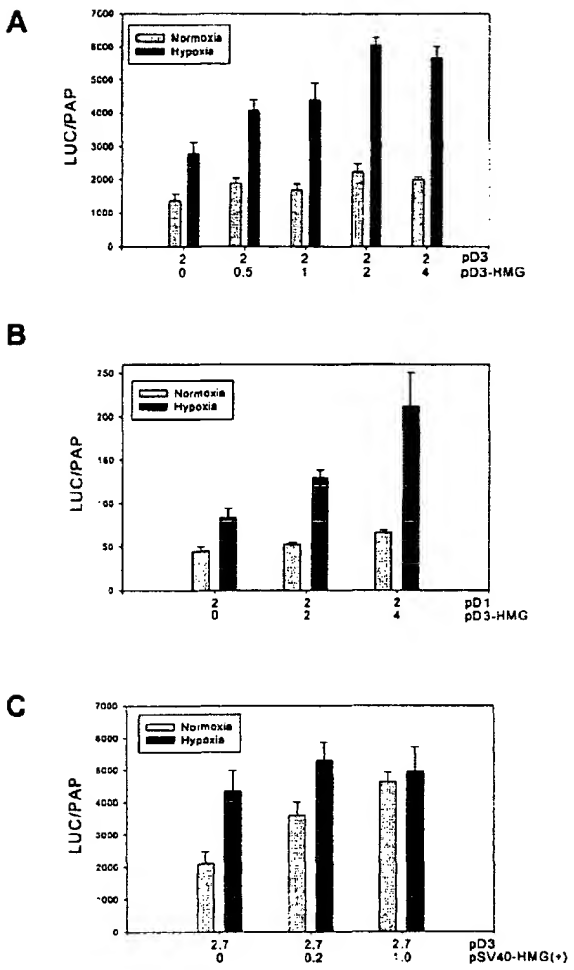

Figure 5. Reporter gene assays using deletion constructs demonstrate that HMG I(Y) upregulates the expression of COX-2 under hypoxic conditions. HUVECs were cotransfected with either 2 μg of pD3, a luciferase reporter that demonstrates full COX-2 promoter activity in hypoxia (A and C), or pD1, a similar luciferase reporter ligated to a basal COX-2 promoter (B), and either 0.5 to 4 μg of pD3-HMG expression plasmid (A and B) or the constitutively active pSV-HMG(+) overexpression vector in the sense orientation (C). The nonexpressing plasmid pBS-HMG was used to control DNA concentration so that the total for all conditions was equal. Also, 0.5 μg of the alkaline phosphatase plasmid pSV2PAP was used in each experiment for correcting the efficiency of transfection. Four to six independent transfections were performed for each dose. Cell lysates were harvested 24 hours after treatment with hypoxia and assayed for luciferase activity and alkaline phosphatase activity. Data were expressed as mean±SEM of LUC/PAP ratios.

of COX-1 cDNA[29]; the negative control was obtained using cDNA for pBluescript II SK(+). Figure 6 illustrates the comparison between COX-1 and COX-2 transcripts obtained from nuclei from HUVECs that had been treated for 30 minutes, 2 hours, and 4 hours of hypoxia versus normoxia. Although transcription of the COX-1 gene did not change during hypoxia, transcription of the COX-2 gene was increased by hypoxia.

Regulation of HMG I(Y) Gene Expression by Hypoxia in HUVECs

We investigated how hypoxia regulated the HMG I(Y) gene expression in HUVECs. Data are shown in Figure 7. We found that steady-state levels of HMG I(Y) mRNA were nearly doubled by hypoxia by 2 hours (Figure 7A). The peak prevalence of HMG I(Y) mRNA was reached between 2 and 6 hours with the hypoxia treatment and subsequently tailed off. The change in mRNA was relatively small compared with the >5-fold in increase HMG I(Y) protein caused by hypoxia (Figure 7B). We observed that protein prevalence also began to decrease after 6 hours of hypoxia.

Effects of Sense and Antisense HMG I(Y) on COX-2 Gene Expression

We expressed sense and antisense HMG I(Y) RNA by transfecting HUVECs with constitutively active vectors [pSV40-HMG(+) and pSV40-HMG(−), respectively]. The effect of pSV40-HMG(+) on hypoxia-mediated increases in COX-2 immunoreactive protein are illustrated in Figure 8. All cells were exposed to equal amounts of DNA through balance transfection with empty vectors. This was important, since we found that transfected cells produced less COX-2 than did cells that had not been transfected with a given amount of DNA. We found that overexpression of HMG proteins led to progressive increases in COX-2 due to hypoxia. Since there was virtually no COX-2 produced at baseline, we could not decrease COX-2 by antisense overexpression in our model. However, using relative reporter gene activity as an index as illustrated in Figure 9, we documented that pSV40-HMG(−) inhibited and pSV40-HMG(+) stimulated luciferase reporter gene activity linked to the COX-2 promoter. These experiments indicate a specific role for HMG I(Y) proteins in the regulation of COX-2 gene expression by hypoxia.

Endothelial PGE_2 in Hypoxia

The radioimmunoassay for PGE was performed on HUVEC media directly after 2 hours, 10 hours, 24 hours, and 48 hours of hypoxic or normoxic stimulation. Direct assay of cell culture medium for immunoactive PGE_2 levels has been reported previously.[30] Assays on the normoxic cells were performed as controls for basal synthesis of PGE_2. Parallel hypoxic cells at each point were also pretreated with 4 μg/mL indomethacin to block the cyclooxygenase activity. As shown in Figure 10, the PGE_2 level was not changed after 2 hours of hypoxic stimulation but was slightly increased by hypoxia after 10 hours and 24 hours. PGE_2 was significantly increased after 48 hours of hypoxia compared with normoxia. Furthermore, pretreatment of cells with indomethacin eliminated the hypoxia-induced enhancement of the PGE_2 synthesis. The time course of the PGE_2 response also corresponds to that of COX-2 protein induction by hypoxia,[16] suggesting that the enhancement of the PGE_2 synthesis by hypoxia is dependent on increased COX-2 protein.

Discussion

The present study reveals for the first time that HMG I(Y) is upregulated by hypoxia in HUVECs. The time course of the

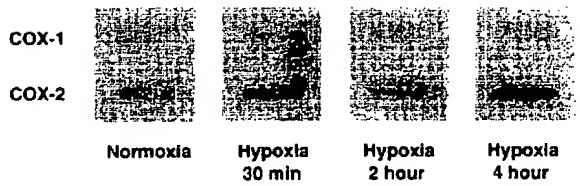

Figure 6. Nuclear runoff of nascent RNA transcripts reveals increased transcription of the COX-2 gene in hypoxia. Radiolabeled RNA from nuclei obtained from HUVECs that had been exposed to normoxia or hypoxia was hybridized to immobilized pBS-hgCOX-2-3', containing the 3' end (bases 4490 to 10488) of the human genomic COX-2 sequence.[28] The positive control was demonstrated by hybridization to pBS-hCOX-1, containing a 1750-bp insert of COX-1 cDNA.[29] COX-2 transcription was demonstrably increased during hypoxia; no effect was seen on the positive control COX-1. The negative control pBluescript II SK(+) is not shown.

response indicates that HMG I(Y) upregulation is an early event. The data herein suggest that HMG I(Y) proteins are constituents of an enhanceosome that regulates hypoxia-mediated transcription of COX-2 in a manner analogous to the synergistic roles of HMG I(Y) and NF-κB protein factors in induction of the human interferon-β gene.[14,31] The specific role of the HMG I(Y) protein family is indicated by direct effects of this protein on DNA-protein interactions and COX-2 gene expression, along with the ability of antisense RNA of HMG I(Y) to decrease COX-2 promoter activity.

The cyclooxygenases catalyze the rate-limiting step in the synthesis of prostaglandins from arachidonic acid. Since the time course of the PGE_2 response to hypoxia in our experiments corresponds with that of COX-2 protein in hypoxia[16] and the change in PGE_2 is inhibited by the cyclooxygenase inhibitor indomethacin, we propose that hypoxia increases the PGE_2 level in human vascular endothelial cells via inducible COX-2 synthesis. Other studies have shown that the transcription of the HMG I(Y) gene is inducible in human lymphoid cells by phorbol esters and calcium ionophore stimulation.[2] However, the time course of the HUVEC HMG I(Y) response to hypoxia is shorter than that in response to phorbol ester in lymphoid tissue. HMG I(Y) has been linked

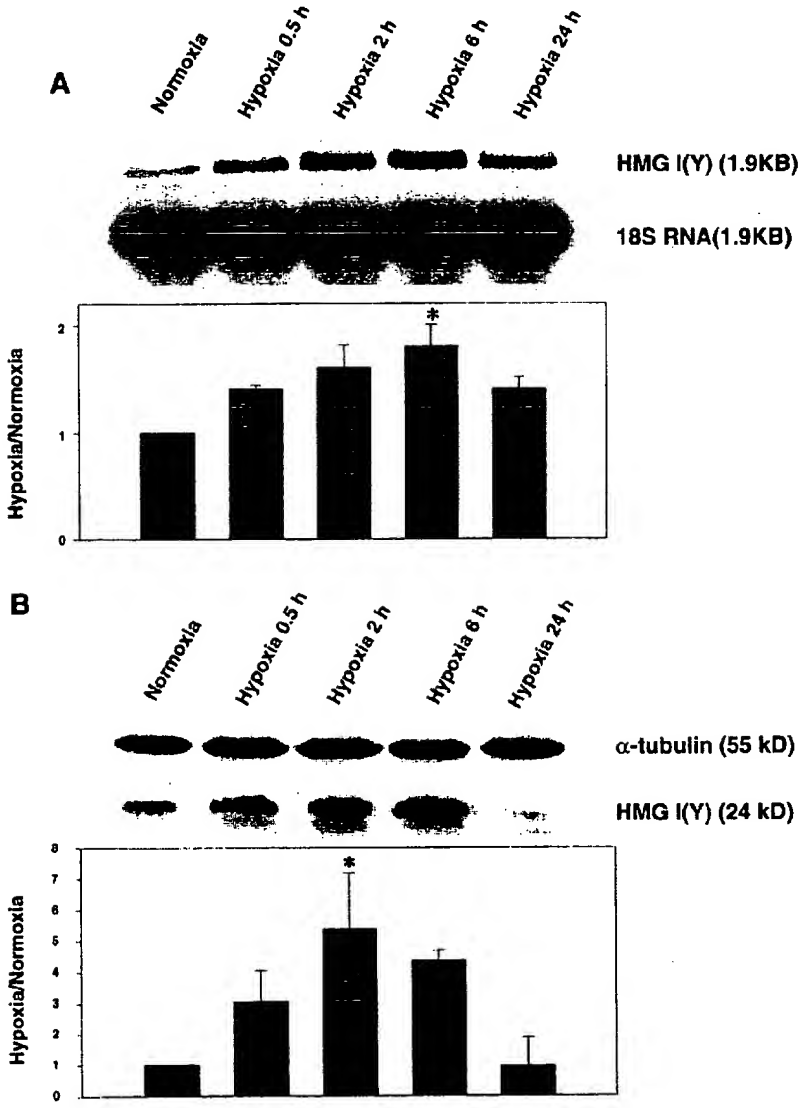

Figure 7. Upregulation of HMG I(Y) gene expression by hypoxia in HUVECs and the consequences of this upregulation on COX-2 expression. A, Northern blot analysis of HMG I(Y) mRNA. Total RNA (20 μg) was loaded in each lane. The total RNA was extracted from HUVECs treated with normoxia and a time course of hypoxia as indicated. Hybridization of 18S RNA was performed as a comparative control using a probe with fewer radioactive counts than the HMG I(Y) probe for clarity. The steady-state levels of HMG I(Y) mRNA nearly doubled during hypoxia. This blot is representative of 3 separate experiments; the bar graph represents the corresponding mean±SEM phosphorescent image density corrected for 18S as an index of lane loading (*$P<0.05$ vs normoxia). B, Western blot analysis of HMG I(Y) protein. Whole-cell lysate (30 μg) was loaded in each lane. HUVECs were treated with normoxia and a time course of hypoxia before lysis. Hybridization with anti-α-tubulin was performed as a lane-loading control. HMG I(Y) protein was increased 5-fold by hypoxia, as illustrated in a bar graph of relative band density (mean±SEM, corrected for α-tubulin) from 3 separate experiments (*$P<0.05$ vs normoxia).

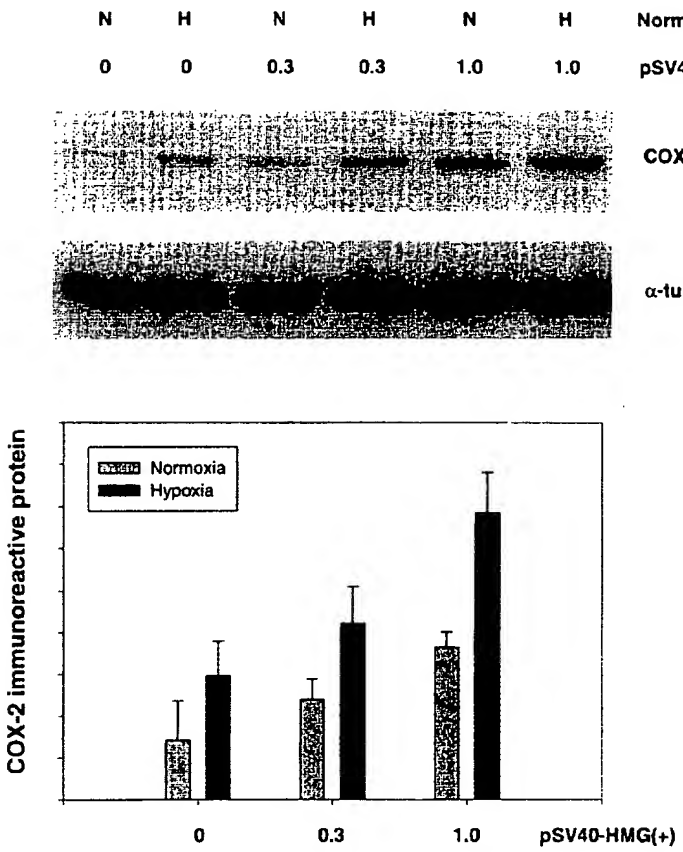

Figure 8. Effect of increasing HMG I(Y) expression on COX-2 protein in hypoxic HUVECs. Cells were transfected with 1.0 μg total DNA [pSV40-HMG(+) or a blank pGL-2]. COX-2 protein was progressively increased by hypoxia and HMG overexpression. The bar graph demonstrates the direction of the dose-response relationship of hypoxia, HMG I(Y), and COX-2 immunoreactive protein (corrected for α-tubulin) from 3 separate experiments.

to carcinogenesis in pulmonary hamartomas[32] and uterine leiomyomata.[33] We speculate, on the basis of our data, that HMG I(Y), COX-2, and PGE_2 are part of a proliferative, proinflammatory, and angiogenic response to hypoxia in cardiovascular diseases.

COX-2 mRNA metabolism has been linked to the "AUUUA" motif in its 3′ untranslated region.[23] There does not appear to be such a motif in the HMG I(Y) 3′ untranslated region.[1] Therefore, another negative-feedback mechanism may be responsible for the reduction of HMG I(Y) RNA in HUVECs after prolonged hypoxia (24 hours). The transcriptional regulation afforded by HMG I(Y) is a function of the prevalence of the HMG I(Y) protein.[17,34,35] Our results have shown that HMG I(Y) protein facilitates nuclear protein binding with NF-κB-3′ and with TATA box elements. The increased HMG I(Y) expressed in hypoxic HUVECs appears to alter the conformation of the protein-DNA complex and the interaction between the basal transcription complex and promoter activity of genes including COX-2. Beyond a certain point, excess HMG I(Y) diminishes both NF-κB-3′ and TATA binding to nuclear protein in hypoxia. This finding correlates with previous work documenting repression of transcription by excess HMG I(Y).[9]

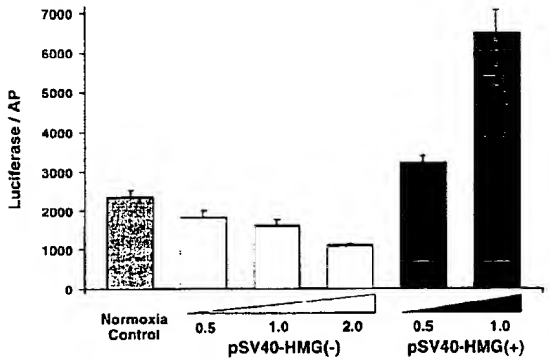

Figure 9. Cotransfection of HUVECs with pD3, a luciferase promoter vector ligated to the COX-2 promoter region, and either pSV40-HMG(−) or pSV40-HMG(+) is illustrated in a bar graph of luciferase reporter gene activity, corrected for alkaline phosphatase (AP) activity, from 3 separate experiments. We found that the antisense HMG I(Y) vector led to decreased COX-2 promoter activity and that the sense HMG I(Y) vector increased COX-2 promoter activity (*$P<0.05$ vs control).

High-level expression of HMG I(Y) is also found during embryonic development.[36] Previous studies demonstrate that HMG I(Y) stimulates the binding of Sp1, NF-κB, and activating transcription factor-2 to DNA and that it can interact with TBP.[5,9,10,31] We propose that HMG I(Y) mediates the induction of COX-2 by hypoxia on 3 levels: (1) HMG I(Y) may bind to the TATA box and interact with TBP, altering basal promoter activity; (2) HMG I(Y) may facilitate Sp1, NF-κB, and activating transcription factor-2 binding to DNA as a cofactor, increasing COX-2 enhanceosome function at the promoter; and (3) binding of HMG I(Y) to A·T-rich elements may change the conformation of DNA itself, focally altering the helical structure of DNA and thereby acting

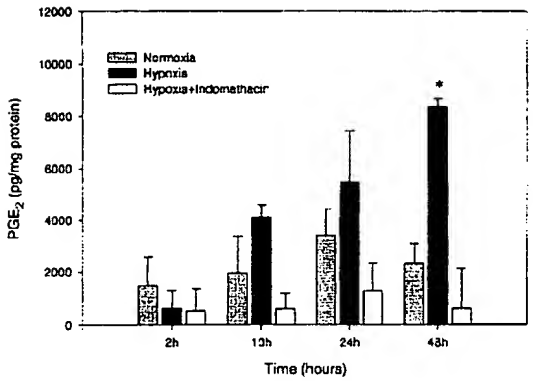

Figure 10. HUVEC production of PGE_2 is increased during hypoxia by a cyclooxygenase-dependent mechanism. Cells were incubated for 2 hours, 10 hours, 24 hours, and 48 hours under normoxic or hypoxic conditions. Some hypoxic cells were also pretreated with 4 μg/mL indomethacin to block the cyclooxygenase activity. PGE_2 levels were assayed by radioimmunoassay of culture medium. PGE_2 levels from normoxic cells are presented as a control. Results are expressed in picograms per milligram protein as the mean±SEM (n=3). *$P<0.05$ compared with normoxia and hypoxia+indomethacin.

as a facilitator (or, when in excess, an inhibitor) of enhanceosome-mediated transcription.

HMG I(Y) is a unique multifunctional regulator because it interacts with both DNA and many other factors. HMG I(Y) is known to cooperate with NF-κB and compete with NF-AT factors in binding to DNA.[11] HMG I(Y) can directly recognize and alter the structure of localized regions of chromatin,[17,35] thereby facilitating, inhibiting, or replacing the binding of some factors.[9,11,12,37,38] The interaction between HMG I(Y) and NF-κB p65 in the induction of COX-2 transcription by hypoxia provides new insight into the mechanisms of promoter-specific transcriptional regulation and cell-specific gene expression. Our data do not point to a one-protein/one-enhancer mechanism of transcription. In the case of COX-2, the enhanceosome model provides a template for our proposal that hypoxia-mediated transcription in vascular endothelium occurs when a specific combination of protein factors binds to specified sites within a promoter region.

Acknowledgments

This study was supported by the John Sealy Memorial Endowment Fund for Biomedical Research. The authors extend their gratitude to Marschall S. Runge for his helpful advice.

References

1. Johnson KR, Lehn DA, Reeves R. Alternative processing of mRNAs encoding mammalian chromosomal high-mobility-group proteins HMG-I and HMG-Y. *Mol Cell Biol.* 1989;9:2114–2123.
2. Friedmann M, Holth LT, Zoghbi HY, Reeves R. Organization, inducible-expression and chromosome localization of the human HMG-I(Y) nonhistone protein gene. *Nucleic Acids Res.* 1993;21:4259–4267.
3. Reeves R, Nissen MS. The AT-DNA-binding domain of mammalian high mobility group I chromosomal proteins. *J Biol Chem.* 1990;265:8573–8582.
4. Maher JF, Nathans D. Multivalent DNA-binding properties of the HMG-I proteins. *Proc Natl Acad Sci U S A.* 1996;93:6716–6720.
5. Falvo JV, Thanos D, Maniatis T. Reversal of intrinsic DNA bends in the IFNβ gene enhancer by transcription factors and the architectural protein HMG I(Y). *Cell.* 1995;83:1101–1111.
6. Leger H, Sock E, Renner K, Grummt F, Wegner M. Functional interaction between the POU domain protein Tst-1/Oct- 6 and the high-mobility-group protein HMG-I/Y. *Mol Cell Biol.* 1995;15:3738–3747.
7. John S, Reeves RB, Lin J-X, Child R, Leiden JM, Thompson CB, Leonard WJ. Regulation of cell-type-specific interleukin-2 receptor α-chain gene expression: potential role of physical interactions between Elf-1, HMG-I(Y), and NF-κB family proteins. *Mol Cell Biol.* 1995;15:1786–1796.
8. Wood LD, Farmer AA, Richmond A. HMGI(Y), and Sp1 in addition to NF-κB regulate transcription of the MGSA/GRPα gene. *Nucleic Acids Res.* 1995;23:4210–4219.
9. Du W, Maniatis T. The high mobility group protein HMG I(Y) can stimulate or inhibit DNA binding of distinct transcription factor ATF-2 isoforms. *Proc Natl Acad Sci U S A.* 1994;91:11318–11322.
10. French SW, Schmidt MC, Glorioso JC. Involvement of a high-mobility-group protein in the transcriptional activity of herpes simplex virus latency-active promoter 2. *Mol Cell Biol.* 1996;16:5393–5399.
11. Klein-Hessling S, Schneider G, Heinfling A, Chuvpilo S, Serfling E. HMG I(Y) interferes with the DNA binding of NF-AT factors and the induction of the interleukin 4 promoter in T cells. *Proc Natl Acad Sci U S A.* 1996;93:15311–15316.
12. Ge H, Roeder RG. The high mobility group protein HMG1 can reversibly inhibit class II gene transcription by interaction with the TATA-binding protein. *J Biol Chem.* 1994;269:17136–17140.
13. Abdulkadir SA, Krishna S, Thanos D, Maniatis T, Strominger JL, Ono SJ. Functional roles of the transcription factor Oct-2A and the high mobility group protein I/Y in HLA-DRA gene expression. *J Exp Med.* 1995;182:487–500.
14. Thanos D, Maniatis T. The high mobility group protein HMG I(Y) is required for NF-κB-dependent virus induction of the human IFN-β gene. *Cell.* 1992;71:777–789.
15. Aizawa S, Nishino H, Saito K, Kimura K, Shirakawa H, Yoshida M. Stimulation of transcription in cultured cells by high mobility group protein 1: essential role of the acidic carboxyl-terminal region. *Biochemistry.* 1994;33:14690–14695.
16. Schmedtje JF Jr, Ji Y-S, Liu W-L, DuBois RN, Runge MS. Hypoxia induces cyclooxygenase-2 via the NF-κB p65 transcription factor in human vascular endothelial cells. *J Biol Chem.* 1997;272:601–608.
17. Reeves R, Wolffe AP. Substrate structure influences binding of the non-histone protein HMG-I(Y) to free and nucleosomal DNA. *Biochemistry.* 1996;35:5063–5074.
18. Goppelt-Struebe M. Regulation of prostaglandin endoperoxide synthase (cyclooxygenase) isozyme expression. *Prostaglandins Leukot Essent Fatty Acids.* 1995;52:213–222.
19. Wu KK. Cyclooxygenase 2 induction: molecular mechanism and pathophysiologic roles. *J Lab Clin Med.* 1996;128:242–245.
20. Xie WL, Herschman HR. Transcriptional regulation of prostaglandin synthase 2 gene expression by platelet-derived growth factor and serum. *J Biol Chem.* 1996;271:31742–31748.
21. Zembowicz A, Jones SL, Wu KK. Induction of cyclooxygenase-2 in human umbilical vein endothelial cells by lysophosphatidylcholine. *J Clin Invest.* 1995;96:1688–1692.
22. Inoue H, Yokoyama C, Hara S, Tone Y, Tanabe T. Transcriptional regulation of human prostaglandin-endoperoxide synthase-2 gene by lipopolysaccharide and phorbol ester in vascular endothelial cells: involvement of both nuclear factor for interleukin-6 expression site and cAMP response element. *J Biol Chem.* 1995;270:24965–24971.
23. Appleby SB, Ristimäki A, Neilson K, Norko K, Hla T. Structure of the human cyclo-oxygenase-2 gene. *Biochem J.* 1994;302:723–727.
24. Srivastava SK, Tetsuka T, Daphna-Iken D, Morrison AR. IL-1β stabilizes COX II mRNA in renal mesangial cells: role of 3'-untranslated region. *Am J Physiol.* 1994;267:F504–F508.
25. Xie W, Fletcher BS, Andersen RD, Herschman HR. v-src induction of the TIS10/PGS2 prostaglandin synthase gene is mediated by an ATF/CRE transcription response element. *Mol Cell Biol.* 1994;14:6531–6539.
26. Bradford MM. A rapid and sensitive method for the quantitation of microgram quantities of protein using the principle of protein-dye binding. *Anal Biochem.* 1976;72:248–254.
27. Semenza GL, Jiang B-H, Leung SW, Passantino R, Concordet J-P, Maire P, Giallongo A. Hypoxia response elements in the aldolase A, enolase 1, and lactate dehydrogenase A gene promoters contain essential binding sites for hypoxia-inducible factor 1. *J Biol Chem.* 1996;271:32529–32537.
28. Hla T, Neilson K. Human cyclooxygenase-2 cDNA. *Proc Natl Acad Sci U S A.* 1992;89:7384–7388.
29. Eberhart CE, Coffey RJ, Radhika A, Giardiello FM, Ferrenbach S, DuBois RN. Up-regulation of cyclooxygenase 2 gene expression in

human colorectal adenomas and adenocarcinomas. *Gastroenterology*. 1994;107:1183–1188.
30. Andley UP, Hebert JS, Morrison AR, Reddan JR, Pentland AP. Modulation of lens epithelial cell proliferation by enhanced prostaglandin synthesis after UVB exposure. *Invest Ophthalmol Vis Sci*. 1994;35:374–381.
31. Thanos D, Maniatis T. Virus induction of human IFN β gene expression requires the assembly of an enhanceosome. *Cell*. 1995;83:1091–1100.
32. Xiao S, Lux ML, Reeves R, Hudson TJ, Fletcher JA. *HMGI(Y)* activation by chromosome 6p21 rearrangements in multilineage mesenchymal cells from pulmonary hamartoma. *Am J Pathol*. 1997;150:901–910.
33. Williams AJ, Powell WL, Collins T, Morton CC. HMGI(Y) expression in human uterine leiomyomata: involvement of another high-mobility group architectural factor in a benign neoplasm. *Am J Pathol*. 1997;150:911–918.
34. Kel OV, Romaschenko AG, Kel AE, Wingender E, Kolchanov NA. A compilation of composite regulatory elements affecting gene transcription in vertebrates. *Nucleic Acids Res*. 1995;23:4097–4103.
35. Nissen MS, Reeves R. Changes in superhelicity are introduced into closed circular DNA by binding of high mobility group protein I/Y. *J Biol Chem*. 1995;270:4355–4360.
36. Chiappetta G, Avantaggiato V, Visconti R, Fedele M, Battista S, Trapasso F, Merciai BM, Fidanza V, Giancotti V, Santoro M, Simeone A, Fusco A. High level expression of the HMG I(Y) gene during embryonic development. *Oncogene*. 1996;13:2439–2446.
37. Zappavigna V, Falciola L, Citterich HM, Mavilio F, Bianchi ME. HMG1 interacts with HOX proteins and enhances their DNA binding and transcriptional activation. *EMBO J*. 1996;15:4981–4991.
38. Farnet CM, Bushman FD. HIV-1 cDNA integration: requirement of HMG I(Y) protein for function of preintegration complexes in vitro. *Cell*. 1997;88:483–492.
39. Yokoyama C, Tanabe T. Cloning of human gene encoding prostaglandin endoperoxide synthase and primary structure of the enzyme. *Biochem Biophys Res Commun*. 1989;165:888–894.

STIC-ILL NPL

From: Brannock, Michael
Sent: Tuesday, May 29, 2001 3:18 PM
To: STIC-ILL
Subject: 09378046

Please provide the following refs:

Whiteway M et al., Molecular and Cellular Biology 14(5)3223-9, 1994

Ji YS et al., Circulation Research 83(3)295-304, 1998

Franchimont N, J. Clinical Investivation 100(7)1797-1803, 1997.

Li, J., et al., Molecular Endocrinology 10(3)252-64, 1996

Thank you,

Michael T. Brannock, Ph.D.
Patent Examiner, AU 1646
Crystal Mall One, 10E18
(703) 306-5876

Interleukin 6 Is Autoregulated by Transcriptional Mechanisms in Cultures of Rat Osteoblastic Cells

Nathalie Franchimont,* Sheila Rydziel,* and Ernesto Canalis*‡§

*Department of Research and ‡Department of Medicine, Saint Francis Hospital and Medical Center, Hartford, Connecticut 06105; and §The University of Connecticut School of Medicine, Farmington, Connecticut 06030

Abstract

Interleukin 6 (IL-6), a cytokine produced by skeletal cells, stimulates osteoclast recruitment. The IL-6 soluble receptor (sIL-6R) increases IL-6 activity, and IL-6 and sIL-6R levels are increased in conditions of increased bone resorption. We examined the production of IL-6 by primary rat osteoblasts (Ob cells) cultured in the presence of IL-6 and sIL-6R. IL-6 alone did not induce IL-6 transcripts, but IL-6 was stimulatory in the presence of sIL-6R. Furthermore, sIL-6R by itself increased IL-6 transcripts. Cycloheximide superinduced IL-6 transcripts and did not prevent the effect of IL-6 and sIL-6R. IL-6 in the presence of sIL-6R stimulated IL-6 rates of transcription and the activity of IL-6 promoter fragments in transiently transfected Ob cells. 5′ deletions of the IL-6 promoter and targeted mutations of the multiple response element (MRE)/cAMP responsive element (CRE), the nuclear factor for IL-6 (NF-IL-6), and the nuclear factor-κB (NF-κB) binding sites indicated that NF-IL-6 and NF-κB, in combination with MRE/CRE, binding sites are required for the induction of the IL-6 promoter by IL-6. In conclusion, IL-6 induces its own synthesis in osteoblasts by transcriptional mechanisms. This positive feedback may be important in conditions of increased bone resorption. (*J. Clin. Invest.* 1997. 100:1797–1803.) Key words: bone remodeling • osteoporosis • cytokines • DNA-binding sites • transcription factors

Introduction

Interleukin 6 (IL-6), a pleiotropic cytokine with osteotropic activities, is produced by multiple cells in the skeletal tissue, including cells of the osteoblast and osteoclast lineage (1, 2). IL-6 is considered an autocrine or paracrine mediator of bone resorption since it stimulates the development of osteoclasts from precursor cells (2, 3). IL-6 production in skeletal cells is stimulated by hormones, such as parathyroid hormone and 1,25-dihydroxyvitamin D_3, and by local cytokines, such as TNF and IL-1 (4–7). IL-6 may be an important intermediary in the effects of these agents on bone resorption, and it appears to mediate the bone loss observed in the estrogen-deficient state (8). Myeloma cells are a source of IL-6, and thus, this cytokine may also be responsible for the increased bone resorption observed in patients with multiple myeloma (9–11).

Although IL-6 appears to play a pivotal role in bone resorption, its mechanism of action is poorly understood. In coculture systems of mouse osteoblasts and bone marrow cells, IL-6 stimulates the formation of multinucleated osteoclast-like cells in the presence but not in the absence of the IL-6 soluble receptor (sIL-6R)[1] (12). sIL-6R can be generated by proteolytic cleavage of the IL-6 membrane–bound receptor, an 80-kD glycoprotein (gp-80), or by translation of an alternatively spliced RNA (13–15). Signal transduction occurs after the binding of IL-6 to gp-80 and the association of the complex with two 130-kD glycoproteins (gp-130). The cytoplasmic domain of gp-80 is not required for IL-6 signaling, and the sIL-6R can mediate IL-6 signals since it retains ligand-binding activity (16).

sIL-6R has been detected in biological fluids such as plasma, urine, and synovial fluid of healthy humans, and its levels, like those of IL-6, are elevated in conditions of increased bone resorption, such as multiple myeloma and estrogen deficiency (17–19). This suggests that not only IL-6 but also its soluble receptor play a role in bone resorption.

In this study, we examined whether IL-6 stimulates IL-6 production in cultures of osteoblast-enriched cells from 22-d fetal rat calvariae (Ob cells). We also postulated that the sIL-6R potentiates this autoregulation. Since IL-6 and sIL-6R levels are increased in conditions of increased bone resorption, IL-6 autoregulation in osteoblasts may be critical for IL-6 paracrine effects on osteoclast development and bone resorption. We determined the mechanisms involved and studied the regulatory elements of the rat IL-6 gene promoter responsible for the stimulatory effects of IL-6 and sIL-6R on IL-6 expression.

Methods

Cell culture. The culture method used was described in detail previously (20, 21). Parietal bones were obtained from 22-d-old fetal rats immediately after the mothers were killed by blunt trauma to the nuchal area. This project was approved by the Animal Care and Use Committee of Saint Francis Hospital and Medical Center. Cells were obtained by five sequential digestions of the parietal bone using bacterial collagenase (CLS II; Worthington Biochemical Corp., Freehold, NJ). Cell populations harvested from the third to fifth digestions were cultured as a pool. These cells were shown previously to express osteoblastic characteristics, including the production of type I collagen, high levels of alkaline phosphatase activity and osteocalcin,

Address correspondence to Ernesto Canalis, M.D., Department of Research, Saint Francis Hospital and Medical Center, 114 Woodland Street, Hartford, CT 06105-1299. Phone: 860-714-4068; FAX: 860-714-8053.

Received for publication 19 June 1997 and accepted in revised form 12 August 1997.

J. Clin. Invest.

0021-9738/97/10/1797/07 $2.00
Volume 100, Number 7, October 1997, 1797–1803
http://www.jci.org

1. *Abbreviations used in this paper:* AP-1, activation protein-1; CMV, cytomegalovirus; CRE, cAMP responsive element; gp-80 and gp-130, 80- and 130-kD glycoproteins; MRE, multiple response element; NF-IL-6, nuclear factor for IL-6; NF-κB, nuclear factor-κb; Ob cells, primary rat osteoblastic cells; sIL-6R, IL-6 soluble receptor.

and an increase in cAMP after exposure to parathyroid hormone (22). Ob cells were plated at a density of 8,000–12,000 cells/cm^2 and cultured in a humidified 5% CO_2 incubator at 37°C, maintaining a pH of 7.5. Cells were cultured in DME supplemented with nonessential amino acids (Life Technologies, Grand Island, NY) and 10% FBS (Summit, Fort Collins, CO). For RNA analysis, cells were grown to confluence ($\sim$ 50,000 cells/cm^2), transferred to serum-free medium for 20–24 h, and exposed to test agents in serum-free medium for 2–48 h, as indicated in the text and legends. For treatments lasting 48 h, test and control cultures were replaced with fresh solutions after 24 h. For the nuclear run-on experiment, subconfluent cultures of Ob cells were trypsinized, subcultured at 1:10 dilution, and grown to confluence in DME supplemented with 10% FBS. Cells were serum-deprived for 24 h, and treated for 2 or 6 h in serum-free DME. For transient transfections, cells were grown to 70% confluence, transfected in 10% FBS, serum-deprived, and treated. Recombinant human IL-6 and sIL-6R (R & D Systems, Inc., Minneapolis, MN) were dissolved in PBS containing 0.1% BSA; an equal amount of PBS containing BSA was added to control cultures. Cycloheximide (Sigma Chemical Co., St. Louis, MO) was added directly to the culture medium.

Northern blot analysis. Total cellular RNA was isolated with guanidine thiocyanate, at acid pH, followed by phenol-chloroform (Sigma Chemical Co.) extraction, or isolated by RNeasy Kit per manufacturer's instructions (QIAGEN Inc., Chatsworth, CA) (23). RNA was precipitated with isopropanol, resuspended, and reprecipitated with ethanol. The RNA recovered was quantitated by spectrometry, and equal amounts of RNA from control or test samples were loaded on a formaldehyde agarose gel after denaturation. The gel was stained with ethidium bromide to visualize rRNA, documenting equal RNA loading of the various experimental samples. RNA was then blotted onto GeneScreen Plus charged nylon (DuPont, Wilmington, DE), and the uniformity of transfer was documented by revisualization of rRNA. A 900-bp BamHI/PstI restriction fragment of rat IL-6 cDNA, and a 700-bp BamHI/SphI fragment of a mouse 18S rRNA cDNA clone (both from American Type Culture Collection, Rockville, MD) were purified by agarose gel electrophoresis (24). IL-6 and 18S rRNA cDNAs were labeled with [α-^{32}P]dATP and [α-^{32}P]dCTP (50 μCi each at a specific activity of 3,000 Ci/mmol; DuPont) using the random hexanucleotide primed second-strand synthesis method (25). Hybridizations were carried out at 42°C for 16–48 h, and posthybridization washes were performed at 65°C in 1× SSC. The bound radioactive material was visualized by autoradiography on X-AR5 film (Eastman Kodak Co., Rochester, NY), employing Cronex Lightning Plus intensifying screens (DuPont). Relative hybridization levels were determined by densitometry. Northern blot analyses shown are representative of three or more cultures.

Nuclear run-on assay. To examine changes in the rate of transcription, nuclei were isolated by Dounce homogenization in a Tris buffer, pH 7.4, containing 0.5% NP-40 (26). Nascent transcripts were labeled by incubation of nuclei in a reaction buffer containing 500 μM each ATP, CTP, and GTP, 150 U RNasin (Promega Corp., Madison, WI), and 250 μCi [α-^{32}P]UTP (3,000 Ci/mmol; DuPont) (27). RNA was isolated by treatment with DNase I and proteinase K, followed by phenol-chloroform extraction and ethanol precipitation. Linearized plasmid DNA containing $\sim$ 1 μg cDNA was immobilized onto GeneScreen Plus by slot blotting according to manufacturer's directions (DuPont). The plasmid vector pGL2-Basic (Promega Corp.) was used as a control for nonspecific hybridization, and a mouse 18S rRNA cDNA clone was used to estimate uniformity of the loading. Equal counts per minute of ^{32}P-RNA from each sample were hybridized to cDNAs at 42°C for 72 h and washed in 1× SSC at 65°C for 20 min. Hybridized cDNAs were visualized by autoradiography, and IL-6 hybridization levels were determined by densitometry.

Transient transfections. To determine changes in promoter activity, chimeric constructs of the 5′ flanking region of the IL-6 promoter and the luciferase reporter gene (kindly provided by Dr. G. Fey, Friedrich-Alexander Universität, Erlangen, Germany) were tested (28). Ob cells were cultured to $\sim$ 70% confluence and transiently transfected by calcium phosphate–DNA coprecipitation as described (29). A construct containing the cytomegalovirus (CMV) promoter-driven β-galactosidase gene (Clontech, Palo Alto, CA) was used to control for transfection efficiency. After 4 h, cells were exposed for 3 min to 10% glycerol. Ob cells were allowed to recover in serum-containing DME for 24 h, serum-deprived for 20–24 h, and exposed to control or test medium for 6–24 h as described in text and legends. Cells were washed with PBS and harvested in reporter lysis buffer (Promega Corp.). Luciferase activity was measured using a luciferase assay kit (Promega Corp.), and β-galactosidase activity was measured using Galacton reagent (Tropix, Inc., Bedford, MA), both in accordance with manufacturer's instructions. Luciferase activity was corrected for β-galactosidase activity, and data were expressed as treated/control ratios. Data are presented as means±SEM. Statistical differences were determined by ANOVA and post hoc examination by Ryan-Einot-Gabriel-Welsh F test (30, 31).

Site-directed mutagenesis. Site-directed mutagenesis was performed using the method of gene splicing by overlap extension or by using the Morph Mutagenesis Kit (5 Prime → 3 Prime, Inc., Boulder, CO) (32). The Morph Mutagenesis Kit was used in accordance with manufacturer's instructions to create targeted mutations of the multiple response element (MRE)/cAMP responsive element (CRE) and of the nuclear factor for IL-6 (NF-IL-6), alone or in combination (Fig. 1). Gene splicing by overlap extension was used to create mutations of the nuclear factor-κB (NF-κB), alone or in combination with NF-IL-6 (double mutation) or with MRE/CRE and NF-IL-6 (triple mutation). For this purpose, wild-type and mutant constructs were generated by PCR using a 5′ primer containing a SacI restriction site on the 5′ end and the sequence corresponding to bp −257 to −249 of the rat IL-6 promoter (5′-AGGCGAGCTCAAAGAAAGA-3′), in the presence of a 3′ primer corresponding to bp +6 to +20 of the rat IL-6 gene that included an XhoI restriction site on the 3′ end (5′-CCGCTCGAGA-CAGAATGA-3′). A chimeric construct containing bp −257 to +20 of the IL-6 promoter was used as a template. Mutant sense and antisense primers, used to synthesize the intermediate products, contained nucleotide sequences corresponding to the known consensus sequences of the binding sites with two or three altered bases, creating the desired targeted mutations (Fig. 1). Targeted multiple mutations of NF-IL-6 and NF-κB (double mutation) or MRE/CRE, NF-IL-6, and NF-κB (triple mutation) were generated by PCR using mutant sense and antisense primers for NF-κB in the presence of the

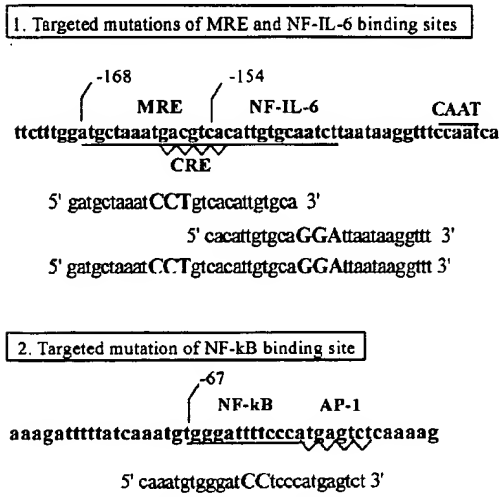

Figure 1. Oligonucleotides used for targeted mutation analysis of the IL-6 gene. *Bold*, Wild-type sequence of the IL-6 promoter. Capital letters within the primers indicate mutations used to alter the sequence of MRE/CRE, NF-IL-6, and NF-κB binding sites.

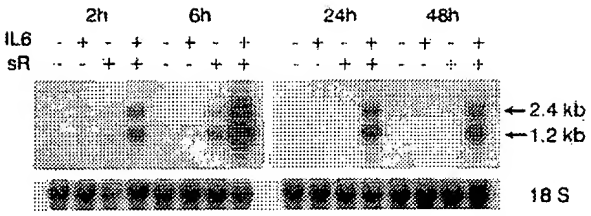

Figure 2. Effect of IL-6 at 100 and sIL-6R (*sR*) at 125 ng/ml, singly and in combination, on IL-6 mRNA levels in cultures of Ob cells treated for 2–48 h. Total RNA from control or treated cells was subjected to Northern blot analysis and hybridized with an [α-^{32}P]-labeled IL-6 cDNA. IL-6 transcripts of 1.2 and 2.4 kb were visualized by autoradiography. Blots were stripped and rehybridized with an [α-^{32}P]-labeled 18S rRNA cDNA. *Upper panel*, IL-6 transcripts. *Lower panel*, 18S rRNA transcripts.

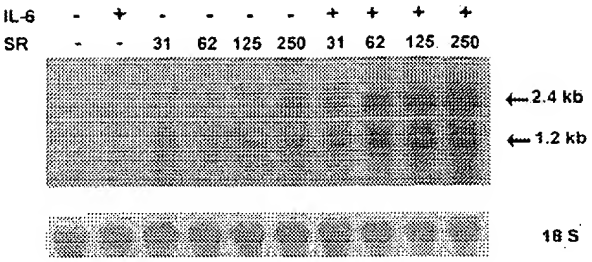

Figure 4. Effect of sIL-6R (*SR*) at 31–250 ng/ml in the presence (+) or absence (−) of IL-6 on IL-6 mRNA levels in cultures of Ob cells treated for 6 h. Total RNA from control, IL-6–, or sIL-6R–treated cells was subjected to Northern blot analysis and hybridized with an [α-^{32}P]-labeled IL-6 cDNA. IL-6 transcripts of 1.2 and 2.4 kb were visualized by autoradiography. Blots were stripped and rehybridized with an [α-^{32}P]-labeled 18S rRNA cDNA. *Upper panel*, IL-6 transcripts. *Lower panel*, 18S rRNA transcripts.

NF-IL-6 or MRE/CRE and NF-IL-6 mutated constructs as a template. Newly synthesized wild-type and target-mutated IL-6 promoter fragments were cloned into pGL-3 Basic (Promega Corp.) containing a luciferase reporter gene. Sequences of the wild-type and mutated constructs generated by either the Morph Mutagenesis Kit or PCR were confirmed by DNA sequence analysis using the Sequenase Version 2.0 DNA sequencing kit (United States Biochemical Corp., Cleveland, OH).

Results

Northern blot analysis of total RNA from serum-deprived confluent Ob cells revealed limited expression of a 1.2- and a 2.4-kb IL-6 transcript. IL-6 by itself did not induce IL-6 transcripts, but in the presence of sIL-6R, IL-6 caused a time- and dose-dependent stimulation of IL-6 mRNA levels (Figs. 2 and 3). IL-6 at 100 ng/ml in the presence of sIL-6R at 125 ng/ml induced IL-6 mRNA levels after 2 h; the effect was maximal after 6 h, and was sustained for 24–48 h (Fig. 2). In the presence of sIL-6R, the effect of IL-6 was observed at concentrations of 1–300 ng/ml (Fig. 3). sIL-6R at 31–250 ng/ml also caused a dose-dependent induction of IL-6 mRNA, and this effect was observed in the presence and absence of IL-6 at 100 ng/ml (Fig. 4). To determine whether the autoregulation of IL-6 was dependent on protein synthesis, Ob cells were treated for 6 h with IL-6 at 100 and sIL-6R at 125 ng/ml in the presence or absence of the protein synthesis inhibitor cycloheximide at 3.6 μM. Cycloheximide superinduced IL-6 mRNA levels and did not prevent the effect of IL-6 and sIL-6R (Fig. 5).

To analyze the mechanisms involved in the autoregulation of IL-6, we examined the effects of IL-6 and sIL-6R on the rate of transcription of the IL-6 gene by a nuclear run-on assay performed on nuclei from Ob cells exposed to control medium or to IL-6 at 100 and sIL-6R at 50 ng/ml for 2 and 6 h. After 6 h, IL-6 in the presence of sIL-6R increased IL-6 transcription rates 2–2.5-fold, demonstrating a transcriptional effect (Fig. 6).

To confirm that IL-6 autoregulation occurs by transcriptional mechanisms, and to define gene elements responsible for the effect, Ob cells were transfected transiently with chimeric constructs containing fragments of the IL-6 promoter linked to the reporter gene luciferase. The effects of IL-6 at 100 and sIL-6R at 125 ng/ml alone or in combination were tested for 6–24 h on a bp −2906 to +20 fragment of the rat IL-6 promoter. IL-6 or sIL-6R alone caused a small, for the most part not statistically significant, stimulatory effect on promoter

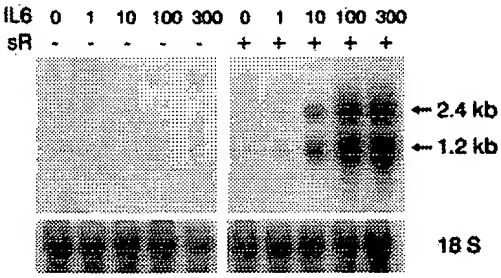

Figure 3. Effect of IL-6 at 1–300 ng/ml in the presence (+) and absence (−) of sIL-6R (*sR*) at 125 ng/ml on IL-6 mRNA levels in cultures of Ob cells treated for 6 h. Total RNA from control, IL-6–, or sIL-6R–treated cells was subjected to Northern blot analysis and hybridized with an [α-^{32}P]-labeled IL-6 cDNA. IL-6 transcripts of 1.2 and 2.4 kb were visualized by autoradiography. Blots were stripped and rehybridized with an [α-^{32}P]-labeled 18S rRNA cDNA. *Upper panel*, IL-6 transcripts. *Lower panel*, 18S rRNA transcripts.

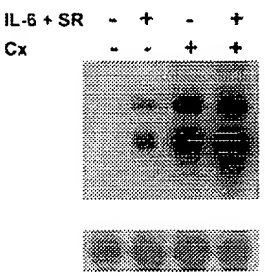

Figure 5. Effect of IL-6 at 100 and sIL-6R (*SR*) at 125 ng/ml in the presence (+) or absence (−) of cycloheximide (*Cx*) at 3.6 μM on IL-6 mRNA levels in cultures of Ob cells treated for 6 h. Total RNA from control, cycloheximide-, or IL-6 + sIL-6R–treated cells was subjected to Northern blot analysis and hybridized with an [α-^{32}P]-labeled IL-6 cDNA. IL-6 transcripts of 1.2 and 2.4 kb were visualized by autoradiography. Blots were stripped and rehybridized with an [α-^{32}P]-labeled 18S rRNA cDNA. *Upper panel*, IL-6 transcripts. *Lower panel*, 18S rRNA transcripts.

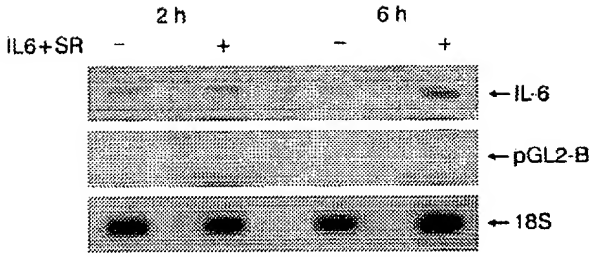

Figure 6. Effect of IL-6 at 100 ng/ml in the presence of sIL-6R (*SR*) at 50 ng/ml on IL-6 transcription rates in cultures of Ob cells treated for 2 and 6 h. Nascent transcripts from control (−) or IL-6– and sIL-6R (+)-treated cultures were labeled in vitro with [α-^{32}P]UTP, and the labeled RNA was hybridized to immobilized cDNA for IL-6. 18S rRNA cDNA was used to demonstrate loading, and pGL2-Basic vector DNA was used as a control for nonspecific hybridization.

activity (Fig. 7). However, IL-6 at 100 ng/ml, in the presence of sIL-6R at 125 ng/ml, caused an eightfold increase in promoter activity after 6 h, and a 13–16-fold stimulation after 16 and 24 h (Figs. 7 and 8). To characterize the regulatory elements involved, 5′ deletion constructs of the IL-6 promoter ranging from bp −2906 to +20 to bp −34 to +20 were tested in six different experiments. 5′ deletions from bp −2906 to −257 of the IL-6 promoter resulted in a decrease in the basal activity of the IL-6 promoter (not shown), but did not preclude the response to IL-6 in the presence of sIL-6R. IL-6 with sIL-6R induced the bp −276 to +20 and the bp −257 to +20 of the IL-6 promoter construct by 11- and 8-fold, respectively. In individual experiments, we were unable to detect consistent differences in the response of these two constructs. Deletion to bp −154 and to bp −105 resulted in a partial loss of the stimulatory effect of IL-6 and its soluble receptor, and together they increased the activity of the two constructs five- to sixfold (Fig. 8). The basal activity of the bp −34 to +20 IL-6 promoter fragment was decreased dramatically (not shown), and IL-6, with sIL-6R, did not modify the activity of this construct. These results suggest that MRE/CRE, NF-IL-6, and NF-κB binding sites contained in the bp −257 to +20 region of the IL-6 gene are potentially necessary for the response to IL-6 and sIL-6R.

To define the elements responsible for the autoregulation of IL-6, a bp −257 to +20 fragment of the IL-6 promoter was cloned into pGL-3 Basic, and targeted mutations of the known consensus sequences of MRE/CRE, NF-IL-6, and NF-κB binding sites were made singly or in combination and tested in two separate experiments, which revealed analogous results. In the experiment shown in Fig. 9, IL-6 and sIL-6R increased the activity of the bp −257 to +20 wild-type IL-6 construct sixfold. Targeted single mutations of NF-IL-6, NF-κB, or MRE/CRE binding sites resulted in a decrease in the response to IL-6 and its soluble receptor (all $P < 0.05$ vs. wild-type). The combined NF-IL-6 and NF-κB or MRE/CRE and NF-IL-6 mutations resulted in a comparable decrease in the response to IL-6

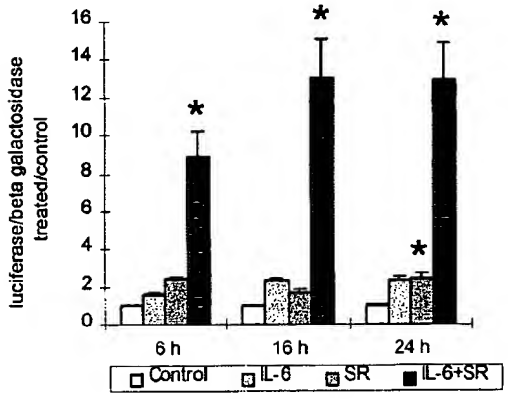

Figure 7. Effect of IL-6 at 100 and sIL-6R (*SR*) at 125 ng/ml, singly and in combination, on IL-6 promoter activity in transiently transfected Ob cells. Ob cells were transfected with 35 μg DNA of a chimeric construct containing the rat IL-6 promoter sequence of bp −2906 to +20 linked to a luciferase reporter gene by calcium phosphate–DNA coprecipitation. To control for transfection efficiency, 10 μg of a CMV–β-galactosidase expression vector was cotransfected. 24 h after transfection, Ob cells were serum-deprived for 20–24 h and exposed to IL-6 or sIL-6R singly and in combination for the indicated periods of time. Cells were harvested, and luciferase activity was determined, corrected for β-galactosidase activity, and expressed as treated/control ratios for each individual time period studied. Values are means±SEM of 18–24 observations pooled from four independent experiments; SEM not shown were too small to be depicted. *Significantly different from control ($P < 0.05$).

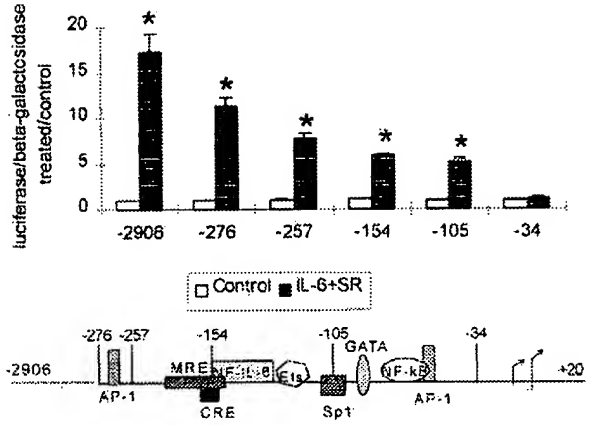

Figure 8. Effect of IL-6 at 100 ng/ml, in the presence of sIL-6R (*SR*) at 125 ng/ml, on IL-6 promoter activity in transiently transfected Ob cells. Ob cells were transfected with 35 μg DNA of chimeric constructs containing fragments of the IL-6 promoter linked to a luciferase reporter gene by calcium phosphate–DNA coprecipitation. The 5′ deletion endpoints of the IL-6 promoter are indicated (*bottom*). To control for transfection efficiency, 10 μg of a CMV–β-galactosidase expression vector was cotransfected. 24 h after transfection, Ob cells were serum-deprived for 20–24 h and exposed to IL-6 in the presence of sIL-6R for 16 h. Cells were harvested and analyzed, and luciferase activity was determined, corrected for β-galactosidase activity, and expressed as treated/control ratios for each construct tested. Values are means±SEM of 22–33 observations, pooled from six independent experiments; SEM not shown were too small to be depicted. *Significantly different from respective control ($P < 0.05$). (*Bottom*) Putative *cis*-regulatory elements of the rat IL-6 promoter with their approximate locations relative to the major start site. *Bars*, 5′ deletion points of the truncated constructs used.

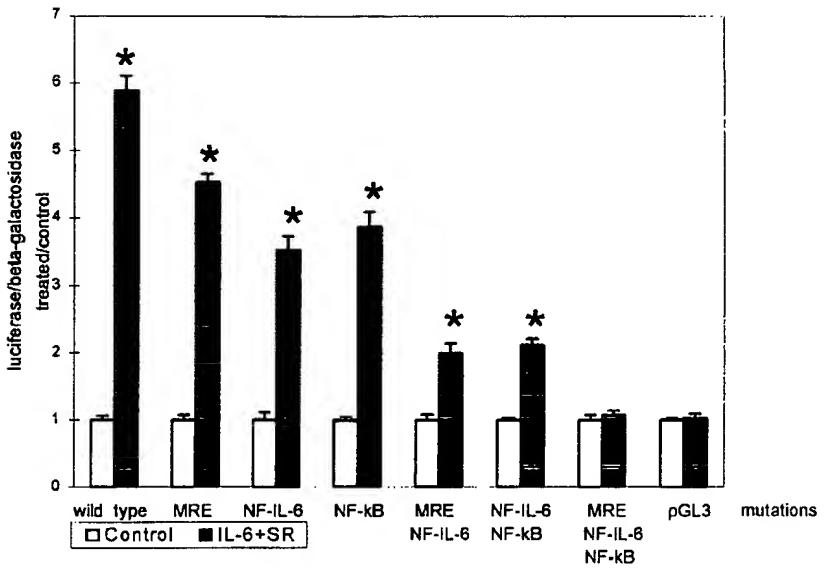

Figure 9. Effect of IL-6 at 100 ng/ml, in the presence of sIL-6R (*SR*) at 125 ng/ml, on IL-6 promoter activity in transiently transfected Ob cells. Ob cells were transfected with 35 μg of a chimeric construct containing a bp −257 to +20 fragment of the IL-6 promoter, with or without mutations of MRE, NF-IL-6, and NF-κB alone or mutations of the combinations MRE and NF-IL-6, NF-IL-6 and NF-κB, and MRE, NF-IL-6, and NF-κB. Constructs were linked to a luciferase reporter gene and transfected by calcium phosphate–DNA coprecipitation. To control for transfection efficiency, 10 μg of a CMV–β-galactosidase expression vector was cotransfected. 24 h after transfection, Ob cells were serum-deprived for 20–24 h and exposed to IL-6 in the presence of sIL-6R for 16 h. Cells were harvested, and luciferase activity was determined, corrected for β-galactosidase activity, and expressed as treated/control ratios for each construct tested. Values are means±SEM of six observations. *Significantly different from control ($P < 0.05$).

and sIL-6R, which was more pronounced than the decrease observed with single mutations ($P < 0.05$). The triple mutation of MRE/CRE, NF-IL-6, and NF-κB resulted in a total loss of the IL-6 promoter response to IL-6 and sIL-6R ($P < 0.05$ vs. wild-type, and all constructs with single or double mutations).

Discussion

In these studies, we have demonstrated that IL-6 in the presence of its soluble receptor induces IL-6 mRNA in Ob cells. Although IL-6 has been shown to induce IL-6 mRNA in the osteoblastic cells MC3T3-E1, the effect was small and only detected by reverse transcription-PCR (33). The lack of an IL-6 effect when tested alone is probably due to the low level of expression of the membrane-bound IL-6 receptor in Ob cells or due to receptor downregulation. IL-6 binds an 80-kD surface glycoprotein, and the IL-6/surface receptor complex associates with gp-130 molecules, which activate the JAK/STAT signal transduction pathway (34). A soluble form of the IL-6 receptor is present in human and mouse serum and was found to enhance the effects of IL-6 in various cell types, including osteoclasts (12, 17, 35). Similarly, we showed that the effects of IL-6 on IL-6 transcripts in Ob cells were observed in the presence of its soluble receptor. Moreover, increasing concentrations of sIL-6R induced IL-6 transcripts in the absence of exogenous IL-6, suggesting that endogenous IL-6 is produced in sufficient amounts to induce its own synthesis in the presence of its soluble receptor.

The sIL-6R is a 55-kD protein generated by proteolytic cleavage of the membrane-bound receptor at a site adjacent to the transmembrane domain, or by translation of an alternatively spliced RNA (13–15, 36, 37). The sIL-6R binds IL-6 with similar affinity as the membrane-bound receptor, and the complex can elicit IL-6 signaling in cells that do not express cell surface–associated receptor, provided that they express gp-130 (14). This indicates that the sIL-6R is sufficient to mediate IL-6 action. sIL-6R can be measured in human serum, and elevated levels are associated with conditions of increased bone resorption, such as multiple myeloma or estrogen deficiency (18, 19). However, it is not known whether or not osteoblasts or other cells present in the bone environment produce sIL-6R. The concentrations of sIL-6R used in these studies are similar to those found in serum, suggesting that the amplification of the IL-6 effect by its soluble receptor is physiologically or pathologically relevant.

To study the mechanisms of IL-6 stimulation of its own synthesis, we tested the effect of the protein synthesis inhibitor cycloheximide. As previously described, cycloheximide superinduced IL-6 transcripts, suggesting stabilization of IL-6 mRNA (38). In the presence of cycloheximide, IL-6 and sIL-6R had an additive effect on IL-6 mRNA levels, demonstrating that IL-6 autoregulation is not protein synthesis dependent. In addition, we have shown that the autoregulation of IL-6 occurs at the transcriptional level, since IL-6 in the presence of sIL-6R enhanced IL-6 rates of transcription and promoter activity. Using 5′ deletion constructs, we demonstrated that a bp −257 to +20 fragment of the IL-6 promoter is responsive to IL-6 and sIL-6R. The −257 to + 20 region of the IL-6 gene contains important sequences, including MRE/CRE, NF-IL-6, and NF-κB binding sites, and these sequences are essential for the response of IL-6 to IL-1 and TNF-α (39, 40). In hepatocytes, IL-6 increases NF-IL-6 mRNA levels and NF-IL-6 binding activity (40, 41). In this study, we demonstrated that an NF-IL-6 binding site is necessary for the response of the IL-6 promoter to IL-6, but mutation of the NF-IL-6 binding site was not sufficient to abolish the response to IL-6. Even though experiments using 5′ deletion constructs indicated that MRE/CRE or NF-κB binding sites are involved in the response to IL-6 and its soluble receptor, single targeted mutations of MRE/CRE or NF-κB did not abrogate the response of the IL-6 promoter. When NF-

IL-6 and NF-κB binding sites were mutated in combination, the response of the IL-6 promoter to IL-6 and sIL-6R was decreased further, and when all three binding sites were mutated, no response to IL-6 and sIL-6R was observed. These results indicate that MRE/CRE, NF-IL-6, and NF-κB could operate synergistically, an observation supported by previous work demonstrating that both NF-IL-6 and NF-κB binding sites are required for the regulation of immune and acute-phase response genes such as the IL-6 gene (42). Similar to our results, prostaglandin and cAMP activation of the IL-6 gene require MRE, NF-IL-6, and NF-κB binding sites as well as an activation protein-1 (AP-1) binding site (43). In this study, we were unable to detect consistent differences in the response of the bp −276 to +20 and bp −257 to +20 construct to IL-6 and sIL-6R, indicating that the AP-1 site located at bp −263 to −269 of the IL-6 promoter probably does not play a central role in the autoregulation of IL-6 in osteoblasts. Additional regulatory binding sites upstream of bp −276 may be required for the IL-6 promoter response to IL-6 and sIL-6R, since deletions from bp −2906 to −276 resulted in a decrease in the response to IL-6 and sIL-6R.

In conclusion, IL-6 synthesis is autoinduced in osteoblastic cells by transcriptional mechanisms, an effect that requires the presence of sIL-6R. IL-6 autoregulation may play a central role in the effects of IL-6 on bone resorption.

Acknowledgments

The authors thank Dr. G. Fey for providing IL-6 promoter constructs, Cathy Boucher, Bari Gabbitas, and Deena Durant for technical assistance, and Mrs. Margaret Nagle for secretarial help.

This work was supported by grant AR-21707 from the National Institute of Arthritis and Musculoskeletal and Skin Diseases, National Institutes of Health. Dr. N. Franchimont was supported by a fellowship award from the Catherine Weldon Donaghue Foundation.

References

1. Roodman, G.D. 1992. Interleukin-6: an osteotropic factor? *J. Bone Miner. Res.* 7:475–478.

2. Löwik, C.W.G.M. 1992. Differentiation inducing factors: leukemia inhibitory factor and interleukin-6. *In* Cytokines and Bone Metabolism. M. Gowen, editor. CRC Press, Inc., London. 299–324.

3. Kurihara, N., C. Civin, and G.D. Roodman. 1991. Osteotropic factor responsiveness of highly purified populations of early and late precursors for human multinucleated cells expressing the osteoclast phenotype. *J. Bone Miner. Res.* 6:257–261.

4. Feyen, J.H., P. Elford, F.E. Di Padova, and U. Trechsel. 1989. Interleukin-6 is produced by bone and modulated by parathyroid hormone. *J. Bone Miner. Res.* 4:633–638.

5. Franchimont, N., Y. Vrindts, S. Gaspar, M. Lopez, R. Gathy, D. DeGroote, J.Y. Reginster, and P. Franchimont. 1993. Parathyroid hormone (1-34) stimulates and $1,25(OH)_2$ vitamin D_3 inhibits leukemia inhibitory factor (LIF) production by osteoblasts *in vitro*. *In* Proceedings 1993: Fourth International Symposium on Osteoporosis and Consensus Development Conference. C. Christiansen and B. Riis, editors. Handelstrykkeriet Aalborg ApS, Aalborg, Denmark. 249–250.

6. Helle, M., J.P.J. Brakenhoff, E.R. DeGroot, and L.A. Aarden. 1988. Interleukin-6 is involved in interleukin-1 induced activities. *Eur. J. Immunol.* 18: 957–959.

7. Littlewood, A.J., J. Russell, G.R. Harvey, D.E. Hughes, R.G.G. Russell, and M. Gowen. 1991. The modulation of the expression of IL-6 and its receptor in human osteoblasts in vitro. *Endocrinology.* 129:1513–1520.

8. Jilka, R.L., G. Hangoc, G. Girasole, G. Passeri, D.C. Williams, J.S. Abrams, B. Boyce, H. Broxmeyer, and S.C. Manolagas. 1992. Increased osteoclast development after estrogen loss: mediation by interleukin-6. *Science (Wash. DC).* 257:88–91.

9. Kawano, M., T. Hirano, T. Matsuda, T. Taga, Y. Horii, K. Iwato, H. Asaoku, B. Tang, O. Tanabe, H. Tanaka, et al. 1988. Autocrine generation and requirement of BSF-2/IL-6 for human multiple myeloma. *Nature (Lond.).* 332: 83–85.

10. Klein, B., X.G. Zhang, Z.Y. Lu, and R. Bataille. 1995. Interleukin-6 in human multiple myeloma. *Blood.* 85:863–872.

11. Bataille, R., D. Chappard, and B. Klein. 1992. The critical role of interleukin-6, interleukin-1B and macrophage colony-stimulating factor in the pathogenesis of bone lesions in multiple myeloma. *Int. J. Clin. Lab. Res.* 21: 283–287.

12. Tamura, T., N. Udagawa, N. Takahashi, C. Miyaura, S. Tanaka, Y. Yamada, Y. Koishihara, Y. Ohsugi, K. Kumaki, T. Taga, et al. 1993. Soluble interleukin-6 receptor triggers osteoclast formation by interleukin 6. *Proc. Natl. Acad. Sci. USA.* 90:11924–11928.

13. Müllberg, J., H. Schooltink, T. Stoyan, M. Günther, L. Graeve, G. Buse, A. Mackiewicz, P.C. Heinrich, and S. Rose-John. 1993. The soluble interleukin-6 receptor is generated by shedding. *Eur. J. Immunol.* 23:473–480.

14. Rose-John, S., M. Ehlers, J. Grötzinger, and J. Müllberg. 1995. The soluble interleukin-6 receptor. *Ann. NY Acad. Sci.* 762:207–221.

15. Lust, J.A., K.A. Donovan, M.P. Kline, P.R. Greipp, R.A. Kyle, and N.J. Maihle. 1992. Isolation of an mRNA encoding a soluble form of the human interleukin-6 receptor. *Cytokine.* 4:96–100.

16. Taga, T., M. Hibi, Y. Hirata, K. Yamasaki, K. Yasukawa, T. Matsuda, T. Hirano, and T. Kishimoto. 1989. Interleukin-6 triggers the association of its receptor with a possible signal transducer, gp130. *Cell.* 58:573–581.

17. Frieling, J.T.M., R.W. Sauerwein, J. Wijdenes, T. Hendriks, and C.J. van der Linden. 1994. Soluble interleukin 6 receptor in biological fluids from human origin. *Cytokine.* 6:376–381.

18. Gaillard, J.-P., R. Bataille, H. Brailly, C. Zuber, K. Yasukawa, M. Attal, N. Maruo, T. Taga, T. Kishimoto, and B. Klein. 1993. Increased and highly stable levels of functional soluble interleukin-6 receptor in sera of patients with monoclonal gammopathy. *Eur. J. Immunol.* 23:820–824.

19. Girasole, G., M. Pedrazzoni, N. Giuliani, G. Passeri, and M. Passeri. 1995. Increased serum soluble interleukin-6 receptor levels are induced by ovariectomy, prevented by estrogen replacement and reversed by alendronate administration. *J. Bone Miner. Res.* 10:S160. (Abstr.)

20. Centrella, M., T.L. McCarthy, W.F. Kusmik, and E. Canalis. 1991. Relative binding and biochemical effects of heterodimeric and homodimeric isoforms of platelet-derived growth factor in osteoblast-enriched cultures from fetal rat bone. *J. Cell. Physiol.* 147:420–426.

21. Centrella, M., T.L. McCarthy, and E. Canalis. 1989. Platelet-derived growth factor enhances deoxyribonucleic acid and collagen synthesis in osteoblast-enriched cultures from fetal rat parietal bone. *Endocrinology.* 125:13–19.

22. McCarthy, T.L., M. Centrella, and E. Canalis. 1988. Further biochemical and molecular characterization of primary rat parietal bone cell cultures. *J. Bone Miner. Res.* 3:401–408.

23. Chomczynski, P., and N. Sacchi. 1987. Single-step method of RNA isolation by acid guanidinium thiocyanate-phenol-chloroform extraction. *Anal. Biochem.* 162:156–159.

24. Northemann, W., T.A. Braciak, M. Hattori, F. Lee, and G.H. Fey. 1989. Structure of the rat interleukin 6 gene and its expression in macrophage-derived cells. *J. Biol. Chem.* 264:16072–16082.

25. Feinberg, A.P., and B. Vogelstein. 1984. A technique for radiolabeling DNA restriction endonuclease fragments to high specific activity. *Anal. Biochem.* 137:266–267.

26. Ausubel, F.M., R. Brent, R.E. Kingston, D.D. Moore, J.G. Seidman, J.A. Smith, and K. Struhl. 1995. Preparation and analysis of RNA. *In* Current Protocols in Molecular Biology. John Wiley & Sons Inc., New York. 4.10.5–4.10.9.

27. Greenberg, M.E., and E.B. Ziff. 1984. Stimulation of 3T3 cells induces transcription of the c-*fos* proto-oncogene. *Nature (Lond.).* 311:433–438.

28. Baffet, G., T.A. Braciak, R.G. Fletcher, J. Gauldie, G.H. Fey, and W. Northemann. 1991. Autocrine activity of interleukin 6 secreted by hepatocarcinoma cell lines. *Mol. Biol. Med.* 8:141–156.

29. Pash, J.M., A.M. Delany, M.L. Adamo, C.T. Roberts, Jr., D. LeRoith, and E. Canalis. 1995. Regulation of insulin-like growth factor I transcription by prostaglandin E_2 in osteoblast cells. *Endocrinology.* 136:33–38.

30. Godfrey, K. 1985. Statistics in practice. Comparing the means of several groups. *N. Engl. J. Med.* 313:1450–1456.

31. Wall, F.J. 1986. Statistical Data Analysis Handbook. McGraw-Hill Inc., New York.

32. Horton, R.M. 1993. In vitro recombination and mutagenesis of DNA. SOEing together tailor-made genes. *In* Methods in Molecular Biology, Volume 15. B.A. White, editor. Humana Press Inc., Totowa, NJ. 251–261.

33. Greenfield, E.M., S.M. Shaw, S.A. Gornik, and M.A. Banks. 1995. Adenyl cyclase and interleukin 6 are downstream effectors of parathyroid hormone resulting in stimulation of bone resorption. *J. Clin. Invest.* 96:1238–1244.

34. Bellido, T., N. Stahl, T.J. Farruggella, V. Borba, G.D. Yancopoulos, and S.C. Manolagas. 1996. Detection of receptors for interleukin 6, interleukin 11, leukemia inhibitory factor, oncostatin M, and ciliary neurotrophic factor in bone marrow stromal/osteoblastic cells. *J. Clin. Invest.* 97:431–437.

35. Suzuki, H., K. Yasukawa, T. Saito, M. Narazaki, A. Hasegawa, T. Taga, and T. Kishimoto. 1993. Serum soluble interleukin-6 receptor in MRL/1pr mice is elevated with age and mediates the interleukin-6 signal. *Eur. J. Immunol.* 23: 1078–1082.

36. Heinrich, P.C., L. Graeve, S. Rose-John, J. Schneider-Mergener, E. Dit-

trich, A. Erren, C. Gerhartz, H. Ulrike, C. Lütticken, U. Wegenka, et al. 1995. Membrane-bound and soluble interleukin-6 receptor: studies on structure, regulation of expression, and signal transduction. *Ann. NY Acad. Sci.* 762:222–237.

37. Stoyan, T., U. Michaelis, H. Schooltink, M. Van Dam, R. Rudolph, P.C. Heinrich, and S. Rose-John. 1993. Recombinant soluble human interleukin-6 receptor. Expression in *Escherichia coli*, renaturation and purification. *Eur. J. Biochem.* 216:239–245.

38. Walther, Z., L.T. May, and P. B. Sehgal. 1988. Transcriptional regulation of the interferon-β_2/B cell differentiation factor BSF-2/hepatocyte-stimulating factor gene in human fibroblasts by other cytokines. *J. Immunol.* 140: 974–977.

39. Sehgal, P.B. 1992. Regulation of IL6 gene expression. *Res. Immunol.* 143:724–734.

40. Akira, S., H. Isshiki, T. Nakajima, S. Kinoshita, Y. Nishio, S. Hashimoto, S. Natsuka, and T. Kishimoto. 1992. A nuclear factor for the IL-6 gene (NF-IL6). *Chem. Immunol.* 51:299–322.

41. Akira, S., H. Isshiki, T. Sugita, O. Tanabe, S. Kinoshita, Y. Nishio, T. Nakajima, T. Hirano, and T. Kishimoto. 1990. A nuclear factor for IL-6 expression (NF-IL6) is a member of a C/EBP family. *EMBO (Eur. Mol. Biol. Organ.) J.* 9:1897–1906.

42. Matsusaka, T., K. Fujikawa, Y. Nishio, N. Mukaida, K. Matsushima, T. Kishimoto, and S. Akira. 1993. Transcription factors NF-IL6 and NF-κB synergistically activate transcription of the inflammatory cytokines, interleukin 6 and interleukin 8. *Proc. Natl. Acad. Sci. USA.* 90:10193–10197.

43. Dendorfer, U., P. Oettgen, and T.A. Libermann. 1994. Multiple regulatory elements in the interleukin-6 gene mediate induction by prostaglandins, cyclic AMP, and lipopolysaccharide. *Mol. Cell. Biol.* 14:4443–4454.

STIC-ILL

From: Brannock, Michael
Sent: Tuesday, May 29, 2001 3:18 PM
To: STIC-ILL
Subject: 09378046

Please provide the following refs:

Whiteway M et al., Molecular and Cellular Biology 14(5)3223-9, 1994

Ji YS et al., Circulation Research 83(3)295-304, 1998

Franchimont N, J. Clinical Investivation 100(7)1797-1803, 1997.

Li, J., et al., Molecular Endocrinology 10(3)252-64, 1996

Thank you,

Michael T. Brannock, Ph.D.
Patent Examiner, AU 1646
Crystal Mall One, 10E18
(703) 306-5876

MOLECULAR AND CELLULAR BIOLOGY, May 1994, p. 3223–3229
0270-7306/94/$04.00+0

Vol. 14, No. 5

Genetic Identification of Residues Involved in Association of α and β G-Protein Subunits†

MALCOLM WHITEWAY,* KAREN L. CLARK, EKKEHARD LEBERER, DANIEL DIGNARD, AND DAVID Y. THOMAS

Eukaryotic Genetics Group, National Research Council, Biotechnology Research Institute, Montreal, Quebec, Canada H4P 2R2

Received 16 December 1993/Returned for modification 24 January 1994/Accepted 7 February 1994

The *GPA1*, *STE4*, and *STE18* genes of *Saccharomyces cerevisiae* encode the α, β, and γ subunits, respectively, of a G protein involved in the mating response pathway. We have found that mutations G124D, W136G, W136R, and ΔL138 and double mutations W136R L138F and W136G S151C of the Ste4 protein cause constitutive activation of the signaling pathway. The W136R L138F and W136G S151C mutant Ste4 proteins were tested in the two-hybrid protein association assay and found to be defective in association with the Gpa1 protein. A mutation at position E307 of the Gpa1 protein both suppresses the constitutive signaling phenotype of some mutant Ste4 proteins and allows the mutant α subunit to physically associate with a specific mutant Gβ subunit. The mutation in the Gpa1 protein is adjacent to the hinge, or switch, region that is required for the conformational change which triggers subunit dissociation, but the mutation does not affect the interaction of the α subunit with the wild-type β subunit. Yeast cells constructed to contain only the mutant α and β subunits mate and respond to pheromones, although they exhibit partial induction of the pheromone response pathway. Because the ability of the modified Gα subunit to suppress the Ste4 mutations is allele specific, it is likely that the residues defined by this analysis play a direct role in G-protein subunit association.

Heterotrimeric G proteins function to transmit signals from a variety of cell surface receptor proteins to intracellular signaling components through a common molecular mechanism (32). The α and βγ subunits of heterotrimeric G proteins undergo an association-dissociation cycle in response to the interaction between the cell surface receptor and the receptor's cognate ligand. This association-dissociation cycle is regulated by guanine nucleotides. Unstimulated receptors are coupled to nonactivated G proteins in which the subunits are associated, and GDP is bound to the α subunit. The ligand-bound receptor stimulates exchange of the bound GDP for GTP, and this exchange triggers subunit dissociation; subsequent GTP hydrolysis allows reassociation of the subunits and a return to the resting state. This cycle predicts that the α subunit of G proteins is capable of undergoing a conformational change which modifies its affinity for the βγ subunit (9).

We have used a genetic approach to identify specific regions of the G protein α and β subunits that are important for their proper association with each other. The strategy of defining molecular interactions through genetics can supplement or even correct direct structural studies and can provide a high level of resolution (13, 33, 45). Previous approaches to investigating the associations among G-protein subunits have shown that deletion of the amino terminus of Gα blocks association of the Gα and Gβ subunits (10), while mutations in the switch box of G_s α prevent α-β dissociation in response to ligand stimulation of receptor (23). Furthermore, mutation of Cys-215 of G_o α prevents cross-linking to βγ, although the mutant α subunit still binds to βγ (38). In addition, several regions of transducin β have been implicated in the α-β interaction, because antibodies raised to peptides defining the amino terminus, codons 127 to 136 and codons 256 to 265, of transducin β1 block interaction with transducin α (25). These results provide a general map of potential sites of α-β interactions but lack the resolution that can be provided by a mutant selection approach.

The mating response of the yeast *Saccharomyces cerevisiae* is controlled by a hererotrimeric G protein (22) encoded by the *GPA1* (*SCG1*), *STE4*, and *STE18* genes (11, 24, 43). The Ste4 and Ste18 proteins associate to form the βγ dimer (7), which serves to activate downstream signaling components, such as the Ste20 kinase (20). The Gpa1 protein also associates with the Ste4 protein (7); the role of Gpa1 is to shut off the pheromone response by forming the inactive heterotrimer. Mutations which delete or inactivate the *GPA1* gene result in constitutive activation of the signaling pathway (11, 24). A similar phenotype is created by a dominant mutation of the *STE4* gene that activates the pathway (2). The behavior of this allele, designated Hpl because activation of the pathway causes cell cycle arrest and such alleles are thus haploid lethal, is consistent with the creation of a Ste4 protein with a reduced affinity for the α subunit.

We screened mutagenized libraries of the *STE4* gene to identify additional mutant Gβ subunits that could activate the response pathway, in this case, even in the presence of high levels of the Gpa1 protein. We used the two-hybrid protein association assay (6, 12) to determine whether these mutant proteins were defective in association with the wild-type α subunit, and we also used the mutant Gβ subunits in a search for suppressor mutations which occurred within the Gpa1 protein. This genetic approach has identified specific residues which are important in the proper association of the yeast α and β subunits.

MATERIALS AND METHODS

Strains, transformations, and media. Strain W303-1A has the genotype *MATa ade2 his3 leu2 trp1 ura3 can1*. SY2366 is an

* Corresponding author. Mailing address: Eukaryotic Genetics Group, National Research Council, Biotechnology Research Institute, 6100 Royalmount Ave., Montreal, Quebec, Canada H4P 2R2. Phone: (514) 496-6146. Fax: (514) 496-6213.

† NRCC publication 36165.

a/α diploid that is homozygous for the markers Δ*gal4* Δ*gal80* *his3* *leu2* *pGAL1-lacZ* (7). Strain DC17 has the genotype *MATα* *his1* (20). Standard genetic techniques were used (30), and yeast transformations were performed essentially by the lithium acetate procedure (15). Rich yeast medium was 1% yeast extract plus 2% Bacto Peptone containing either 2% glucose (YPD medium) or 2% galactose (YPGal). Selective yeast medium contained 0.67% yeast nitrogen base without amino acids, supplemented with the appropriate amino acids and nutrients and containing 2% of the desired carbon source (glucose, galactose, or sucrose).

Plasmids. Plasmid pL38 (21) contains the *STE4* gene under the control of the *GAL1* promoter (*pGAL1*) on the vector pRS313 (31). Plasmids pL38-21-1 and pL38-21-3 are mutants from the oligonucleotide-directed mutagenized pL38 library (21). YCpGAL-GPA1 contains the *GPA1* gene under the control of the *GAL1* promoter (34). Plasmids YCpGALG PA1-4.3 and YCpGAL-GPA1-A are mutants from the hydroxylamine-mutagenized YCpGAL-GPA1 library (34). Plasmid pC3 (11), a gift from J. Kurjan, contains the *GPA1* (*SCG1*) gene on plasmid YEp13 (5). Plasmid pSB234 (39) contained a *FUS1* promoter region regulating expression of the *lacZ* gene and was a gift from G. Fink.

pMA424 and pGAD2F were gifts of S. Fields (6). Plasmids pGAD2F.N, pKB40.1, and pKB33.23 were constructed as described before (7). Plasmids pKB85.8 and pKB86.80 were made essentially as described for pKB40.1. However, oligonucleotides KOLI-23 (5′-TTTTCCTTTTGCGGCCGCCTA TTGATAACCTGGAGACC-3′) and KOLI-24 (5′-GGTGA TCACGATGTCTGCAGCACATCAG-3′) were used as primers, and plasmids pL38-21-1 and pL38-21-3, containing the *STE4* Hpl 21-1 and *STE4* Hpl 21-3 mutations, respectively, were used as the templates. The presence of the mutation in each of these plasmids was confirmed by sequencing (29). Plasmid pKB77.1 was made as described for pKB33.23 except that plasmid YCpGAL-GPA1-4.3 was used as the template. That pKB77.1 contained the E307K mutation of *GPA1* was confirmed by sequencing (29).

***STE4* mutant selections.** Mutant libraries of plasmid pL38 (21) were transformed into strain W303-1A containing pC3 and scored for growth on galactose plates, selecting for the two plasmids. Approximately 300 transformants were scored for each library; only library 21 gave galactose-sensitive transformants. Plasmids were isolated from these colonies and transformed into *Escherichia coli*, and the sequences of the mutant genes were determined by the dideoxy procedure (29). The entire gene was sequenced for mutations 21-18 and 21-143, while only the mutagenized region was sequenced for plasmids carrying mutations 21-1, 21-3, and 21-4. In addition, the original Hpl mutation was repaired from the chromosome of strain DJ706-2-4, a gift from D. Jenness, by gap repair with an *Mlu*I deletion of plasmid M81p12 as described before (7) and then sequenced.

***GPA1* mutant selections.** The Hls mutations were identified from a library of hydroxylamine-mutagenized plasmid YCp-GAL-GPA1 (34) transformed into strain W303-1A containing pL38 with the Hpl 21-3 version of *STE4*. Approximately 3,200 transformants were screened for growth on galactose-containing medium, and two colonies which exhibited plasmid-dependent growth were identified. The entire *GPA1* gene from these plasmids was sequenced (29) to determine the site of the mutations.

Gene replacements and strain characterization. The wild-type alleles of the *GPA1* and *STE4* loci were replaced by the Hls 4.3 and Hpl 21-3 alleles, respectively, in a two-step process. A *Hin*dIII-*Sna*BI fragment including the Hls 4.3 mutation and all but the amino terminus of the *GPA1* gene was cloned between the *Sma*I and *Nru*I sites of YIp5 (37) to create M247p2. This plasmid was targeted to the *GPA1* locus by partial cleavage with *Pvu*II. Duplication of *GPA1* flanking vector sequences was confirmed by Southern blotting; resolution of the duplication was selected by growing the transformants on medium containing 5-fluoroorotic acid, which selects against the *URA3*$^+$ marker of YIp5 (3). Colonies that retained only the E307K mutation were identified by amplifying the *GPA1* region by PCR (28) with primers PCR1 (5′-CACA GAATTCGATGCTGAAACGGTGACGCA-3′) and PCR3 (5′-AAAGAATTCGAGATAATACCCTG-3′) and sequencing the region around position 307. Similarly, an *Eco*RV-*Sal*I fragment including the Hpl mutation and all but the amino terminus of the *STE4* gene was cloned into pRS306 (31) cut with *Sma*I and *Sal*I. The resulting plasmid, M248p12 was targeted to the genome by cleavage with *Mlu*I, creating a duplication of most of the *STE4* locus. Resolution of the duplication was selected by using 5-fluoroorotic acid, either for diploid strains or for haploid strains containing the Hls 4.3 allele of *GPA1*, to allow growth of the Hpl 21-3 mutant strains. Strains with the Hpl 21-3 version of *STE4* were identified by amplifying the *STE4* locus with primers KOLI-11 (5′-GGT GATCACGATGGCAGCACATCAGATGG-3′) and KOLI-23 (see above) and cleaving the resulting fragment with *Sph*I, which is diagnostic for the Hpl 21-3 mutation. A diploid strain heterozygous for the *STE4* Hpl 21-3 and for the *GPA1* Hls 4.3 alleles (DM353) was dissected, and the genotypes of the resulting segregants were determined by PCR analysis of the *STE4* and *GPA1* genes, as described above.

Growth rates, pheromone response, and mating assays. A set of isogenic segregants of DM353 containing the three viable combinations of *STE4* Hpl and *GPA1* Hls alleles were compared in several assays. The growth rates of the strains were determined by diluting overnight cultures into YPD and measuring their increase in cell density over a period of 8 h. The pheromone response of the strains was determined by embedding roughly equivalent numbers of cells in YPD agar and spotting them with various amounts of α-factor dissolved in 90% methanol (43). The pheromone response ratios were calculated as the reciprocal of the amount of α-factor required to give identically sized zones of growth inhibition; the size of the wild-type zone was defined as 1.0. Mating assays were performed as described before (43), with strain DC17 as the mating tester strain. Mating efficiency was defined as the number of diploids formed divided by the number of input haploids whose mating was being tested.

β-Galactosidase assays. To determine the basal levels of *FUS1* expression, we transformed strains with plasmid pSB234 (39), which contains the *lacZ* gene under the control of the *FUS1* promoter. Cultures were grown overnight in SD medium lacking uracil, diluted into the same medium, grown for 3 h, and harvested. For the interaction assay, transformants of strain SY2366 were grown overnight in sucrose medium lacking histidine and leucine, diluted into the same medium, and grown to the exponential phase for 5 h. In all cases, cells were harvested and assayed for β-galactosidase activity as described before (17).

Immunoblot analysis. Immunoblot analysis was performed as described before (7). Briefly, cultures were grown overnight in sucrose medium without histidine and leucine, diluted into the same medium, and grown to the exponential phase for 8 h, and total cellular protein was harvested by a boiling method. Equal amounts of extract (3×10^6 cell equivalents) of each sample were resolved by sodium dodecyl sulfate-polyacrylamide gel electrophoresis (SDS-PAGE) on a 10% polyacrylamide

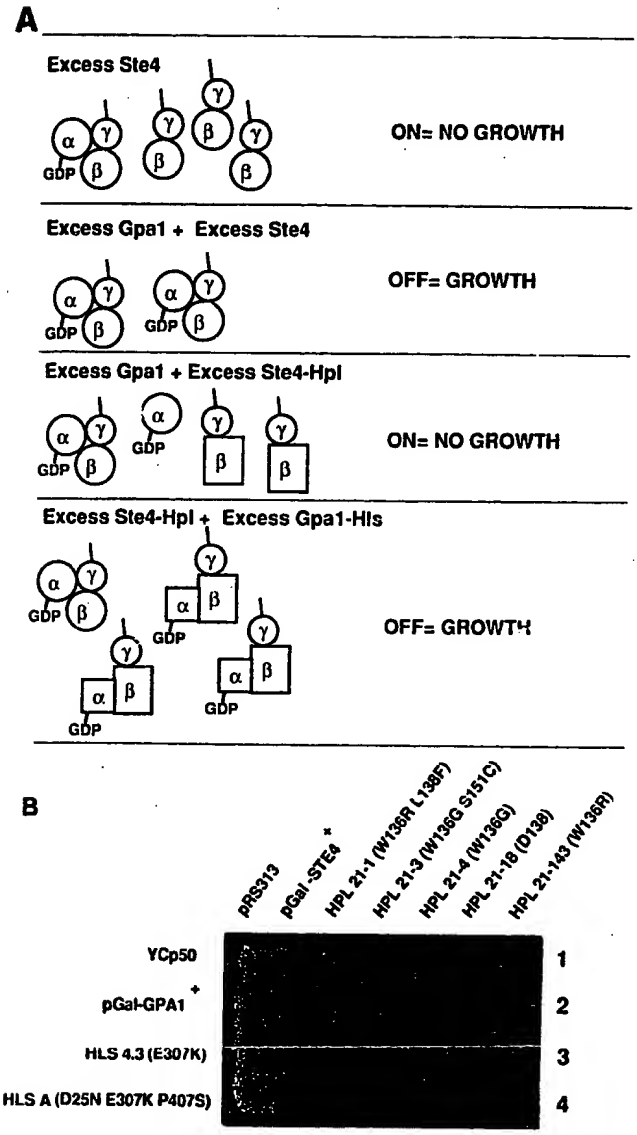

FIG. 1. (A) Model of mutant selections. In the first panel, strains that overexpress the Ste4 protein (β) have an activated pheromone response pathway and are growth arrested because of the presence of free βγ (8, 26, 44). Shaded subunits represent active signaling molecules. In the second panel, strains that overexpress both Ste4 and Gpa1 (α) have no free βγ and are able to grow (8, 26, 44). In the third panel, strains that overexpress the Hpl versions of the Ste4 protein, represented by the rectangular β, still signal in the presence of excess Gpa1 and are growth arrested. In the last panel, Hls versions of Gpa1, represented by the square α, can associate with the Hpl Ste4 proteins and prevent growth arrest. (B) Characterization of Hpl and Hls mutations. Cultures of strain W303-1A carrying either pL38, pL38 with the various Hpl mutations of *STE4* (Hpl 21-1, 21-3, 21-4, 21-18, and 21-143), or the vector pRS313 (31) were cotransformed either with vector plasmid YCp50 (27) or with plasmid YCpGAL-GPA1, containing either the wild-type *GPA1* gene or the Hls mutant allele 4.3 or A of *GPA1*. These transformants were grown on glucose-containing medium that selected for plasmid maintenance and then replica plated to galactose-containing medium. In lane 1, the transformants all contain the vector YCp50; only the strain containing the vector pRS313 is able to grow because the other plasmids all direct overexpression of a signaling-competent version of Ste4 (either wild type or Hpl). In lane 2, all the transformants contain the wild-type version of Gpa1; this allows suppression of the growth arrest of the cells containing wild-type Ste4 (column 2) but not the growth arrest of the cells containing the Hpl alleles of Ste4. In lane 3, all the transformants contain Gpa1 Hls mutant 4.3; this allows suppression of the cellular arrest created by Ste4 and the Ste4 Hpl mutants 21-1 (weak), 21-3, 21-4, and 21-18 but not Hpl 21-143. In lane 4, all the transformants contain Gpa1 Hls mutant A; this allows suppression of the cellular arrest caused by Ste4 and the Hpl mutants 21-1 (weak), 21-3, 21-4, and 21-18 but not Hpl 21-143.

gel and analyzed by immunoblotting with goat anti-rabbit immunoglobulin G coupled to horseradish peroxidase (Bio-Rad) and a chemiluminescent substrate (ECL System; Amersham, Inc.). The primary antiserum, a gift of J. Hopper, was rabbit antiserum to full-length Gal4, used at a 1:2,500 dilution.

RESULTS

Isolation of haploid-lethal alleles of *STE4*. Overproduction of Gpa1 normally corrects the cell cycle arrest phenotype created by overexpression of Ste4 (8, 26, 44). We used this observation to develop an assay for new Hpl mutants (Fig. 1A). We screened populations of mutagenized Ste4 proteins for those which still caused a cell cycle arrest phenotype when overexpressed from the strong, regulated *GAL1* promoter in cells containing a high level of the *GPA1* gene product. Such Ste4 proteins were insensitive to the action of Gpa1 but were still functional in signaling (Fig. 1B). Five independent mutants were identified in two screens of libraries created by oligonucleotide-directed random mutagenesis of the entire *STE4* sequence (21). All of these mutations were in the region between the codons for amino acids 126 and 151; no mutations were identified elsewhere in the gene even though the mutagenesis was extensive (10 to 30% sterile cells) throughout the gene (21). These five alleles were sequenced; three, Hpl 21-4 (W136G), Hpl 21-143 (W136R), and Hpl 21-18 (D138) had single amino acid changes, and two, Hpl 21-3 (W136G S151C) and Hpl 21-1 (W136R L138F), had double changes. We also sequenced the original Hpl mutation (2) and determined it to be a change of glycine 124 to aspartic acid. Thus, a small region of the Ste4 protein appears to be necessary for proper interaction with the Gpa1 protein but not for other facets of Ste4 function.

Isolation of compensatory suppressor alleles of *GPA1*. We next looked for *GPA1* alleles that could suppress the constitutive arrest created by the *STE4* mutations (Fig. 1A). A library of hydroxylamine-mutagenized *GPA1* genes (34) was screened for suppressors of the Hpl 21-3 (W136G S151C) allele of *STE4*; this allele was selected because it introduced a new *Sph*I site into the *STE4* gene that could facilitate allele identification. Two independent mutations in *GPA1* were identified and sequenced. Mutant 4.3 had a single amino acid change, E307K, while mutant A had the E307K change as well as changes D25N and P407S.

We determined the ability of these two mutants to suppress the lethality of our five Hpl alleles on galactose medium (Fig. 1B). *GPA1* variant Hls (haploid-lethal suppressor) 4.3 efficiently suppressed mutations 21-3 (W136G S151C), 21-4 (W136G), and 21-18 (D138); it poorly suppressed 21-1 (W136R L138F); and it did not significantly modify the phenotype created by mutation 21-143 (W136R). *GPA1* variant Hls A failed to suppress 21-143, suppressed 21-1 and 21-18 poorly, and suppressed 21-3 and 21-4 reasonably well. Hence, the Hpl allele containing the W136R mutation in combination with the L138F mutation was weakly suppressed by the Hls 4.3 mutation, although the allele having just the single W136R mutation was not suppressed. These results point to complex

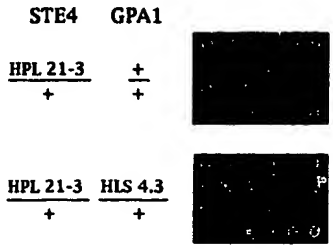

FIG. 2. (Top) Dissection of strain DM348-4, which is heterozygous for the Hpl 21-3 allele of *STE4*. Only two spores from each ascus give rise to viable colonies; the other spores germinate but arrest after one to several divisions as large, morphologically aberrant, unbudded cells. This behavior is characteristic of cells constitutively expressing the pheromone response pathway (2, 11, 24). (Bottom) Dissection of diploid DM353, which is heterozygous for both the Hpl 21-3 allele of the *STE4* gene and the Hls 4.3 allele of *GPA1*. The inviability of half the spores containing the Hpl 21-3 allele is suppressed by the Hls mutation, so the tetrads frequently contain three or four viable spores per ascus.

TABLE 2. Physical association of Gpa1 and Ste4 fusion proteins

Plasmids	Protein fused to Gal4 at:		Activity[a]
	DNA-binding domain	Transcription activation domain	
pKB33.23 + pKB40.1	Gpa1	Ste4	140
pKB77.1 + pKB40.1	Gpa1 Hls 4.3	Ste4	140
pKB33.23 + pKB86.80	Gpa1	Ste4 Hpl 21.3	<0.07
pKB77.1 + pKB86.80	Gpa1 Hls 4.3	Ste4 Hpl 21.3	2.4
pKB33.23 + pKB85.8	Gpa1	Ste4 Hpl 21.1	<0.07
pKB77.1 + pKB85.8	Gpa1 Hls 4.3	Ste4 Hpl 21.1	
pKB33.23 + pGAD2F.N	Gpa1	NF[b]	<0.07
pKB77.1 + pGAD2F.N	Gpa1 Hls 4.3	NF	<0.07
pMA424 + pKB86.80	NF	Ste4 Hpl 21.3	<0.07
pMA424 + pKB85.8	NF	Ste4 Hpl 21.1	<0.07
pMA424 + pGAD2F.N	NF	NF	<0.07

[a] β-Galactosidase activity of transformants of strain SY2366 harboring the indicated plasmids in the two-hybrid assay. Results are the averages for two to four transformants and varied less than 70% from the mean. Units are modified Miller units (17).
[b] NF, no fusion.

allele-specific interactions between the subunits. Because the single E307K mutation was a more effective suppressor than the triple mutation, it appears that the D25N and P407S changes in Gpa1 are not involved in aiding interaction with the Ste4 proteins containing the Hpl mutations.

Comparison of isogenic strains containing Hpl and Hls mutations. We constructed isogenic strains with the various combinations of Hpl and Hls mutations replaced into the genome to assess the consequences of the amino acid replacements on the yeast mating response. Diploid strains heterozygous for the Hpl 21-3 mutation sporulated to give only two viable spores (Fig. 2); the other two spores germinated but arrested after one or two divisions as the large, unbudded, morphologically aberrant cells characteristically caused by constitutive activation of the response pathway (2, 11, 24). Diploids heterozygous for both the Hpl 21-3 mutation and the Hls 4.3 mutation frequently generated three or four viable spores, consistent with the Hls allele of *GPA1* suppressing the cell cycle arrest caused by the Hpl allele of *STE4* (Fig. 2).

PCR analysis was used to identify cells containing the three viable combinations of alleles, and various physiological aspects of the mating response were measured (Table 1). Wild-type *STE4* strains containing the wild-type or Hls 4.3 allele of the *GPA1* gene were indistinguishable; they had similar growth rates and pheromone sensitivities, low basal expression of the pheromone-inducible *FUS1* promoter, and similar mating efficiencies. In contrast, the *STE4* Hpl *GPA1* Hls double mutant strain grew more slowly, was more pheromone sensitive, and had a higher basal level of *FUS1* promoter expression than the wild-type strain. Thus, the combination of the mutant Gα and Gβ subunits does not reestablish a completely wild-type G protein. All the strains were efficient maters; in fact, the double-mutant strain generated more diploids than would be expected from the input haploid cells, a pattern that could be caused by a fraction of the cells being competent to mate but not to form vegetative colonies.

Physical interaction between mutant proteins. We used the two-hybrid in vivo protein association assay (6, 12) to provide a physical basis for the genetic observations. We had shown previously that this assay could detect the interaction of the wild-type yeast α and β subunits (7). The Hls 4.3 mutation of Gpa1, which did not affect the ability of this subunit to function when combined with Ste4 (Table 1), also did not affect the α-β association detected in the two-hybrid assay (Table 2). In contrast, constitutive activation of the pheromone response pathway by the Ste4 Hpl mutants 21-1 and 21-3 corresponded to a complete disruption of α-β association (Table 2). This was not due to some destabilization of the Ste4 Hpl mutant proteins, because immunoblot analysis showed that the mutant proteins were as stable as the wild type (Fig. 3 and data not shown), although in the case of both the mutant and the wild type, the presence of the Gal4 transcription activation domain-Ste4 fusion protein reduced the amount of Gal4 DNA-binding domain-Gpa1 fusion protein observable by immunoblot assay. When the Hpl 21-3 and Hls 4.3 proteins were assayed, it was found that the suppression of the Hpl 21-3 allele by the Hls 4.3 allele corresponded to reestablishment of a detectable protein-

TABLE 1. Comparison of wild-type and mutant strains

Strain	Allele		Growth rate[a] (h/division)	Relative pheromone response[b]	Mating efficiency[c]	Basal *FUS1* expression[d]
	GPA1	*STE4*				
M353-1B	+	+	3.1 ± 0.2	1.0	0.5 ± 0.1	0.05 ± 0.01
M353-2A	Hls 4.3	+	3.0 ± 0.2	1.0	0.40 ± 0.1	0.10 ± 0.02
M353-2B	Hls 4.3	Hpl 21-3	4.6 ± 0.7	4.5	1.2 ± 0.2	8.0 ± 0.3

[a] The growth rate results are the averages of two experiments ± standard error.
[b] The pheromone response ratios were calculated as the reciprocal of the amount of α-factor required to give identically sized zones of growth inhibition; the size of the wild-type zone was defined as 1.0, and the experiment was repeated three times.
[c] The mating efficiencies are the averages of two to four repeats ± standard error.
[d] Basal *FUS1* expression is represented as β-galactosidase activity (see Materials and Methods) in modified Miller units (17) and represents the average of three repetitions ± standard error. Pheromone-induced levels are approximately 50 U (data not shown).

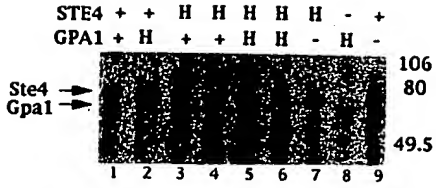

FIG. 3. Immunoblot analysis of Gpa1 and Ste4 fusion proteins. Equal amounts of cell extract (3×10^6 cell equivalents) from transformants of strain SY2366 were immunoblotted with antiserum to full-length Gal4 as described in Materials and Methods. The wild-type Ste4 and Gpa1 fusions (+) and the Hpl and Hls mutants (H) are indicated above the lanes. Lanes marked with dashes contain vectors. Lane 1, pKB40.1 plus pKB33.23 transformant; lane 2, pKB40.1 plus pKB77.1 transformant; lanes 3 and 4, two different pKB86.80 + pKB33.23 transformants; lanes 5 and 6, two different pKB86.80 plus pKB77.1 transformants; lane 7, pKB86.80 plus pMA424 transformant; lane 8, pGAD2F.N plus pKB77.1 transformant; lane 9, pKB40.1 plus pMA424 transformant. The positions of protein molecular mass standards (in kilodaltons) are shown, as are the positions of the Gal4 transactivation domain-Ste4 fusion proteins (Ste4) and the Gal4 DNA-binding domain-Gpa1 fusion proteins (Gpa1).

protein association; this combination of alleles created a G protein which allowed a partial constitutive activation of the response pathway, and the two-hybrid assay detected an association that was about 50 times weaker than for the wild-type proteins (Table 2). Finally, the weak genetic suppression of the Hpl 21-1 allele of *STE4* by the Hls 4.3 allele of *GPA1* did not create a physical association that was strong enough to be detected by the two-hybrid assay (Table 2). These results establish a direct correlation between physical association of the α and β subunits and inactivation of signaling.

DISCUSSION

The pheromone response pathway of *S. cerevisiae* allows the investigation of G-protein function in a genetically tractable system. We have used genetic selections to identify mutations of the α and β G-protein subunits that affect subunit association. These mutants were of two classes: β mutants (Hpl), which disrupted α-β interaction, and α mutants (Hls), which permitted association with these mutant β subunits.

The cluster of *STE4* Hpl mutations all lay within the second copy of the WD-40 repeat characteristic of all Gβ subunits, but

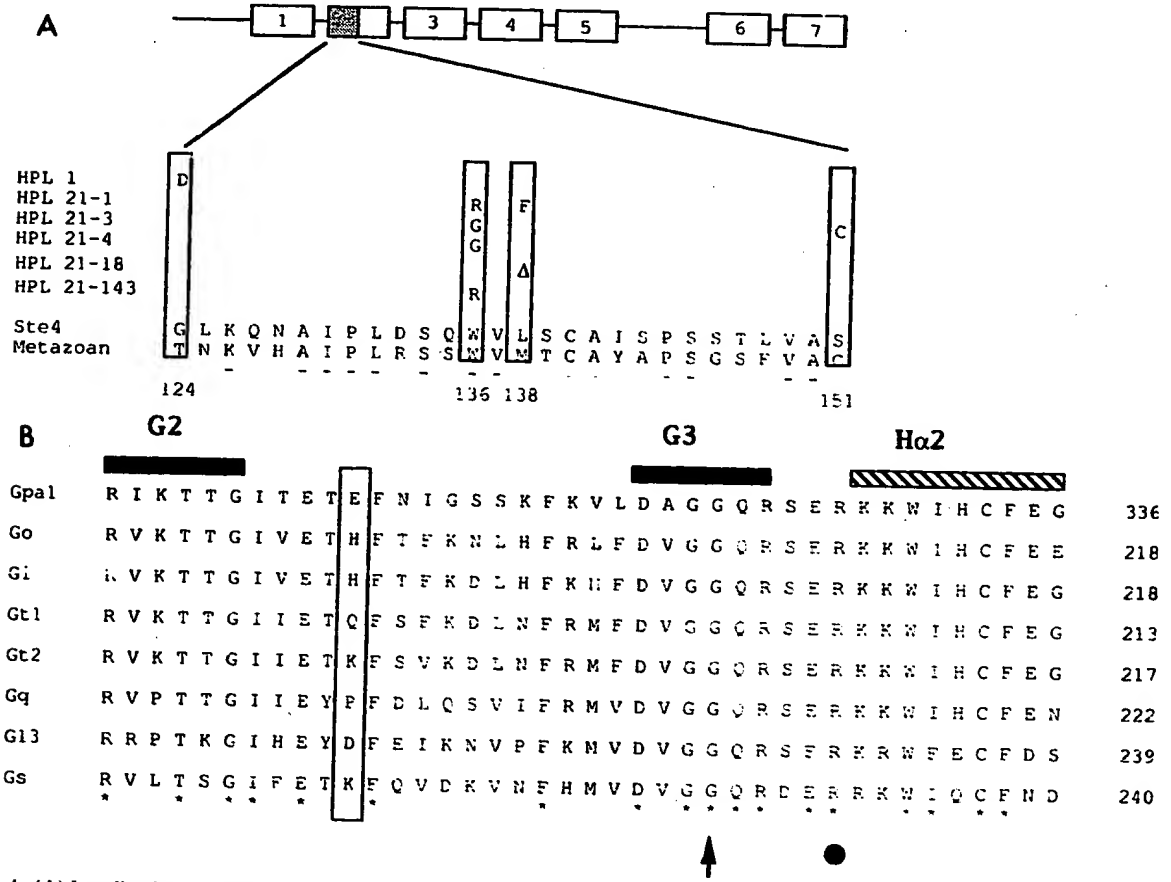

FIG. 4. (A) Localization of Hpl mutations. The seven WD-40 repeats of the Ste4 protein are shown schematically as boxes numbered 1 through 7 (41). The amino terminus and a stretch between repeats 5 and 6 are unique to the Ste4 protein relative to other Gβ proteins (43). The amino-terminal half of the second repeat contains the Hpl mutations; this region is not conserved among the various repeats in Ste4. The Hpl mutations are shown above the sequence of Ste4 from amino acids 124 to 151. The corresponding consensus sequence for metazoan Gβ subunits is also shown; amino acids which are identical between Ste4 and this consensus are underlined. (B) Region of Gpa1 surrounding the Hls mutation. The Gpa1 protein sequence around the E307 position is aligned with mammalian sequences representing various G protein subgroups (4, 16, 18, 35, 36, 40, 42). The G2 and G3 regions and the Hα2 domain are shown above the alignment, and the position 307 equivalent residues are boxed. The G residue mutated in the inactivatable Gα subunits (9, 19, 23, 34) is shown by an arrow. The conserved arginine protected from tryptic cleavage by the binding of nonhydrolyzable GTP analogs (14) is noted by a dot, and residues conserved in all the listed Gα subunits are starred.

W136 is not part of the WD pair (41). All the amino acids that are changed in the Hpl mutant alleles are conserved among metazoan G-protein β subunits; however, with the exception of the W136 residue, the Ste4 protein does not show this conservation of these residues (Fig. 4A). Our results indicate that these residues can be modified to dramatically reduce the interaction between Ste4 and Gpa1 without preventing other aspects of Ste4 function, such as effector interaction and association with Ste18, since the signaling ability of the mutant protein is not compromised. It has recently been determined that overexpression of Gpa1 will suppress the lethality caused by the initial Hpl mutation, the G124D change (46). This result is also consistent with the Hpl mutation's modifying the α-β association. Clearly, other regions of the Ste4 protein could be involved in the interaction with Gpa1, but if these regions were also required for different aspects of Ste4 function, they would not be detected in this assay.

The Hls mutation changes a residue in Gpa1 that lies between the G2 and G3 regions of the Gα subunits (1). It is intriguing that the Gpa1 Hls mutation allowed association between the α subunit and a variety of Hpl mutant Ste4 proteins but did not affect the association with the wild-type Ste4 protein, as measured either functionally or with the two-hybrid assay. It thus appears that the E307K mutation creates an α subunit with a broadened specificity for Gβ subunits. The one Hpl mutation that was not suppressed by the Hls 4.3 allele is the W136R change. From sequence similarity to the Ras protein, the G2 and G3 regions of Gpa1 are believed to be involved in forming the binding pocket for the guanine nucleotides and to lie immediately adjacent to the hinge, or switch, α-helix that undergoes a conformational change in response to guanine nucleotide exchange (9, 25a) (Fig. 4B). Mutations of a conserved glycine (G322 in Gpa1) in the G3 region create a protein that is unable to dissociate from βγ in response to ligand stimulation of the receptor (9, 19, 23, 34). A conserved arginine in this region, R204 in G_{t1} α and R209 in G_o α (R327 in Gpa1), is protected from tryptic cleavage by binding of nonhydrolyzable GTP analogs (14). In addition, mutation of a conserved cysteine, C215, in the hinge α-helix of G_o α (C333 in Gpa1) prevents cross-linking to βγ, although the mutant α subunit can still bind βγ (38). Therefore, Gpa1 amino acid E307 is in a region intimately involved in the structural rearrangements associated with G protein activation and subunit dissociation. It must be emphasized that the Gpa1 mutagenesis strategy was not exhaustive and that the E307 residue clearly will not represent the only site for Hls mutations. Targeted mutagenesis in this region of Gpa1 should be useful in defining potential interactions more specifically.

Recently, the crystal structure of transducin α has been determined (25a). Deletion of the amino terminus of the protein did not disrupt the structure or prevent effector activation but did block βγ binding. This suggests that there are regions of α subunits distinct from the hinge region identified in our study that are involved in βγ interaction.

Although the position equivalent to Gpa1 E307 is flanked by highly conserved regions, the block of approximately 15 amino acids between the G2 and G3 elements (303 to 318 in Gpa1) is divergent. Perhaps significantly, the residue in the mammalian α subunit equivalent to the E307 position in Gpa1 is highly diagnostic for a particular class of mammalian α subunits. In particular, all G_s α subunits contain a lysine at this position (4), all G_o and G_i α subunits contain a histidine (16, 40), t1 transducin α subunits have a glutamine (42), G_q α subunits have a proline (35), and G_{13} α subunits have an aspartic acid (36) (Fig. 4B). This diversity between but not within classes of Gα subunits suggests that the region around E307 of Gpa1 may have a function in defining the specificity of the G protein α subunit; this selectivity could be involved in the binding of βγ complexes, or it could play a role in effector or receptor interactions.

ACKNOWLEDGMENTS

We thank David Stone and Steve Reed for the library of mutant *GPA1* sequences, Rick Stewart for plasmids, Duane Jenness for the strain containing the original Hpl allele, and Thierry Vernet and Henry Bourne for comments on the manuscript.

We thank Glaxo Group Research Limited for partial financial support.

REFERENCES

1. **Berlot, C. H., and H. R. Bourne.** 1992. Identification of effector-activating residues of G_sα. Cell **68**:911–922.
2. **Blinder, D., S. Bouvier, and D. D. Jenness.** 1989. Constitutive mutants in the yeast pheromone response: ordered function of the gene products. Cell **56**:479–486.
3. **Boeke, J. D., J. Trueheart, G. Natsoulis, and G. R. Fink.** 1987. 5-Fluoroorotic acid as a selective agent in yeast molecular genetics. Methods Enzymol. **154**:164–171.
4. **Bray, P. L., A. Carter, C. Simons, V. Guo, C. Puckett, J. Kamholz, A. Spiegel, and M. Nirenberg.** 1986. Human cDNA clones for four species of Gαs signal transduction protein. Proc. Natl. Acad. Sci. USA **83**:8893–8897.
5. **Broach, J. R., J. N. Strathern, and J. B. Hicks.** 1979. Transformation in yeast: development of a hybrid cloning vector and isolation of the *CAN1* gene. Gene **8**:121–133.
6. **Chien, C., P. L. Bartel, R. Sternglanz, and S. Fields.** 1991. The two-hybrid system: a method to identify and clone genes for proteins that interact with a protein of interest. Proc. Natl. Acad. Sci. USA **88**:9578–9582.
7. **Clark, K. L., D. Dignard, D. Y. Thomas, and M. Whiteway.** 1993. Interactions among the subunits of the G protein involved in *Saccharomyces cerevisiae* mating. Mol. Cell. Biol. **13**:1–8.
8. **Cole, G. M., D. E. Stone, and S. I. Reed.** 1990. Stoichiometry of G protein subunits affects the *Saccharomyces cerevisiae* mating pheromone signal transduction pathway. Mol. Cell. Biol. **10**:510–517.
9. **Conklin, B. R., and H. R. Bourne.** 1993. Structural elements of Gα subunits that interact with Gβγ, receptors, and effectors. Cell **73**:631–641.
10. **Denker, B. M., E. J. Neer, and C. J. Schmidt.** 1992. Mutagenesis of the amino terminus of the α subunit of the G protein G_o: in vitro characterization of $\alpha_o\beta\gamma$ interactions. J. Biol. Chem. **267**:6272–6277.
11. **Dietzel, C., and J. Kurjan.** 1987. The yeast *SCG1* gene: a G_α-like protein implicated in the a- and α-factor response pathway. Cell **50**:1001–1010.
12. **Fields, S., and O. Song.** 1989. A novel genetic system to detect protein-protein interactions. Nature (London) **340**:245–246.
13. **Hanes, S., and R. Brent.** 1991. A genetic model for interaction of the homeodomain recognition helix with DNA. Science **251**:426–430.
14. **Hurley, J. B., M. I. Simon, D. B. Teplow, J. D. Robishaw, and A. G. Gilman.** 1984. Homologies between signal transducing G proteins and *ras* gene products. Science **226**:860–862.
15. **Ito, H., Y. Fukuda, K. Murata, and A. Kimura.** 1983. Transformation of intact yeast cells treated with alkali cations. J. Bacteriol. **153**:163–168.
16. **Itoh, H., R. Toyama, T. Kozasa, M. Matsuoka, and Y. Kaziro.** 1988. Presence of three distinct molecular species of Gi protein α subunit: structure of rat cDNAs and human genomic DNAs. J. Biol. Chem. **263**:6656–6664.
17. **Jarvis, E. E., D. C. Hagen, and G. F. Sprague, Jr.** 1988. Identification of a DNA segment that is necessary and sufficient for α-specific gene control in *Saccharomyces cerevisiae*: implications for regulation of α-specific and a-specific genes. Mol. Cell. Biol. **8**:309–320.
18. **Kubo, M., T. Hirano, and M. Kakinuma.** 1991. Molecular cloning and sequence analysis of cDNA and genomic DNA for the human cone transducin α subunit. FEBS Lett. **291**:245–248.

19. **Kurjan, J., J. P. Hirsch, and C. Dietzel.** 1991. Mutations in the guanine nucleotide-binding domains of a yeast Gα protein confer a constitutive or uninducible state to the pheromone response pathway. Genes Dev. **5**:475–483.
20. **Leberer, E., D. Dignard, D. Harcus, D. Y. Thomas, and M. Whiteway.** 1992. The protein kinase homologue Ste20p is required to link the yeast pheromone response G-protein βγ subunits to downstream signalling components. EMBO J. **11**:4815–4824.
21. **Leberer, E., D. Dignard, L. Hougan, D. Y. Thomas, and M. Whiteway.** 1992. Dominant-negative mutants of a yeast G-protein β subunit identify two functional regions involved in pheromone signalling. EMBO J. **11**:4805–4813.
22. **Marsh, L., A. M. Neiman, and I. Herskowitz.** 1991. Signal transduction during pheromone response in yeast. Annu. Rev. Cell Biol. **7**:699–728.
23. **Miller, R. T., S. B. Masters, K. A. Sullivan, B. Beiderman, and H. R. Bourne.** 1988. A mutation that prevents GTP-dependent activation of the α chain of G_s. Nature (London) **334**:712–715.
24. **Miyajima, I., M. Nakafuku, N. Nakayama, C. Brenner, A. Miyajima, K. Kaibuchi, K. Arai, Y. Kaziro, and K. Matsumoto.** 1987. *GPA1*, a haploid essential gene, encodes a yeast homolog of mammalian G protein which may be involved in mating factor signal transduction. Cell **50**:1011–1019.
25. **Murakami, T., W. Simmons, and A. Spiegel.** 1992. Site-specific antibodies directed against G protein β and γ subunits: effects on α and βγ subunit interaction. Biochemistry **31**:2905–2911.
25a. **Noel, J. P., H. E. Hamm, and P. B. Sigler.** 1993. The 2.2Å crystal structure of transducin-α complexed with GTPγS. Nature (London) **366**:654–663.
26. **Nomoto, S., N. Nakayama, K.-I. Arai, and K. Matsumoto.** 1990. Regulation of the yeast pheromone response pathway by G protein subunits. EMBO J. **9**:691–696.
27. **Rose, M., P. Novick, J. H. Thomas, D. Botstein, and G. R. Fink.** 1987. The *Saccharomyces cerevisiae* genomic plasmid bank based on a centromere-containing shuttle vector. Gene **60**:237–243.
28. **Saiki, R. J., D. H. Gelfand, S. Stoffel, S. J. Scharf, R. Higuchi, G. T. Horn, K. B. Mullis, and H. A. Erlich.** 1988. Primer-directed enzymatic amplification of DNA with a thermostable DNA polymerase. Science **239**:487–491.
29. **Sanger, F., S. Nicklen, and A. R. Coulson.** 1977. DNA sequencing with chain terminating inhibitors. Proc. Natl. Acad. Sci. USA **74**:5463–5467.
30. **Sherman, F., G. R. Fink, and J. B. Hicks.** 1982. Methods in yeast genetics. Cold Spring Harbor Laboratory, Cold Spring Harbor, N.Y.
31. **Sikorski, R. S., and P. Heiter.** 1989. A system of shuttle vectors and yeast host strains designed for efficient manipulation of DNA in *Saccharomyces cerevisiae*. Genetics **122**:19–27.
32. **Simon, M. I., M. P. Strathmann, and N. Gautam.** 1991. Diversity of G proteins in signal transduction. Science **252**:802–808.
33. **Staake, D., B. Walter, B. Kisters-Woike, B. von Wilcken-Bergmann, and B. Muller-Hill.** 1990. How Trp repressor binds to its operator. EMBO J. **9**:1963–1967.
34. **Stone, D. E., and S. I. Reed.** 1990. G-protein mutations that alter the pheromone response in *Saccharomyces cerevisiae*. Mol. Cell. Biol. **10**:4439–4446.
35. **Strathman, M., and M. I. Simon.** 1990. G protein diversity: a distinct class of α subunits is present in vertebrates and invertebrates. Proc. Natl. Acad. Sci. USA **87**:9113–9117.
36. **Strathman, M., and M. I. Simon.** 1991. Gα12 and Gα13 subunits define a fourth class of G protein α subunits. Proc. Natl. Acad. Sci. USA **88**:5582–5586.
37. **Struhl, K., D. T. Stinchcomb, S. Scherer, and R. W. Davis.** 1979. High-frequency transformation of yeast: autonomous replication of hybrid DNA molecules. Proc. Natl. Acad. Sci. USA **76**:1035–1039.
38. **Thomas, T. C., C. J. Schmidt, and E. J. Neer.** 1993. G-protein α_o subunit: mutation of conserved cysteines identifies a subunit contact surface and alters GDP affinity. Proc. Natl. Acad. Sci. USA **90**:10295–10299.
39. **Trueheart, J., D. Boeke, and G. R. Fink.** 1987. Two genes required for cell fusion during yeast conjugation: evidence for a pheromone-induced surface protein. Mol. Cell. Biol. **7**:2316–2328.
40. **Tsukamoto, T., R. Toyama, H. Itoh, T. Kozasa, M. Matsuoka, and Y. Kaziro.** 1991. Structure of the human gene and two rat cDNAs encoding the α-chain of GTP-binding regulatory protein G_o: two different mRNAs are generated by alternative splicing. Proc. Natl. Acad. Sci. USA **88**:2974–2978.
41. **van der Voorn, L., and H. Ploegh.** 1992. The WD-40 repeat. FEBS Lett. **307**:131–134.
42. **Van Dop, C., D. C. Medynski, and L. M. Apone.** 1989. Nucleotide sequence for a cDNA encoding the α subunit of retinal transducin (GNAT1) isolated from the human eye. Nucleic Acids Res. **17**:4887–4887.
43. **Whiteway, M. S., L. Hougan, D. Dignard, D. Y. Thomas, L. Bell, G. C. Saari, F. J. Grant, P. O'Hara, and V. L. MacKay.** 1989. The *STE4* and *STE18* genes of yeast encode potential β and γ subunits of the mating factor receptor-coupled G protein. Cell **56**:467–477.
44. **Whiteway, M., L. Hougan, and D. Y. Thomas.** 1990. Overexpression of the *STE4* gene leads to mating response in haploid *Saccharomyces cerevisiae*. Mol. Cell. Biol. **10**:217–222.
45. **Wolberger, C., A. K. Vershon, B. Liu, A. D. Johnson, and C. O. Pabo.** 1991. Crystal structure of a MATα2 homeodomain-operator complex suggests a general model for homeodomain-DNA interactions. Cell **67**:517–528.
46. **Zhang, M., and D. J. Tipper.** 1993. Suppression of a dominant G protein β-subunit mutation in yeast by Gα protein expression. Mol. Microbiol. **9**:813–821.

A.Ponce

QP187.3.M64M6

STIC-ILL

From: Brannock, Michael
Sent: Tuesday, May 29, 2001 3:18 PM
To: STIC-ILL
Subject: 09378046

Please provide the following refs:

Whiteway M et al., Molecular and Cellular Biology 14(5)3223-9, 1994

Ji YS et al., Circulation Research 83(3)295-304, 1998

Franchimont N, J. Clinical Investivation 100(7)1797-1803, 1997.

Li, J., et al., Molecular Endocrinology 10(3)252-64, 1996

Thank you,

Michael T. Brannock, Ph.D.
Patent Examiner, AU 1646
Crystal Mall One, 10E18
(703) 306-5876

Angiotensinogen Gene Activation by Angiotensin II Is Mediated by the Rel A (Nuclear Factor-κB p65) Transcription Factor: One Mechanism for the Renin Angiotensin System Positive Feedback Loop in Hepatocytes

Junyi Li and Allan R. Brasier

Departments of Internal Medicine and
Sealy Center for Molecular Science
University of Texas Medical Branch
Galveston Texas 77550-1060

The renin-angiotensin system controls blood pressure through the enzymatic production of the vasopressor angiotensin II (AII) from the angiotensinogen (AGT) precursor. Intravascular AII production stimulates *de novo* synthesis of its precursor in a positive feedback loop through increased gene expression. In this study, we investigate the effects of AII on AGT gene expression. At nanomolar concentrations, AII activates transcription of the native AGT gene; this region is mapped to the AGT gene multihormone-inducible enhancer (−615 to −470). Within the multihormone-inducible enhancer, site-directed mutations of the acute-phase response element (APRE) that interfere with nuclear factor-κB (NF-κB) transcription factor binding also abolish AII responsiveness. The APRE functions as a rapidly inducible AII-inducible enhancer with peak reporter activity detected after a 4-h stimulation; this effect occurs only when the type 1 AII receptor is expressed. AII induces sequence-specific NF-κB binding to the APRE in HepG2 nuclear extracts. Moreover, AII infusions of primary rat hepatocyte cultures produces a rapid 4-fold increase in sequence-specific NF-κB binding to the APRE. Antibodies against the transcriptional activator subunit, Rel A, quantitatively supershift the nucleoprotein complex, whereas antibodies to other NF-κB members do not, demonstrating that Rel A APRE-binding activity is AII-inducible. Transient overexpression of Rel A(1–551) activates the AGT multihormone-inducible enhancer. AII-inducible domains of Rel A were mapped by cotransfecting a chimeric GAL4-Rel A fusion protein with a reporter gene containing GAL4-binding sites. GAL4-Rel A(1–551) was an AII-inducible transactivator. Deletion of the NH_2-terminal 254 amino acids of Rel A produces a constitutive transactivator, indicating that Rel A is activated by AII in a manner dependent on its NH_2 terminus. These studies define one mechanism for the renin-angiotensin system positive feedback loop in hepatocytes. (Molecular Endocrinology 10: 252–264, 1996)

0888-8809/96/$3.00/0
Molecular Endocrinology

INTRODUCTION

The intravascular renin-angiotensin system (RAS) is a central endocrine regulator of cardiovascular homeostasis in man (1, 2). Exposure of the renal secretory juxtaglomerular apparatus to hypotensive stimuli results in the secretion of renin, an aminopeptidase that initiates sequential proteolysis of the angiotensinogen (AGT) precursor into the potent vasopressor angiotensin II (AII). The AGT gene encodes the only known precursor of the angiotensin peptides (2). Accumulating evidence shows that physiological mediators that alter intravascular AGT concentrations influence the velocity of AII synthesis because intravascular AGT circulates at concentrations far below the Michaelis-Menten constant (K_m) of renin.

AII produces potent vasoconstrictor effects and aldosterone release and serves as a myocardial growth factor and controller of sympathetic nervous system output (1, 2). AII mediates its effects by activation of the pharmacologically distinct type 1 AII receptor (AT_1). Upon binding to AT_1, AII stimulates phospholipase C activity, formation of 1,2 diacylglycerol, production of inositol-1,4,5 trisphosphate (and consequent mobilization of intracellular calcium from intracellular stores), and protein kinase C (PKC) translocation (3–5).

In adrenal glomerulosa cells (6), cardiac myocytes (7, 8), vascular smooth muscle cells (9, 10), and hepatocytes (11), AII activates the expression of the early response c-*fos* protooncogene (among others); c-*fos* mRNA expression is induced within minutes of AII administration in a protein synthesis-independent manner (6, 7, 12, 13).

Intravascular AII formation controls the activity of the RAS through negative feedback regulation of renin secretion and positive feedback regulation of AGT synthesis (14–16). In the hepatocyte, AII stimulates AGT gene expression, in part, through enhanced transcription as documented by nuclear run-on analysis (14). The RAS positive feedback loop is important to insure that sufficient AGT is in supply to respond to any future hypotensive challenges and, moreover, may also play a pathophysiological role in the malignant phase of essential or renovascular hypertension (HTN) where enhanced AGT synthesis sustains the elevated blood pressure (2, 15–18). Understanding the mechanisms for the renin angiotensin system positive feedback loop is therefore of considerable interest.

The identification of the *cis* regulatory element(s) and corresponding transacting factor(s) mediating the positive feedback loop on AGT gene synthesis have remained elusive (3, 14–16). One difficulty in the study of AII-dependent enhancers has been due to the loss of AT_1 expression after isolation of primary hepatocytes and the lack of AT_1 expression in transformed hepatocyte cultures. The molecular cloning of AT_1 has provided an important reagent with which to address the mechanism of the RAS positive feedback loop, where expression of AT_1 results in high affinity AII binding activity functionally coupled to intracellular calcium transients (3). In this study, we examine the relationship between AII stimulation and AGT gene transcription using two systems. First, using transcription and DNA-binding assays in AT_1-complemented human hepatocytes, we identify an AII-inducible enhancer in the AGT promoter that, surprisingly, maps to a previously characterized cytokine-inducible enhancer. AII induces acute phase response element (APRE) DNA-binding activity of a specific nuclear factor-κB (NF-κB) family member (Rel A). Second, Rel A binding to the APRE is increased in freshly isolated AII-infused rat primary hepatocytes (which express functionally coupled AT_1-receptors). Finally, we provide evidence that the potent NF-κB transactivating subunit, Rel A, is an AII-inducible transactivator, a phenomenon dependent on its NH_2-terminal 255 amino acids.

RESULTS

AII Activates AGT Transcription through the Multihormone-Inducible Enhancer

To investigate whether AII activates AGT gene transcription, we performed transient cotransfections of AGT-luciferase reporters along with a eukaryotic expression vector encoding the type-1 AII receptor (AT_1) in human HepG2 hepatocytes. AT_1-complementation was necessary because all cultured hepatocytes tested (Hep G2, H4IIEC3, Hep 3B, and Huh-7) lack high-affinity AII binding. Moreover, although freshly isolated primary hepatocytes express AII receptors when assayed within 4 h after isolation, high affinity ligand binding becomes almost undetectable after 24 h in culture, making primary hepatocytes unsuitable for the relatively longer transfection studies (in our hands, specific [^{125}I]AII binding at 4 h is 1.4×10^{-5} nmol/10^6 cells, whereas by 24 h, specific binding falls to 8.3×10^{-7} nmol/10^6 cells).

Transient transfections of the full length AGT promoter into AT_1-complemented HepG2 cells gave a reproducible ~1.5- to 2-fold induction of luciferase reporter activity in response to nanomolar AII concentrations (Fig. 1B). Moreover, AII-inducible gene activation was localized to the multihormone-inducible enhancer of the AGT gene, spanning nucleotides −615 to −470, termed GCS-LUC (19) (Fig. 1C). In the GCS-LUC reporter, AII rapidly stimulated AGT-driven reporter gene transcription over a physiological dose-responsive range producing a statistically significant 3-fold induction, peaking at the concentration of 10 nM (Fig. 1C), a concentration identical to the dissociation constant (K_d) of the AT_1 (3).

Our previous studies have indicated that, within the multihormone-inducible enhancer, a short sequence termed the APRE was a major target for cytokine induction. This element, located between −545 to −527, is bound by two classes of transcription factors, CCAAT box/enhancer binding protein (C/EBP), and NF-κB that recognize the APRE in a mutually exclusive fashion (20). We tested separately site-directed mutations of the AGT promoter APRE sequences to destroy NF-κB binding sites [APRE M6 (a mutant that binds C/EBP proteins only) or APRE M2 (a mutant that binds neither NF-κB nor C/EBP)]. Both mutations blocked AII-induced reporter gene activity (Fig. 1, B and C). To our surprise, these studies indicate the requirement of NF-κB, a cytokine-inducible transcription factor, for AII activation of AGT gene transcription.

The AGT APRE Is a *Bona Fide* AII-Inducible Enhancer Dependent on the AT_1 Receptor

To more convincingly demonstrate that the APRE is an AII-inducible element and to further characterize whether AT_1 expression is necessary for the effect, an APRE-driven luciferase reporter (20, 21) was transiently transfected into HepG2 cells in the absence or presence of the AT_1 receptor expression vector. In the dose-response experiment shown in Fig. 2A, transfectants were assayed after a 4-h incubation with various AII concentrations. Activity was first detectable at 0.01 nM AII, with the maximal 13-fold induction seen in response to 10 nM AII; at higher doses of up to 100 nM (not shown), less activity than the maximum 13-fold

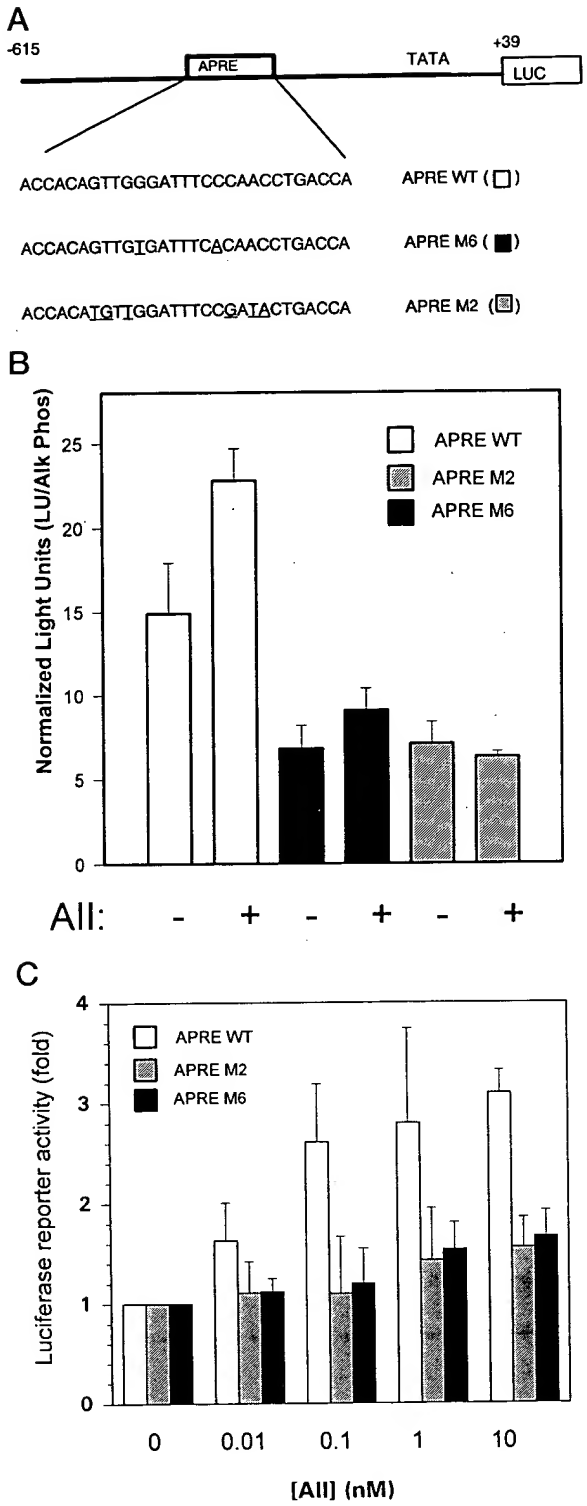

Fig. 1. All Activates AGT Promoter Transcription through the Multihormone-Inducible Enhancer

A, DNA sequence of the APRE and its mutations in AGT gene promoter fragment. A schematic diagram of the AGT gene promoter fragment (−615/+39) containing APRE WT (*white bars*) or its mutations (M2, *hatched bars* or M6, *dark bars*) driving the luciferase reporter gene. B, Induction of the native AGT promoter in receptor-complemented HepG2 cells. The WT AGT gene promoter fragment or its site mutation was transiently transfected to AT_1-complemented HepG2 cells for 44 h. Transient transfectants were stimulated with the indicated doses of All for 4 h before harvest for luciferase reporter and internal control activity assays. Triplicate plates were assayed for each experimental point. Shown is mean ± SD of a representative transfection after normalization to internal control. Only the APRE WT sequences are All-inducible. C, The AGT multihormone-inducible enhancer is sufficient for All-induction. The AGT multihormone-inducible enhancer (−615 to −470) was ligated upstream of the inert AGT promoter driving the expression of the luciferase reporter gene and transfected with internal control β-galactosidase expression vector (4 μg) (as an internal control) into receptor-complemented HepG2 cells. In these and subsequent assays, the luciferase activity is normalized to internal control for each plate and expressed as fold induction relative to the AGT promoter in the absence of All stimulation. Shown is mean ± SD of three independent experiments. All produces a statistically significant induction of APRE WT-containing sequences, peaking at a 3-fold induction at a concentration of 10 nM.

was seen, perhaps due to the well described phenomenon of agonist-induced receptor down-regulation (22). Importantly, All-dependent transcriptional activation was seen only in cells cotransfected with the AT_1 expression vector (Fig. 2A), indicating that AT_1 is absolutely required for this effect.

As with the site-directed mutations within the native AGT multihormone-inducible enhancer (Fig. 1), All stimulation of the APRE is dependent on NF-κB binding because no transcriptional induction was seen by All in either APRE M6 or APRE M2 driving the luciferase reporter gene in response to All (Fig. 2B). In data not shown, the All induction was rapid and transient; treatment with 10 nM All for 4 h produced a maximum induction of 13-fold, and after a 24-h treatment, an induction of only 2-fold was recorded.

All Induces NF-κB Binding to the APRE in Receptor-Complemented HEPG2 Cells and in Primary Rat Hepatocytes

To examine whether All induces changes in APRE DNA-binding complexes, we analyzed the patterns of DNA-binding activities from control and All-stimulated nuclear extracts in transiently transfected HepG2 cells by gel mobility shift assays (Fig. 3A, *left panel*). All increased the abundance of a single complex binding to a ^{32}P-labeled APRE oligonucleotide probe. This inducible complex was a high affinity, sequence-specific DNA-binding activity because inclusion of 5 pmol of unlabeled APRE wild type (WT), but not mutant APRE M6 or APRE M2, competitors abolished its binding (Fig. 3A, *right panel*).

To confirm that NF-κB binding could be observed in cells expressing native amounts of functionally coupled All receptors, we used the well established model of continuous All infusion of isolated primary Sprague-Dawley hepatocytes. Continuously infused primary

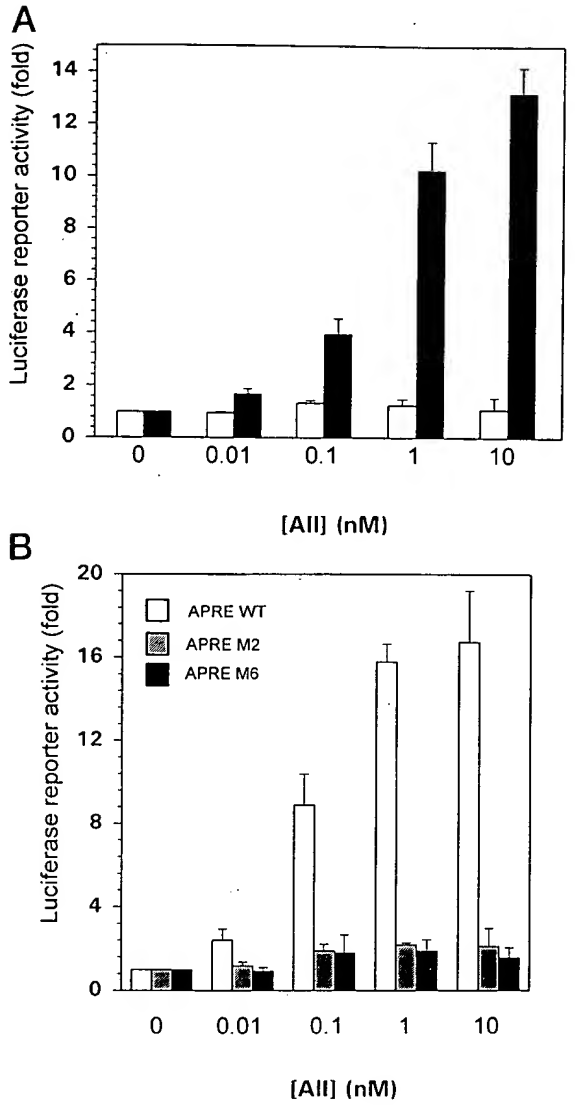

Fig. 2. The APRE Is an AII-Inducible Enhancer

A, AII activates APRE transcription in an AT_1 receptor-dependent fashion. Human hepatoblastoma HepG2 cells were transiently transfected with three APRE copies upstream of the minimal AGT promoter driving luciferase reporter gene in the absence (*white bars*) or presence of AT1 expression vector pEF-Bos (3) (*dark bars*) for 48 h. These constructs initiate transcription at the correct AGT cap site (21). β-Galactosidase expression vector (4 μg) was cotransfected as an internal control. The cells were stimulated and assayed as in Fig. 1. At 10 nM AII, a 13-fold increase in reporter activity is seen, and at concentrations above 10 nM, a decrease in reporter activity is seen. No change in reporter activity is seen in the absence of AT_1 receptor, indicating its expression is absolutely required for the transcriptional effect. B, AII activates APRE enhancer activity through the NF-κB binding sites. AT_1 receptor-complemented HepG2 cells were transiently transfected with three copies of WT APRE (*white bars*) or site mutant APRE (*hatched bars* for M2 and *dark bars* for M6) upstream of the AGT promoter driving the luciferase reporter gene and stimulated and assayed as in Fig. 1. APRE WT, the binding site that recognizes NF-κB (20), is the only template activated by AII.

hepatocytes have been used to demonstrate the AII induction of AGT mRNA and protein [continuous infusions are necessary because AII is rapidly degraded in the primary hepatocyte cultures (23)]. We observed a 4-fold increase of APRE-binding activity in a dose-dependent fashion by AII (Fig. 3B). First detectable at 0.5 nM AII concentrations, APRE-binding activity peaks at a physiological concentration of 5 nM AII (reproduced in four independent experiments). Continuous infusion of 50 nM AII produced no greater stimulation, indicating that the AII effect is saturable. Moreover, the increase in APRE DNA-binding activity was observed as early as 1 h [a time preceding the changes in AGT mRNA (data not shown and Ref. 23)], indicating that AII induction of APRE binding activity is a rapid effect.

AII-activated APRE binding was sequence-specific for the NF-κB protein family as determined by competition analysis. In Fig. 3C, a gel mobility shift assay using nuclear proteins isolated by a separate infusion of rat primary hepatocytes over subnanomolar AII concentrations is shown. As seen in Fig. 3B, maximal APRE-binding effect is seen at 5 nM. In Fig. 3C (*middle and right panels*), a 100-fold molar excess of unlabeled APRE WT coincubated with the radiolabeled probe completely competed for binding. APRE M6, however, competes only slightly for binding as compared with the APRE WT sequences. These results indicate that AII activates AGT APRE-binding activity through changes in NF-κB abundance both in AT_1 receptor-complemented HepG2 hepatocytes and in primary rat hepatocytes. We note that the AII-activated transcriptional activity of the AGT promoter is identical to the binding specificity of the AII-inducible proteins in AII-stimulated hepatocytes (Figs. 1 and 2).

Rel A (NF-κB p65) Subunit Is Contained within the Nucleoprotein Complex

Rel A is the potent transcriptional regulatory subunit of the tumor necrosis factor-α (TNFα)-induced APRE binding NF-κB complex (24). Identification of the composition of NF-κB subunits in the AII-induced nuclear complexes was accomplished using subunit-specific anti-NF-κB antibodies in the gel mobility supershift assay. In the gel mobility supershift assays shown in Fig. 4A, nuclear protein isolated from control or AII-stimulated HepG2 hepatocytes was preincubated 20 min before addition of radiolabeled APRE probe, and the antibody-protein-DNA complexes were separated by nondenaturing PAGE. No supershifted complexes could be observed in HepG2 nuclear proteins using antibodies to NF-κB1, NF-κB2, or C-Rel. By contrast, a slower migrating supershifted band was observed in lanes containing the Rel A antisera. The supershifted complex is produced from the specific AII-inducible complex because its intensity is coincidentally reduced (Fig. 4A; the *lower panel* is a lighter exposure

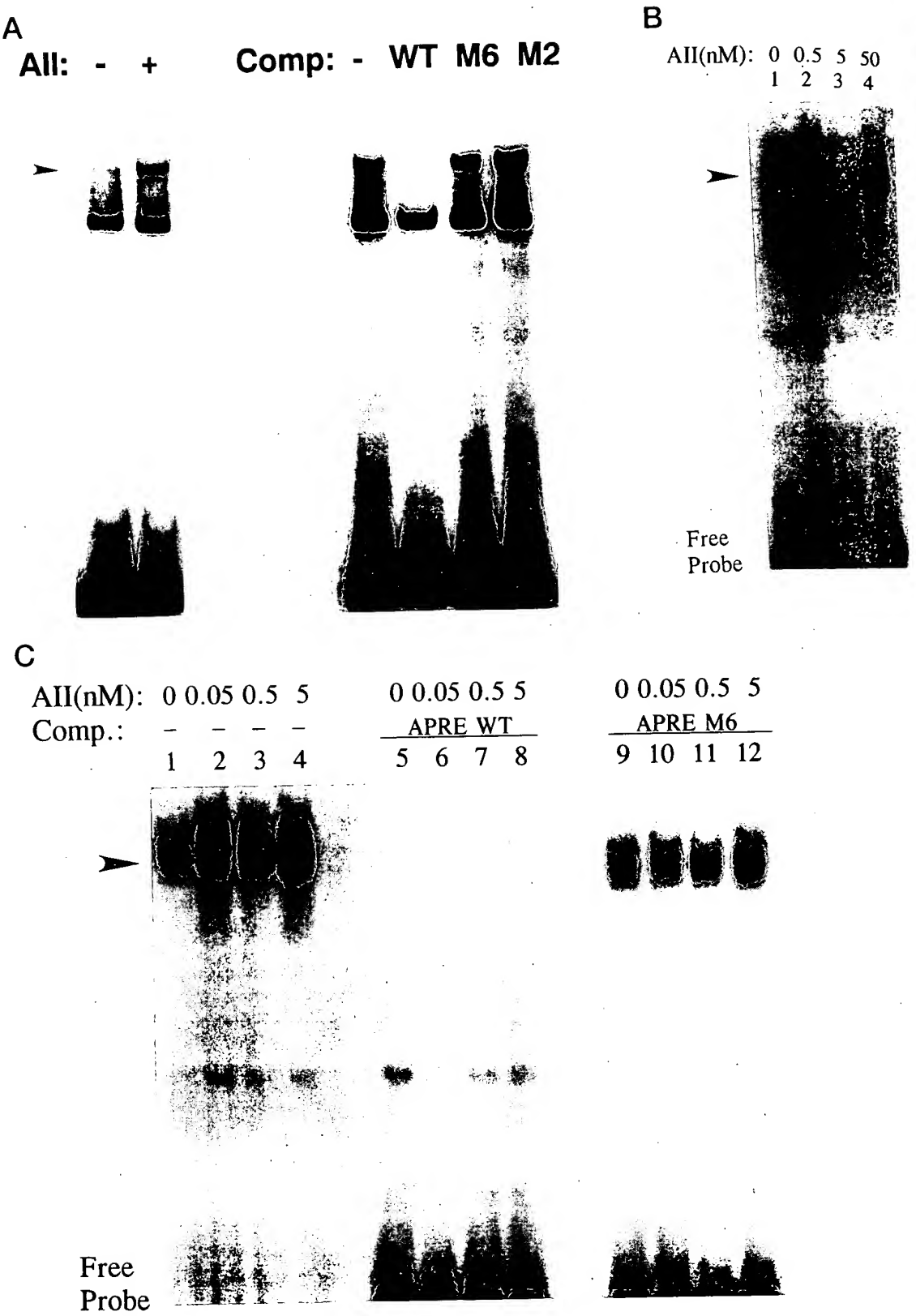

Fig. 3. AII Induces NF-κB Binding to the APRE in Hepatocytes

A, AII induces APRE binding activity in transiently transfected HepG2 hepatocytes. *Left panel*, HepG2 hepatocytes transiently transfected with expression vector encoding the type 1 AT receptor were stimulated with medium alone (AII −) or 20 nM AII (AII +) for 1 h before nuclear protein isolation. Shown is an autoradiogram of a gel mobility shift assay after incubation of 10 μg nuclear protein with ^{32}P-labeled APRE WT DNA (10 fmol; DNA sequences are given in *Materials and Methods*) and fractionation on a 6%

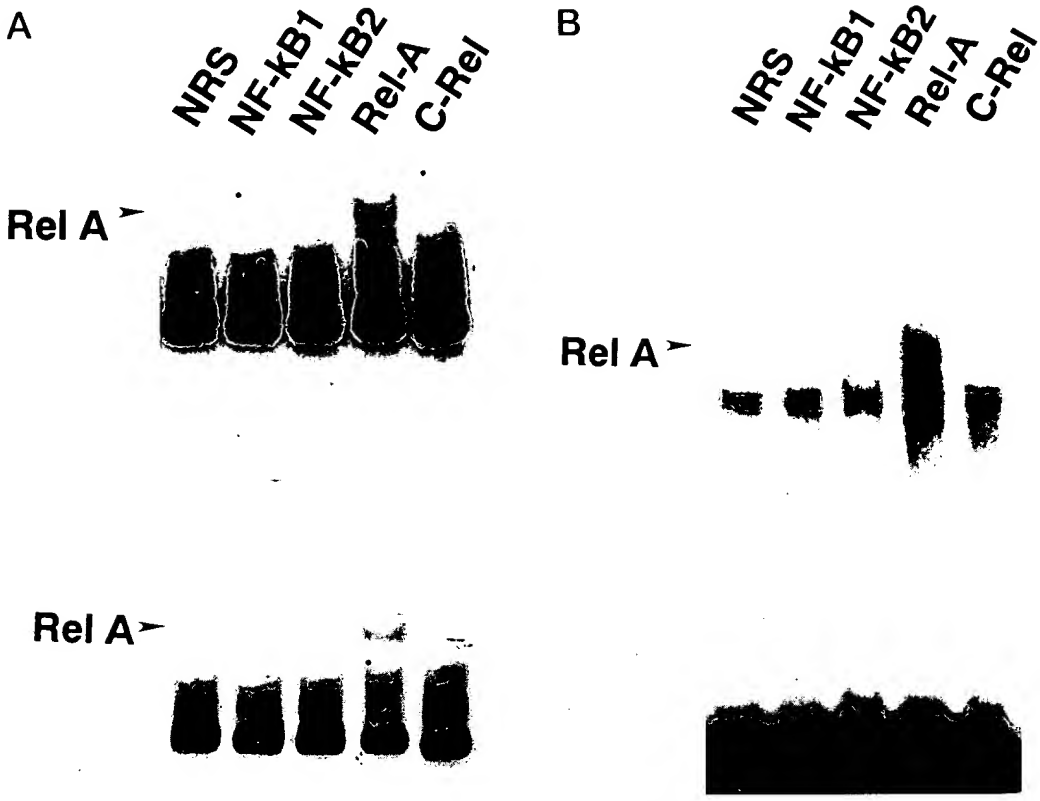

Fig. 4. AII Induction of Rel A DNA-Binding Activity in Primary Hepatocytes

A, Supershift assay of NF-κB subnits in AII-stimulated HepG2 cells. Nuclear proteins from AII-stimulated HepG2 cells transiently transfected with the expression vector for AT_1 receptor were used to bind the ^{32}P-labeled APRE in the presence of affinity-purified NF-κB antibodies to NF-κB1, NF-κB2, Rel-A, and C-Rel (Santa Cruz Biotech). Shown is an autoradiogram of the gel shift after fractionation on a 6% nondenaturing PAG (*bottom panel* is shorter exposure of same autoradiogram). The presence of Rel A antibody quantitatively supershifts the sequence-specific AII-inducible DNA-binding complex (Rel A), indicating that Rel A is the major identifiable NF-κB family member that binds to the AGT APRE. B, Supershift assay of NF-κB subnits in AII-stimulated rat primary hepatocytes. Nuclear proteins from AII-stimulated rat primary hepatocytes were prepared (as described in *Materials and Methods*) and used to bind the ^{32}P-labeled APRE in the presence of affinity-purified NF-κB antibodies to NF-κB1, NF-κB2, Rel-A, and C-Rel. Antibodies to Rel A quantitatively supershift the AII-inducible DNA-binding complex.

of the same autoradiogram), indicating Rel A antibody *quantitatively* supershifts the AII-inducible APRE-binding complex. These observations are reproduced using nuclear extracts from AII-perfused rat hepatocytes (Fig. 4B). Moreover, in data not shown, the Rel A supershifted band is produced by

---

nondenaturing polyacrylamide gel [PAG (20, 53)]. AII induces nuclear APRE DNA-binding activity (*arrow*). *Right panel*, Competition analysis of AII-induced nuclear proteins using 5 pmol unlabeled competitor DNA (representing a 100-fold molar excess) using APRE WT (WT), APRE M6 (M6), or APRE M2 (M2) oligonucleotides. Only APRE WT competes for binding of the AII-inducible complex, indicating the complex is NF-κB-specific. B, AII induces nuclear NF-κB DNA-binding activity in rat primary hepatocytes. Nuclear protein from primary hepatocyte cultures was isolated after a 3-h continuous AII infusion between 0–50 nM. Shown is an autoradiogram of a gel mobility shift assay after incubation with 20 μg ^{32}P-labeled APRE WT DNA (10 fmol; DNA sequences given in *Materials and Methods*) in the presence of poly(dI-dC), and fractionation on a 7% nondenaturing polyacrylamide gel [PAG (20, 53)]. Lane 1, infusion of growth medium alone; lane 2, infusion of medium containing 0.5 nM AII; lane 3, medium with 5 nM AII; lane 4, medium with 50 nM AII. At 0.5 nM AII, a 4-fold increase in APRE binding was observed relative to control. C, AII-inducible APRE DNA-binding activity is specific for NF-κB binding sites. Competition in gel shift assay using a 100-fold molar excess of unlabeled APRE WT probe (*middle panel*, lanes 5–8; sequences given in *Materials and Methods*) and point mutant of the APRE (APRE M6) (*right panel*, lanes 9–12) were mixed with nuclear protein for each lane before adding ^{32}P-labeled APRE probe. Nucleoprotein complexes were resolved on 7% PAG and visualized by autoradiography. Lanes 1, 5, and 9 are control infusions; lanes 2, 6, and 10 are infusions of medium with 0.05 nM AII; lanes 3, 7, and 11 are infusions of medium with 0.5 nM AII; lanes 4, 8, and 12 are infusions of medium with 5 nM AII. A similar induction of APRE-binding activity of 4-fold is seen relative to control (compare lane 4 with lane 1) as shown in Fig. 3B. The AII-inducible APRE-binding proteins are specific for APRE WT DNA-sequences.

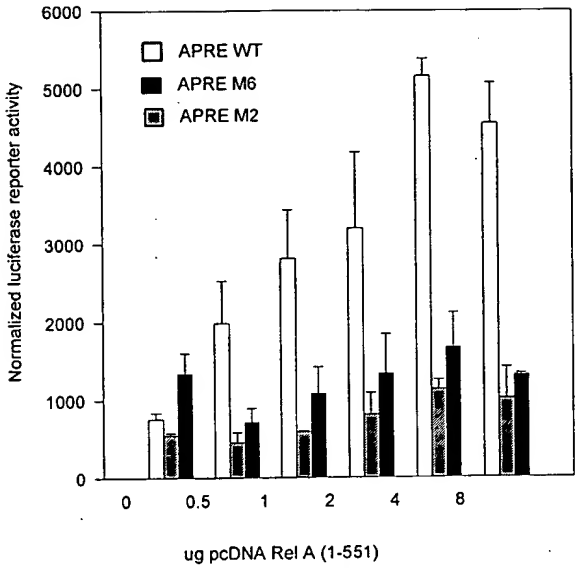

Fig. 5. Rel A Transactivates the AGT Promoter through the APRE

AGT gene promoter fragment (−615 to −470) containing APRE (*white bars*) or its mutations (M2, *hatched bars* or M6, *dark bars*) driving the luciferase reporter gene (GCS-LUC), diagrammed in Fig. 1, were transiently transfected into HepG2 hepatocytes in the presence of increasing concentrations of eukaryotic expression vector (pcDNA) encoding Rel A(1–551). Shown is mean ± SD of normalized luciferase reporter activity from triplicate plates in a representative transfection, reproduced in three independent experiments. Reporter activity of GCS WT increased 2.63-fold (0.5 μg pcDNA Rel A), 3.7-fold (1 μg pcDNA Rel A), 4.2-fold (2 μg pcDNA Rel A), 6.8-fold (4 μg pcDNA Rel A), and 6-fold (8 μg pcDNA Rel A), whereas the APRE site mutations were not significantly inducible. These data indicate that Rel A(1–551) transactivates the multihormone-inducible enhancer through the APRE.

either the NH_2- or COOH-terminally directed antibodies. We conclude that AII activates Rel A DNA binding of the AGT APRE in primary hepatocytes.

Rel A Transactivates the AGT Multihormone-Inducible Enhancer

Rel A, the potent transcriptionally active NF-κB subunit, is sequestered in the cytoplasm of cells through reversible interactions with the IkB inhibitor (25, 26). Demonstration that AII induction of AGT promoter-dependent transcription is dependent on NF-κB binding (Figs. 1 and 2) and identification of Rel A in the AII-inducible nucleoprotein complex (Figs. 3 and 4) required functional analysis of Rel A. In Fig. 5, transient overexpression of native Rel A(1–551) was tested for its ability to transactivate the AGT multihormone-inducible enhancer. High level expression of Rel A(1–551) by the cytomegalovirus (CMV) promoter saturates the IkB inhibitor and results in constitutive Rel A activity (27). Cotransfection of eukaryotic Rel A expression vector, pcDNA-Rel A(1–551), results in a dose-dependent 6-fold activation of the wild-type AGT promoter (Fig. 5). pcDNA-Rel A(1–551) did not activate the site mutations (APRE M2, APRE M6) that block NF-κB binding (20). This indicates that Rel A transactivates the AGT promoter and that transactivation is dependent on the NF-κB binding site in the APRE.

AII Activates Transcriptional Activity of GAL4-Rel A(1–551) Fusion Protein in Hepatocytes

To determine whether Rel A was an AII-inducible transactivator, we transiently expressed a fusion protein of Rel A fused to the DNA-binding domain of the yeast transcription factor GAL4 (amino acids 1–147) at subsaturating levels for IkB (28). Yeast GAL4 is not naturally expressed in mammalian cells. Measuring the activity of GAL4-binding sites linked to the luciferase reporter (UAS-LUC) allows the selective measurement of Rel A(1–551) activity (schematically diagrammed in Fig. 6A). Figure 6B shows the raw and normalized transcriptional activity of UAS-LUC cotransfected with GAL4-Rel A(1–551) in response to physiological AII concentrations (*open boxes*). An AII dose-dependent increase of luciferase reporter activity was seen by GAL4-Rel A(1–551). These results indicate that Rel A is an AII-responsive transcription factor in hepatocytes.

Rel A(1–255) Is Necessary for AII Induction of the GAL4-Rel A Fusion

To identify the regions of Rel A responsive to AII, an NH_2-terminal deletion of 254 amino acid Rel homology domain [Rel A(255–551)] was fused to the GAL4 expression vector, and a transient cotransfection with the UAS LUC reporter was performed (Fig. 6A). GAL4-Rel A(255–551), containing the C-terminal transactivation domain of Rel A, was a potent constitutive activator of UAS-LUC reporter activity (Fig. 6B, *solid boxes*), producing a 20-fold more potent transactivator of GAL4-binding sites than the full length Rel A(1–551) in the absence of hormone. GAL4-Rel A(255–551) was not induced by AII at any concentration (Fig. 6B). Therefore, the 1–254 amino acid NH_2-terminal region of Rel A, containing the IkB inhibitor-interactive domain, is absolutely necessary for AII induction. We note that the activity of GAL4-Rel A(1–551) in response to AII approximates, but does not exceed, the activity of GAL4-Rel A(255–551), perhaps indicating that AII activates Rel A through a mechanism of relieving inhibition conferred by its NH_2 terminus (see *Discussion*).

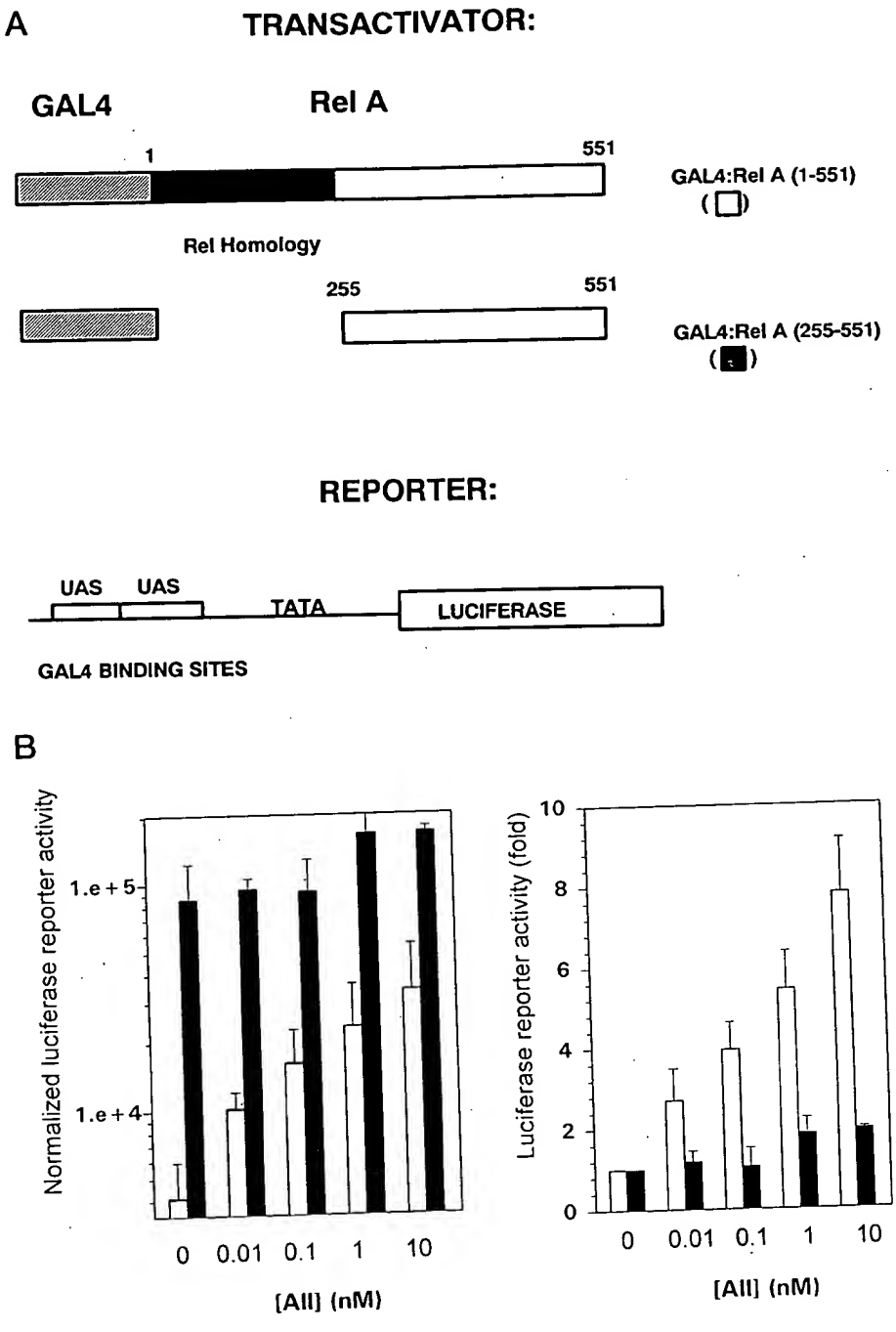

Fig. 6. Rel A Is an AII-Inducible Transcription Factor

A, Schematic diagram of GAL4:Rel A transactivators and reporter. The presence of the GAL4 DNA-binding domain targets the Rel A transactivator to the promoter containing the GAL4-binding sites (UAS LUC). Measurement of UAS-LUC reporter activity is a selective measure of Rel A activity. B, GAL4-Rel A(1–551) is an AII-inducible transcription factor through the NH_2 254 amino acids. AT_1 receptor-complemented HepG2 cells were transiently transfected with the GAL4 DNA-binding sites fused to the luciferase reporter gene (UAS-LUC) in the presence of GAL4-Rel A(1–551) expressing the full length Rel A protein (*white bars*) or GAL4-Rel A(255–551) expressing an N-terminal deletion of 254 amino acids Rel A (*dark bars*) for 48 h. Triplicate plates of cells were stimulated with the indicated AII doses for 4 h before harvest for reporter activity and data analysis. Data are presented in two forms. *Left panel* is the mean ± SD from n = 4 independent transfections plotting normalized luciferase/β galactosidase activity for 0.1 μg (per triplicate) GAL4-Rel A(1–551) expression vector in *open bars*; and 0.1 μg GAL4-Rel A(255–551) expression vector in *dark bars*. In the absence of hormone, GAL4-Rel A(255–551) is a 20-fold more potent activator of UAS-LUC reporter than GAL4-Rel A 1–551); this difference is observed over a wide range of expression vector from 0.01–1.0 μg (not shown). Upon AII stimulation, only GAL4-Rel A(1–551) shows a dose-dependent induction of reporter activity. *Right panel* is the luciferase reporter activity expressed as fold induction relative to the absence of hormone. GAL4-Rel A(1–551) confers a 7.8-fold induction of UAS LUC reporter activity at 10 nM AII; induction is lost upon deletion of the 254 NH_2-terminal amino acids of Rel A.

DISCUSSION

The RAS Positive Feedback Loop Involves the Transcriptional Activation of the AGT Gene

Hepatic AGT gene expression is tightly controlled by multiple physiological stimuli, including 1) steroid hormones and glucocorticoids (19, 29, 30), estrogens (31, 32), and T_3 (33, 34); 2) the state of cellular differentiation (35, 36); and 3) cytokine hormones elaborated as a consequence of the acute-phase response (20, 24, 37). In these examples, AGT transcription is induced through discrete promoter control elements and is due to changes in nuclear abundance of AGT-binding transcription factors. We extend this model to include the mechanism for how the peptide product of AGT processing, AII, controls the synthesis of its own precursor. We are surprised to find that AII stimulates AGT transcription through a previously characterized cytokine-inducible enhancer (APRE) by activating the transcriptionally active NF-κB subunit Rel A.

Numerous studies *in vivo* and *ex vivo* have demonstrated that intravascular AII production directly controls the synthesis of hepatic AGT through the activated AT_1 receptor (15–17, 38). AII stimulation of freshly isolated rat hepatocytes induces AGT mRNA and protein at concentrations between 0.9–9.0 nM, the identical dose-response range seen in our assays, and at AII concentrations close to the K_d for its receptor (3, 38). A 2.5-fold increase in AGT transcription in response to 1 nM AII has previously been demonstrated by nuclear run-on analysis from isolated primary hepatocytes (14). Using transient transfections of AGT multihormone-inducible enhancer-driven luciferase reporter constructs, we observe a rapid and transient 3-fold increase in transcription in response to 10 nM AII; the magnitude and kinetics of induction are remarkably similar in these two studies (14). Moreover, AII-inducible transcription of APRE-driven reporters is absolutely dependent on cotransfection of the AT_1 receptor. Our observations, then, provide additional unambiguous documentation that the effect of AII on AGT gene expression includes a transcriptional component.

The NF-κB p65 Subunit, Rel A, Is a Transactivator Essential for Peptide Hormone Induction of the AGT Gene

The APRE is a high-affinity binding site for various members of the NF-κB trancription factor family. NF-κB is a multiprotein complex encoded by separate genes that share a homologous ~250-amino acid NH_2-terminal DNA-binding region (the Rel homology domain). NF-κB family members include Rel A (NF-κB p65), Rel B, NF-κB1 (p50), and NF-κB2 (p49) (reviewed in Ref. 25), which freely heterodimerize, producing DNA-binding activities with subtle sequence preferences. Rel A is sequestered in the cytoplasm through reversible interactions with the inhibitor protein IkBα (26). The cytokine TNFα activates NF-κB by disrupting the IkB through a coupled phosphorylation/degradation step, where the NH_2-terminal phosphorylation of IkB targets it for proteolysis through the 26S ubiquitin-proteosome complex (25, 39–41). Once freed from its inhibitor, Rel A translocates into the nucleus to activate gene transcription. We have previously shown, using selective mutations of the APRE that disrupt NF-κB1:Rel A binding, that NF-κB is necessary and sufficient for TNFα-inducible transcription (24, 37). In these studies on TNFα induction of AGT, Rel A is the powerful transactivating NF-κB family member that binds to the APRE in conjunction with the inert NF-κB1 (24). In this study, we document, for the first time, that the induction of AGT transcription by its product AII is also dependent on NF-κB binding and that the p65 subunit (Rel A) is an AII-inducible transactivator.

The Rel Homology Domain Is Necessary for AII Induction: A Role for IkB?

Using the GAL4-Rel A chimera, our data indicate that the 254-amino acid NH_2-terminal Rel homology domain is required for AII induction, but not constitutive transcriptional activation. This NH_2-terminal region is a multifunctional domain containing DNA-binding activity, domain(s) for interacting with the IkB inhibitor, nuclear translocation signal(s), dimerization domain(s), and also protein kinase A and PKC phosphoacceptor sites of unknown function (Refs. 25, 27, 42, and references therein). IkB interacts with Rel A through ankyrin repeats in its midmolecule and C-terminal domains to interact with the nuclear localization sequence and inhibit DNA binding of the bound NF-κB dimer (43). NF-κB activators, such as PKC or TNFα, produce phosphorylation of the IkB NH_2 terminus to initiate degradation of IkB through the 26S ubiquitin-proteasome complex (39).

We note that deletion of the 254 NH_2-terminal amino acids of Rel A result in a 20-fold enhanced activity of the GAL4-Rel A(255–551) in the absence of hormone. This large difference occurs over a wide range of transactivator concentrations, arguing that it is unlikely to be due to the trivial explanation that GAL4-Rel A(255–551) is expressed at higher levels than GAL4-Rel A(1–551). In data not shown, basal activity of GAL4-Rel A(1–551) is inhibited by cotransfection of IkBα, but not GAL4-Rel A(255–551). We interpret these data as probably indicating that AII may be acting to relieve repression of Rel A by disrupting its association with the IkB molecule. Whether AII regulates association of Rel A with IkB is directly testable and will be examined in future studies.

AII and TNFα-Induced Signals Are Convergent on NF-κB Rel A

The finding that AII and TNFα activate Rel A indicates that, in some cells (such as hepatocytes), postreceptor cytokine and cardioactive peptide signaling pathways are convergent (Fig. 7). In a wide variety of cell types,

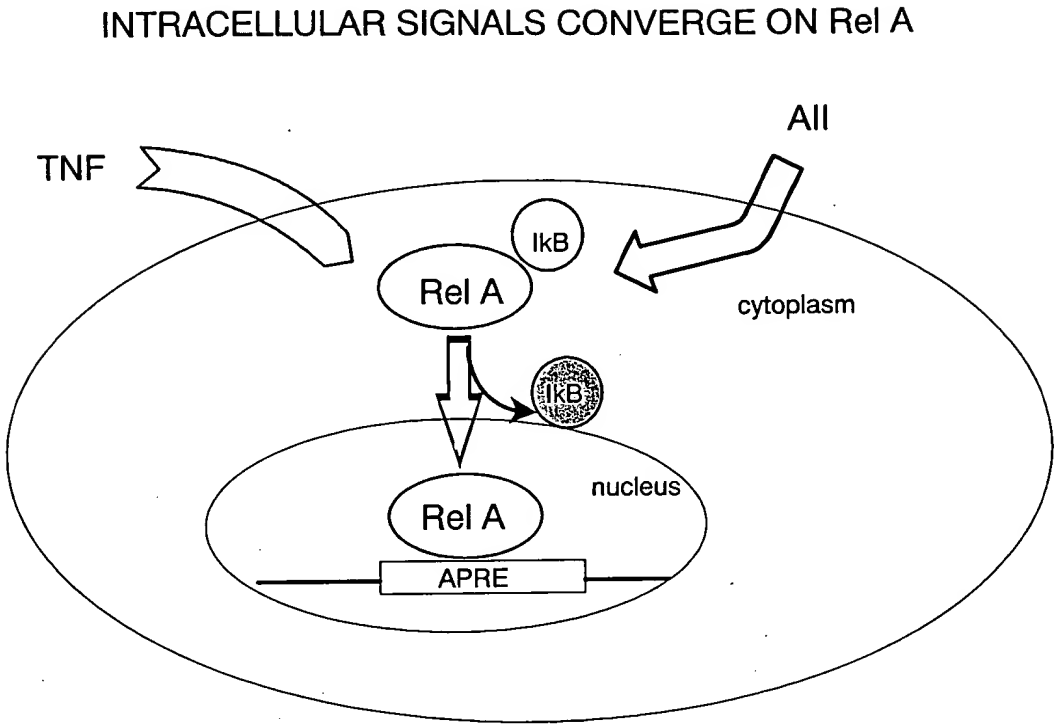

Fig. 7. Schematic Model of Molecular Events in the RAS Positive Feedback Loop: Convergence of AII- and TNFα-Signaling Pathways

NF-κB Rel A is associated with the inhibitory protein IkB as a sequestered, inactive form in resting HepG2 cells. AII produced through the activated RAS stimulates Rel A DNA-binding and transcriptional activity through the AT_1 receptor. Our observations are consistent with a model where the effect of AII binding is to disrupt the Rel A-IkB complex and allow nuclear translocation of Rel A. The inflammatory cytokine TNFα also converges on the Rel A:IkB complex, through a pharmacologically distinct second messenger pathway coupled through the TNF receptor, which also results in Rel A translocation and APRE activation.

TNFα activates NF-κB through two mechanisms: 1) a phosphatidylcholine-specific phospholipase C-coupled activation of an acidic sphingomyelinase with formation of ceramide as a second messenger; and 2) 1,2-diacylglycerol (DAG) formation resulting in PKC activation (44–46). Either of these pathways appears to be sufficient to induce the proteolysis of IkB through a coupled phosphorylation/degradation pathway.

In contrast, upon binding to the hepatocyte type 1 receptor, AII stimulates the formation of DAG with consequent PKC activation, mobilization of intracellular calcium, and inhibition of hormone-stimulated adenylate cyclase activity (3–5). Of these, PKC appears to be an important molecule enabling AII to induce early gene (c-*fos*) synthesis. Chronic exposure to phorbol agonist (to down-regulate PKC) completely inhibits c-*fos* induction in cardiomyocytes (47) and partly antagonizes c-*fos* induction in glomerulosa cells (6) or vascular smooth muscle cells (10). Although the relevant signaling events activated by AII that control NF-κB activity remain speculative, the demonstration that certain PKC isoforms are physically associated with the IkB molecule [kinases that can phosphorylate and inactivate this inhibitor *in vitro*(48)], make PKC a likely candidate for coupling the activated AT_1 receptor to modulating NF-κB activity.

AII as a Physiological Regulator of AGT Synthesis

In comparison to the effects of glucocorticoids on AGT gene expression, where a 10-fold or greater increase in transcriptional rate can be seen (19, 29), AII is a relatively weak inducer of AGT transcription. Within the physiological context of the intravascular renin angiotensin system, a 3- to 4-fold increase in AGT gene expression is nevertheless significant. In transgenic mice overexpressing the AGT gene, 4-fold changes in circulating AGT protein concentrations result in severe AII-dependent HTN (49). In heritable forms of human essential HTN, a significant correlation exists between elevations of 1.5-fold (or less) in circulating AGT concentrations with elevated blood pressure (50). Moreover, the positive feedback loop of the renin angiotensin system plays a central role in blood pressure regulation during the malignant phase of essential HTN and in renovascular HTN (provoked by unilateral renal artery stenosis). These pathological conditions are associated with elevated PRA, increased circulating AII concentrations, and higher circulating levels of

AGT (2). These data indicate that only subtle changes in circulating AGT concentrations can result in a potent biological (pressor) effect.

Is Rel A Involved in the Local RAS?

The RAS is an endocrine system not only confined to the intravascular compartment (circulating or intravascular RAS), but is also active in tissues (local RAS) within the heart, brain, kidney, and arterial wall (reviewed in Ref. 1). Our studies on AII-mediated effects on AGT gene expression in the hepatocyte, the major source of AGT circulating in the plasma, are of particular relevance to regulation of the intravascular RAS. Like the intravascular RAS, AII is also known to activate AGT expression in tissues expressing a local RAS. In cardiac myocytes stimulated with AII, AGT mRNA expression is increased, but given the slow temporal kinetics (requiring 24 h for AGT expression to occur), it is unlikely that AGT expression is mediated through the preformed NF-κB transcription factor. The extent to which Rel A controls this AII-dependent AGT synthesis in other tissues expressing a local RAS will require additional study.

In summary, we present the first evidence that AII-induced AGT gene activation during the RAS positive feedback loop is mediated by the NF-κB subunit Rel A. AII activates transcription of the AGT multihormone-inducible enhancer through the NF-κB binding site in the APRE. The APRE is an element not only necessary for AII induction of the AGT promoter but is also a *bona fide* AII-inducible enhancer by its ability to confer transcriptional activity onto an inert promoter. AII activates Rel A DNA-binding activity in freshly isolated rat primary hepatocytes and the transcriptional activity of a chimeric GAL4-Rel A(1–551). We provide preliminary evidence that Rel A is an AII-inducible transcription factor dependent on its NH_2-terminal 254 amino acids inhibitory domain. That both AII and TNFα act similarly and converge on the Rel A transactivator (diagrammed in Fig. 7) indicate that these hormones produce similar biological responses within the hepatocyte nucleus. These observations argue that Rel A participates in two clearly defined positive feedback systems: 1) The cytokine "cascade" seen during inflammation, and 2) the positive feedback loop of the RAS. We speculate that targeting Rel A activity may have therapeutic potential in secondary human hypertensive disease.

MATERIALS AND METHODS

Materials

Percoll was obtained from Pharmacia Biotech (Uppsala, Sweden). AII, staurosporine, phorbol-12 acetate-13 myristic acid, and synthetic D-luciferin were obtained from Sigma (Saint Louis, MO). Collagenase D, restriction enzymes, and polymerases were obtained from Boehringer-Mannheim (Indianapolis, IN) and were used according to the manufacturer's recommendations. Anti-NH_2-terminal Rel A antibody was obtained from Santa Cruz BioTech (Santa Cruz, CA).

Rat Primary Hepatocyte Isolation and AII Infusion

Animal studies were conducted in accordance with the principles and procedures outlined in the Guidelines for Care and Use of Experimental Animals. Primary hepatocytes were isolated from 250–300 g Sprague-Dawley rats (Texas Animal Specialty, Harlan, TX) using standard techniques (23). In anesthetized rats, the portal vein was cannulated, and the liver was perfused with 200 ml of Solution A (140 mM NaCl, 6 mM KCl, 1.5 mg/ml glucose, 0.5 μg/ml insulin, 10 mM HEPES, pH 7.4) at 12 ml/min followed by 0.05% (wt/vol) collagenase D in solution A with 5.7 mM $CaCl_2$ for 15 min. Hepatocytes were isolated by centrifugation in Percoll gradients, washed, and resuspended to a density of 2×10^6 cells/ml in DMEM/F12 containing 5 μg/ml insulin, 10^{-7} M dexamethasone, 5% Nu-Serum, in a 25-ml flask at 37 C in a shaking water bath. AII was given as a priming dose from 0.05 to 50 nM in different groups and then continuously infused into 15-ml suspension aliquots with infusion rates between 0.03 and 30 ml/h to maintain a constant AII concentration for 3 h (23). Control groups were perfused with the same volume of growth medium.

Transfection and Cell Culture

The human hepatoblastoma cell line HepG2 was obtained from ATCC and maintained in DMEM and cultured in an atmosphere of 5% CO_2 (24, 51). Transient transfections were performed with the calcium phosphate technique in triplicate 60-mm plates using 10 μg luciferase reporter, 1 μg pEF BOS [AT_1-expression vector (3)], 4 μg CMV-β galactosidase (internal control), the indicated concentration of eukaryotic expression vector, and carrier pGEM7Z plasmid to constitute a total of 20 μg DNA for each set of triplicate plates (24). Twenty four hours after transfection, cells were washed, and fresh medium was added. Cells were cultured an additional 20 h. Four hours before harvest, AII was added at the indicated concentrations (at 44 h).

Reporter Assays

Transfected cells were harvested by washing three times in PBS and lysed on the plate by the addition of 0.3 ml lysis buffer (25 mM Tris-phosphate, pH 7.8, 2 mM dithiothreitol (DTT), 2 mM 1.2-diaminocyclohexane-N,N,N′, N′-tetracetic acid, 10% glycerol, 1% Triton X-100). Cytoplasmic lysate (100 μl) was assayed for luciferase and β-galactosidase reporter activities (24). Luciferase activity was determined by subtracting machine background and normalizing each plate to β-Gal activity. Fold induction was calculated by dividing treatment values by unstimulated promoter activity.

Gel Mobility Shift Assays

Nuclear proteins were extracted from suspensions of primary hepatocytes by hypotonic/detergent lysis (24). Soluble nuclear protein was assayed by Coomassie blue G-250 (Bio-Rad Protein Assay, Hercules, CA) for protein concentration and frozen at −70 C until use. Gel mobility shift assays were performed as previously described (19–21, 52) using 20 μg nuclear protein incubated with 2×10^4 cpm of duplex oligonucleotide (labeled by Klenow fill-in using [α^{32}P]dATP) in 20 μl containing 2 μg polydeoxyinosinic-deoxycytidylic acid (polydI-dC). Competition was performed by the addition of excess nonradioactive double-stranded oligonucleotide competitor at the time of addition of radioactive probe. Sequences of APRE WT and mutation oligonucleotides used in

DNA-binding and transfections assays are:

APRE WT:

5′-GATCCACAGTT**GGG**ATTT**CCC**AAC**C**TGACCA-3′
GTGTCAACCCTAAAGGGTTGGACTGGTCTAG

APRE M6:

5′-GATCCACAGTT**GTG**ATTT**CAC**AAC**C**TGACCA-3′
GTGTCAACACTAAAGTGTTGGACTGGTCTAG

APRE M2:

5′-GATCCACATGTT**GG**ATTT**CCG**ATACTGACCA-3′
GTGTACAACCTAAAGGCTATGACTGGTCTAG

Bold type indicates contact points for the NF-κB proteins, *underlines* indicate contact points for the C/EBP proteins (21, 53).

For HepG2 nuclear extracts, antibody supershift assays were performed by adding 1 μl of commercially available affinity-purified IgG (Santa Cruz Biotech) to the binding reaction. For rat liver nuclear extracts, for quantitative supershifting, we found it necessary to first fractionate the APRE binding complex on a DNA-cellulose column (Pharmacia). After incubation for 20 min on ice, the antibody-NF-κB-DNA complexes were electrophoresed on a 6% native PAGE gel (24).

Plasmid Construction

APRE-LUC consists of the trimerized rat AGT APRE WT sequences ligated through *Bam*HI/*Bgl*II ends into the p59 rat AGT minimal promoter driving the expression of the firefly luciferase reporter gene (19–21, 51). Site-directed mutations of the AGT APRE within the context of the native AGT promoter (nucleotides −615 to −470) were produced by PCR amplification and overlap extension (PCR "SOE"ing) and cloned upstream of the AGT promoter (19–21). The GAL4-Rel A expression vector was constructed using the eukaryotic expression vector pSG424 (28) that produces GAL4 (1–147) under control of the SV40 early region promoter/enhancer. Rel A(1–551) and Rel A(255–551) coding sequences were cloned as *Bam*HI −*Xba* 1 fragments into the pSG424 plasmid as described (24). The UAS-LUC reporter plasmid was constructed using tandem GAL4-binding sites ligated upstream of the −59 rat AGT minimal promoter (51). The UAS sequences are (24):

5′-GATCCCGGAGGACTGTCCTCCGCGGAGGACTGTCCTCCGA-3′
GGCCTCCTGACAGGAGGCGCCTCCTGACAGGAGGCTCTAG

All plasmids were prepared on Cesium-chloride gradients before transfection and their concentration determined spectrophotometrically.

Acknowledgments

We wish to thank T.J. Murphy for the gift of the AT_1 expression plasmid pEF-BOS, P. Baeuerle for the gift of the Rel A(1–551) cDNA; Allan Green, E. Aubrey Thompson, and David Konkel for discussions and review of the manuscript; and Becky Soliz for expert secretarial assistance.

Received August 25, 1995. Accepted December 11, 1995.

Address requests for reprints to: Allan R. Brasier, MRB 3.142, University of Texas Medical Branch, 301 University Boulevard, Galveston Texas 77555-1060.

Supported in part by NIH Grant 1 R29 HL-45500. A.R.B. is an Established Investigator of the American Heart Association.

REFERENCES

1. Campbell DJ 1987 Circulating and tissue angiotensin systems. J Clin Invest 79:1–6
2. Peach MJ 1977 Renin-angiotensin system: biochemistry and mechanisms of action. Physiol Rev 57:313–370
3. Murphy TJ, Alexander RW, Griendling KK, Runge MS, Bernstein KE 1991 Isolation of a cDNA encoding the vascular type-1 angiotensin II receptor. Nature 351: 233–236
4. Griendling KK, Rittenhouse SE, Brock TA, Ekstein LS, Gimbrone Jr MA, Alexander RW 1986 Sustained diacylglycerol formation from inositol phospholipids in angiotensin II-stimulated vascular smooth muscle cells. J Biol Chem 261:5901–5906
5. Lang U, Valloton MB 1987 Angiotensin II but not potassium induces subcellular redistribution of protein kinase C in bovine adrenal glomerulosa cells. J Biol Chem 262:8047
6. Clark AJ, Balla T, Jones MR, Catt KJ 1992 Stimulation of early gene expression by angiotensin II in bovine adrenal glomerulosa cells: roles of calcium and protein kinase C. Mol Endocrinol 6:1889–1898
7. Sadoshima J, Izumo S 1993 Signal transduction pathways of angiotensin II-induced c-fos gene expression in cardiac myocytes *in vitro*. Roles of phospholipid-derived second messengers. Circ Res 73:424–438
8. Neyses L, Nouskas J, Luyken J, Fronhoffs S, Oberdorf S, Pfeifer U, Williams RS, Sukhatme VP, Vetter H 1993 Induction of immediate-early genes by angiotensin II and endothelin-1 in adult rat cardiomyocytes. J Hypertens 11:927–934
9. Lyall F, Dornan ES, McQueen J, Boswell F, Kelly M 1992 Angiotensin II increases proto-oncogene expression and phosphoinositide turnover in vascular smooth muscle cells via the angiotensin II AT1 receptor. J Hypertens 10:1463–1469
10. Taubman MB, Berk BC, Izumo S, Tsuda T, Alexander RW, Nadal Ginard B 1989 Angiotensin II induces c-fos mRNA in aortic smooth muscle. Role of Ca^{2+} mobilization and protein kinase C activation. J Biol Chem 264: 526–530
11. Gonzalez-Espinosa C, Garcia Sainz JA 1992 Angiotensin II and active phorbol esters induce proto-oncogene expression in isolated rat hepatocytes. Biochim Biophys Acta 1136:309–314
12. Gonzalez-Espinosa C, Garcia-Sainz JA 1992 Angiotensin II and active phorbol esters induce proto-oncogene expression in isolated rat hepatocytes. Biochim Biophys Acta 1136:309–314
13. Naftilan AJ, Pratt RE, Dzau VJ 1989 Induction of platelet-derived growth factor A-chain and c-myc gene expressions by angiotensin II in cultured rat vascular smooth muscle cells. J Clin Invest 83:1419–1424
14. Eggena P, Zhu JH, Clegg K, Barrett JD 1993 Nuclear angiotensin receptors induce transcription of renin and angiotensinogen mRNA. Hypertension 22:496–501
15. Hilgenfeldt U, Schwind S 1993 Angiotensin II is the mediator of the increase in hepatic angiotensinogen synthesis after bilateral nephrectomy. Am J Physiol 265:E414-E418
16. Nakamura A, Iwao H, Fukui K, Kimura S, Tamaki T, Nakanishi S, Abe Y 1990 Regulation of liver angiotensinogen and kidney renin mRNA levels by angiotensin II. Am J Physiol 258:E1-E6
17. Kohara K, Brosnihan KB, Ferrario CM, Milsted A 1992 Peripheral and central angiotensin II regulates expression of genes of the renin-angiotensin system. Am J Physiol 262:E651-E657
18. Morishita R, Higaki J, Okunishi H, Tanaka T, ishii K, Nagano M, Mikami H 1991 Changes in gene expression of the renin-angiotenin system in two kidney, one clip hypertensive rats. J Hypertension 9:187–192
19. Brasier AR, Ron D, Tate JE, Habener JF 1990 Synergistic enhansons located within an acute phase responsive enhancer modulate glucocorticoid induction of angiotensinogen gene transcription. Mol Endocrinol 4:1921–1933

20. Brasier AR, Ron D, Tate JE, Habener JF 1990 A family of constitutive C/EBP-like DNA binding proteins attenuate the IL-1 alpha induced, NF kappa B mediated transactivation of the angiotensinogen gene acute-phase response element. EMBO J 9:3933–3944
21. Ron D, Brasier AR, Wright KA, Tate JE, Habener JF 1990 An inducible 50-kilodalton NF kappa B-like protein and a constitutive protein both bind the acute-phase response element of the angiotensinogen gene. Mol Cell Biol 10: 1023–1032
22. Bouscarel B, Blackmore PF, Exton JH 1988 Characterization of the angiotensin II receptor in primary cultures of rat hepatocytes. J Biol Chem 263:14913–14919
23. Klett C, Nobiling R, Gierschik P, Hackenthal E 1993 Angiotensin II stimulates the synthesis of angiotensinogen in hepatocytes by inhibiting adenylylcyclase activity and stabilizing angiotensinogen mRNA. J Biol Chem 268: 25095–25107
24. Brasier AR, Li J, Wimbish KA, Tumor necrosis factor activates angiotensinogen gene expression by the Rel A transactivator. J Hypertens, in press
25. Baeuerle PA 1991 The inducible transcription activator NF-kappa B: regulation by distinct protein subunits. Biochim Biophys Acta 1072:63–80
26. Urban MB, Baeuerle PA 1990 The 65-kD subunit of NF-kappa B is a receptor for I kappa B and a modulator of DNA-binding specificity. Genes Dev 4:1975–1984
27. Schmitz ML, Baeuerle PA 1991 The p65 subunit is responsible for the strong transcription activating potential of NF-κB. EMBO J 12:3805–3817
28. Sadowski I, Ptashne M 1989 A vector for expressing GAL4 (1–147) in mammalian cells. Nucleic Acids Res 17:7539
29. Coezy E, Bouhnik J, Clauser E, Pinot F, Philippe M, Menard J, Corvol P 1984 Effects of glucocorticoids and antiglucocorticoids on angiotensinogen production by hepatoma cells in culture. In Vitro 20:528–534
30. Brasier AR, Philippe J, Campbell DJ, Habener JF 1986 Novel expression of the angiotensinogen gene in a rat pancreatic islet cell line: transcriptional regulation by glucocorticoids. J Biol Chem 261:16148–16154
31. Campbell DJ, Habener JF 1986 Angiotensinogen gene is expressed and differentially regulated in multiple tissues of the rat. J Clin Invest 78:31–39
32. Gordon MS, Chin WW, Shupnik MA 1992 Regulation of angiotensinogen gene expression by estrogen. J Hypertens 10:361–366
33. Hong-Brown LQ, Descchepper CF 1992 Effects of thyroid hormones on angiotensinogen gene expression in rat liver, brain, and cultured cells. Endocrinology 130: 1231–1237
34. Kimura S, Iwao H, Fukui K, Abe Y, Tanaka S 1990 Effect of thyroid hormone on angiotensinogen and renin mRNA levels in rat. Jpn J Pharmacol 52:281–285
35. Saye JA, Cassis LA, Sturgill TW, Lynch KR, Peach MJ 1989 Angiotensinogen gene expression in mouse 3T3-L1 cells. Am J Physiol 256:C448-C451
36. McGehee Jr RE, Ron D, Brasier AR, Habener JF 1993 Differentiation-specific element: a cis-acting developmental switch required for the sustained transcriptional expression of the angiotensinogen gene during hormonal-induced differentiation of 3T3-L1 fibroblasts to adipocytes. Mol Endocrinol 7:551–560
37. Ron D, Brasier AR, Habener JF 1990 Transcriptional regulation of hepatic angiotensinogen gene expression by the acute-phase response. Mol Cell Endocrinol 74: C97–104
38. Klett C, Hackenthal E 1987 Induction of angiotensinogen synthesis and secretion by angiotensin II. Clin Exp Hypertens A9:2027–2047
39. Brown K, Gerstberger S, Carlson L, Franzoso G, Siebenlist U 1995 Control of IkB-alpha proteolysis by site-specific, signal-induced phosphorylation. Science 267: 1485–1488
40. Lin Y-C, Brown K, Siebenlist U 1995 Activation of NF-κB requires proteolysis of the inhibitor IkB-a: Signal-induced phosphorylation of IkB-α alone does not release active NF-κB. Proc Natl Acad Sci USA 92:552–556
41. Henkel T, Machleidt T, Alkalay I, Kronke M, Ben-Neriah Y, Baeuerle PA 1993 Rapid proteolysis of I kappa B-alpha is necessary for activation of transcription factor NF-kappa B. Nature 365:182–185
42. Hayashi T, Sekine T, Okamoto T 1993 Identification of a new serine kinase that activates NF kappa B by direct phosphorylation. J Biol Chem 268:26790–26795
43. Ernst MK, Dunn LL, Rice NR 1995 The PEST-like sequence of IkB is responsible for inhibition of DNA binding but not for cytoplasmic retention of c-Rel or Rel A homodimers. Mol Cell Biol 15:872–882
44. Meichle A, Schutze S, Hensel G, Bruming D, Kronke M 1990 Protein kinase C-independent activation of NF-κB by TNF. J Biol Chem 265:8339–8343
45. Wiegmann K, Schutze S, Machleidt T, Witte D, Kronke M 1994 Functional dichotomy of neutral and acidic sphingomyelinases in TNF signalling. Cell 78:1005–1015
46. Wiegmann K, Schutze S, Kampen E, Himmler A, Machleidt T, Kronke M 1992 Human 55 kDa receptor for tumor necrosis factor coupled to signal tranduction cascades. J Biol Chem 267:17997–18001
47. Sadoshima J-I, Izumo S 1993 Signal transduction pathways of angiotensin II-induced c-fos gene expression in cardiac myocytes *in vitro*. Circ Res 73:424–438
48. Diaz-Meco MT, Dominguez I, Sanz L, Dent P, Lozano J, Municio MM, Berrn E, Hay RT, Sturgill TW, Moscat J 1994 epsilonPKC induces phosphorylation and inactivation of IkBα *in vitro*. EMBO J 13:2842–2848
49. Kimura S, Mullins JJ, Bunnemann B, Metzger R, Hilgenfeldt U, Zimmermann F, Jacob H, Fuxe K, Ganten D, Kaling M 1992 High blood pressure in transgenic mice carrying the rat angiotensinogen gene. EMBO J 11: 821–827
50. Jeunemaitre X, Soubrier F, Kotelevtsev YV, Lifton RP, Williams CS, Charru A, Hunt SC, Hopkins PN, Williams RR, Lalouel JM 1992 Molecular basis of human hypertension: role of angiotensinogen. Cell 71:169–180
51. Brasier AR, Tate JE, Ron D, Habener JF 1989 Multiple cis-acting DNA regulatory elements mediate hepatic angiotensinogen gene expression. Mol Endocrinol 3:1022–1034
52. Brasier AR, Ron D 1992 Luciferase reporter gene assay in mammalian cells. Methods Enzymol 216:386–397
53. Brasier AR, Kumar A 1994 Identification of a novel determinant for basic domain-leucine zipper (bZIP) DNA-binding activity in the acute-phase inducible nuclear factor-interleukin 6 transcription factor. J Biol Chem 269: 10341–10351